PROFILING L-SERINE TRANSPORT THROUGHOUT GROWTH AND MEIOTIC MATURATION IN MOUSE OOCYTES

Han Zhang

This thesis is submitted to the Faculty of Graduate and Postdoctoral Studies as a partial fulfillment of the M.Sc. program in

Cellular and Molecular Medicine.

Department of Cellular and Molecular Medicine

Faculty of Medicine

University of Ottawa

Abstract

With the increasing demand for assisted reproduction, more knowledge and understanding towards health requirements of oocytes and their inner workings are required. With current IVF success rates of approximately 40%, oocyte and embryo culture conditions *in vitro* can be improved by first understanding the finer details of oocyte function. As such, there is a need to better understand the mechanisms through which oocytes can acquire certain nutrients. This thesis focuses on the amino acid serine, which has been shown to improve outcome in developing embryos and also plays a variety of roles in the body that may carry over to oocyte health as well. Using radiolabeled [^{3}H] serine, we measured uptake of serine as a function of time throughout growth and meiotic maturation in mouse oocytes. Serine transport appeared in oocytes during growth and became absent in mature eggs. With a competition assay using substrates diagnostic for several different amino acid transporter systems and culture with and without sodium in the external medium, I identified Na^{+}-dependent SNAT7 of the System A/N (SLC38) family to be the most likely transporter in oocytes. Quantitative RT-PCR was consistent with this result. Transporter activity is also not activated by progression of meiotic maturation, as indicated by unperturbed transport when dbcAMP was provided to maintain meiotic arrest. However, a biological regulator of arrest, NPPC, resulted in enhanced transport activity *in vitro*. This may be due to signalling mechanisms of the NPPC pathway affecting regulation of serine uptake, which presents a direction for future research.

Table of Contents

List of Figures

List of Tables:

List of Abbreviations

3PG: 3-phosphoglycerate

ABC: ATP-binding cassette

ADCY: Adenylyl cyclase

AMP: adenosine monophosphate

ANOVA: analysis of variance

AREG: amphiregulin

ATP: adenosine triphosphate

BHMT: betaine--homocysteine methyltransferase

BLIMP1: B lymphocyte-induced maturation protein 1

BMP15: bone morphogenetic protein

BTC: betacellulin

bp: base pair

cAMP: cyclic adenosine monophosphate

CDC25B: cell division cycle 25B

CDK1: cyclin-dependent kinase 1

Chdh: choline dehydrogenase

cGMP: cyclic guanosine monophosphate

COC: cumulus-oocyte complex

CPM: counts per minute

dbcAMP: dibutyryl cyclic adenosine monophosphate

DHEA: dehydroepiandrosterone

DMR: differentially methylated regions

DNA: deoxyribonucleic acid

DNMT: DNA methyltransferase

E2: estradiol

EAAT: excitatory amino acid transporter

ECM: extracellular matrix

EGF: epidermal growth factor

ER: endoplasmic reticulum

EREG: epiregulin

FF: follicular fluid

FSH: follicle stimulating hormone

FOLR: folate receptor

GDF9: growth differentiation factor 9

GPR3: G protein coupled receptor 3

GSH: glutathione

GV: germinal vesicle

GVBD: germinal vesicle breakdown

HA: hyaluronic acid

hCG: human chorionic gonadotropin

HDL: high density lipoprotein

HEPES: 4-(2-hydroxyethyl)-1-piperazineethane-sulfonic acid

HMT: histone methyltransferase

ICM: inner cell mass

ICR: imprinting control region

IMPDH: inosine-5’-monophosphate dehydrogenase

i.p.: intraperitoneally

IU: international units

IVF: *in vitro* fertilization

IVM: *in vitro* maturation

KSOM: K+ supplemented optimized medium

LH: luteinizing hormone

LHR: luteinizing hormone receptor

MAT: methionine adenosyltransferase

MAPK: mitogen-activated protein kinase

MI: meiosis I

MII: meiosis II

MPF: maturation promoting factor

mtDNA: mitochondrial DNA

MTHFR: methyl tetrahydrofolate reductase

NMDA: N-methyl-D-aspartate

NOBOX: NOBOX oogenesis homeobox

NPPA: atrial natriuretic peptide

NPPB: brain natriuretic peptide

NPPC: natriuretic peptide C

NPR: natriuretic peptide receptor

P1-P21: post-natal day 1-21

PCR: polymerases chain reaction

PDE3A: phosphodiesterase 3A

PGC: primordial germ cell

PI: preimplantation

PHGDH: phosphoglycerate dehydrogenase

PMSG: pregnant mare serum gonadotropin

PSAT: phosphoserine aminotransferase

PSPH: phosphoserine phosphatase

PVA: polyvinyl alcohol

PKA: protein kinase A

PPP: pentose phosphate pathway

PRDM4: Positive regulatory domain 4

PTX3: pentraxin-related protein 3

PLP: pyridoxal phosphate

qRT-PCR: quantitative reverse transcription polymerase chain reaction

RFC: reduced-folate carrier

RNA: ribonucleic acid

SAH: s-adenosylhomocysteine

SAM: s-adenosylmethionine

SHMT: serine hydroxymethyltransferase

SOHLH1: spermatogenesis and oogenesis specific basic helix-loop-helix 1

SPT/AGT: serine:pyruvate/alanine:glyoxyate aminotransferase

SLC: solute carrier

TACE/ADAM17: tumour necrosis factor alpha converting enzyme

TE: trophectoderm

TET: ten-eleven translocation enzyme

THF: tetrahydrofolate

ZP: zona pellucida

Acknowledgements

This thesis and the work presented therein were completed under the supervision of Dr. Jay M Baltz (Department of Cellular and Molecular Medicine, University of Ottawa, Ottawa Hospital Research Institute, Chronic Disease Program, Obstetrics and Gynecology). His expertise as both a brilliant scientist and an excellent mentor resulted in the best graduate experience I could have hoped for. Throughout my Master's studies, he has provided endless support and patient guidance in my efforts seeking academic excellence and indulging scientific curiosity. For all this, I would like to express my most sincere gratitude.

I also wish to thank the members of my Thesis Advisory Committee: Dr. Barbara Vanderhyden (Department of Cellular and Molecular Medicine, University of Ottawa, Ottawa Hospital Research Institute, Centre for Cancer Therapeutics), Dr. Johnny Ngsee (Department of Cellular and Molecular Medicine, University of Ottawa, Ottawa Hospital Research Institute, Neuroscience Program), and Dr. Christopher Kennedy (Department of Cellular and Molecular Medicine, University of Ottawa, Ottawa Hospital Research Institute, Chronic Disease Program). I greatly appreciate their contribution of time and expertise. Their insights and questions have challenged me to examine my results in more depth and also expand my knowledge of the field.

Additionally, I would like to thank fellow members of the Baltz lab, past and present. I'd like to acknowledge Mrs. Megan Meredith and Dr. Chenxi Zhou, who taught me the basics of oocyte and embryo handling and provided significant technical guidance and advice. I would also like to thank Dr. Allison Tscherner, who kindly contributed her expertise in the designing of my qPCR protocols for this thesis. In addition, to Dr. Jane Fenelon, Dr. Angus Maccaulay, Ms. Taylor McClatchie, and Ms. Kyla Young, I would like to extend my thanks for their technical advice, friendship, and moral support.

Finally, I would like to express my gratitude for my family and friends for their support. My parents especially have been my rock, and their unconditional love and support have been a blessing throughout all the highs and lows of my journey.

I also acknowledge the support of Canadian Institutes of Health Research (CIHR) (MOP97972) obtained by Dr. Baltz.

1. Introduction

1.1 Oogenesis and Folliculogenesis

Female fertility in mammals depends heavily on the quality of oocytes, which are female germ cells. In embryos, they will contribute half the genetic materials as well as a plethora of nutrients and developmental support. Oocytes grow in ovaries and require regulated growth and maturation processes. The physiology described in this thesis will refer to mice unless otherwise stated.

As is shown in Figure 1, oocytes begin as primordial germ cells (PGCs), which become distinctly detectable in the early embryonic stages. This occurs at approximately embryonic day (E) 7.5 (Ginsburg et al., 1990). At around E10.5, PGCs migrate to the genital ridge, where they will proliferate mitotically and eventually give rise to oogonia (Monk & Mclaren, 1981). Success of these processes relies on transcription factors such as BLIMP1 and PRDM14 to support proliferation and migration, as well as many factors and proteins that support PGC survival (Lawson et al., 1999; Ohinata et al., 2005). These events also correspond with sex differentiation of the developing embryo (Bowles & Koopman, 2010).

PGC proliferation leads to the formation of germ cell nests containing primary oocytes. As mitosis gives way to meiosis, the primary oocytes become arrested in prophase I of meiosis (Borum, 1961). It is at this point that the germ cell nests formed previously break down to form primordial follicles, a process that occurs before birth in humans, but occurs in mice immediately after birth. During this process, a large quantity of oocytes is lost, potentially through a process of quality control (Pepling, 2006). The primordial follicles that form consist of the fertility potential for the entire female reproductive life. Recruitment of follicles will occur in cohorts to create fully mature oocytes (Kezele et al., 2007).

1.1.1 Folliculogenesis

The recruitment of primordial follicles occurs cyclically, with the exception of the initial recruitment (Wassarman et al., 1979). In mice, the first wave of folliculogenesis occurs shortly after birth, where a cohort of follicles develop in sync and reach full growth by approximately post-natal day 21 (P21). Once a primordial follicle is recruited, it activates and proceeds with follicle growth. Other follicles remain arrested and maintain a follicular pool (Fortune, 2003).

In primordial follicles the oocyte is surrounded by flattened granulosa cells, which develop into a single layer of cuboidal granulosa cells, giving rise to primary follicles. Progression to the primary follicle stage requires transcription factors NOBOX and SOHLH1, both of which have been shown to be critical to these early stages (Pangas et al., 2006; Rajkovic et al., 2004). As the granulosa cells proliferate, more layers of these somatic cells form around the oocyte and form the secondary, or preantral follicle (Pedersen & Peters, 1968).

Up to this stage, growth has been gonadotropin-independent. Rather, this process is driven by local paracrine factors that are produced by theca cells, granulosa cells, and the oocyte itself (Sánchez & Smitz, 2012). Secondary follicles become responsive to gonadotropins at this stage and begin to express follicle stimulating hormone (FSH) and luteinizing hormone (LH) receptors, which are required for further follicle development (Fortune & Eppig 1979; Wu et al. 2000). Along with continued growth of the oocyte, granulosa cells proliferate as well into multiple layers due to oocyte-secreted BMP15 and GDF9, the latter of which is also crucial in FSH receptor (FSHR) expression (Orisaka et al., 2006; Otsuka et al., 2000; Vitt et al., 2000). This gives rise to the secondary follicle, where formation of a theca cell layer also occurs, separated from the oocyte and layers of granulosa cells by a basement membrane.

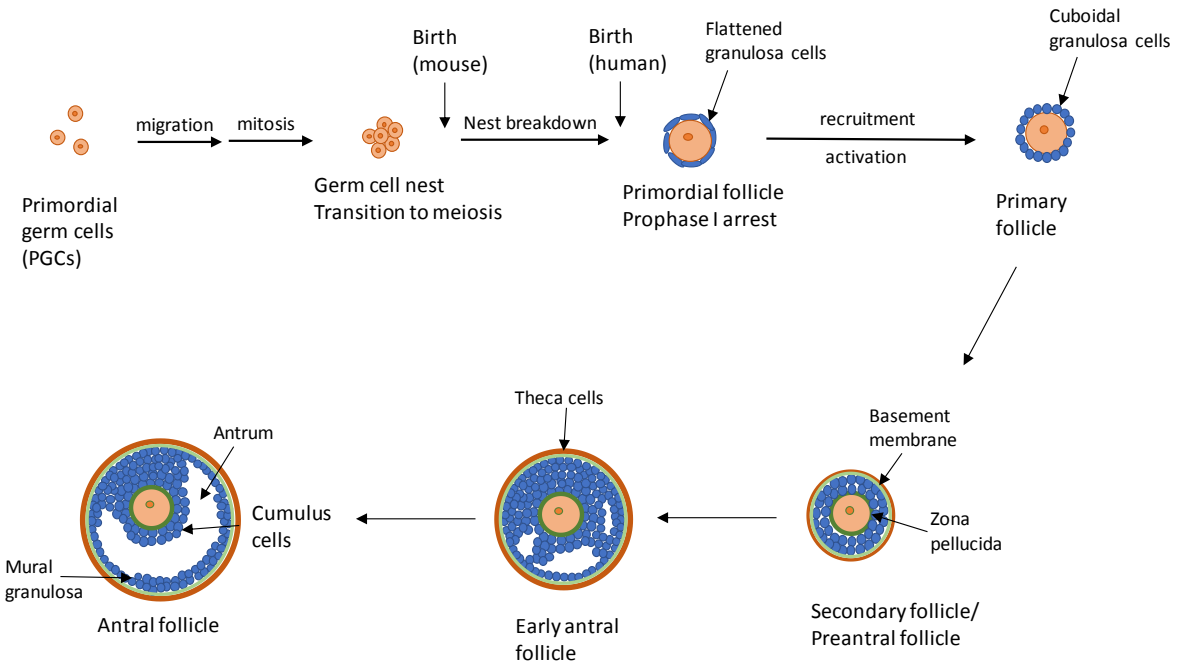

Figure 1. Depiction of oogenesis and folliculogenesis. The primordial germ cells migrate to the genital ridge. There, they divide by mitosis to form the germ cell nest and transition into meiosis. Upon nest breakdown, the primordial follicle is formed, marking the beginning of folliculogenesis. Blue shows somatic granulosa cells, and orange shows the germ cell. Green indicates the basement membrane, and red shows the thecal cell layer.

An antral cavity begins to form, and both the follicle and cavity size increases as folliculogenesis continues (Sánchez & Smitz, 2012).

During antral development, the granulosa cells also begin differentiating into cumulus and mural cells. This process is driven largely by FSH but in precisely regulated levels, as an excess can interfere with granulosa cell differentiation. The aforementioned BMP15 and GDF9 both function in regulating cumulus cell function, which play important supporting roles in oocyte growth and development (Moore et al., 2003; Vitt et al., 2000). The antral cavity is filled with follicular fluid and separates the cumulus cells surrounding the oocyte from the mural granulosa cells on the periphery of the antral follicle (Szybek, 1972).

1.1.2 Maintenance of meiotic arrest

During folliculogenesis, the arrested oocytes are not only increasing in size but also need to acquire meiotic competence as well as developmental competence to be fit for ovulation and fertilization. Meiotic competence refers to the oocyte's capacity to undergo meiotic resumption. Developmental competence addresses the oocyte's preparedness for embryo development after fertilization.

Oocytes achieve meiotic competence at approximately 80% of full size, which corresponds to the stage of antrum formation. This permits oocytes to resume meiosis and undergo meiotic maturation, though this will not occur until developmental competence is likewise achieved. Developmental competence requires the accumulation of various factors and transcripts necessary for embryo development (Szybek, 1972).

Prior to stimulation of ovulation, the oocyte is kept meiotically arrested in the follicle (Figure 2). This arrest is maintained through several pathways that function together. The key

mechanism is a high intracellular concentration of cAMP in the oocyte produced endogenously that maintains meiotic arrest (Downs et al., 1989). In the oocyte, meiotic maturation is initiated by maturation promoting factor (MPF), which is a heterodimer composed of cyclin-dependent kinase 1 (CDK1) and cyclin B (Hashimoto & Kishimoto, 1988). CDK1 is activated by the enzyme M-phase inducer phosphatase 2 (CDC25B). Maintaining elevated levels of cAMP results in persistent activation of protein kinase A (PKA) through phosphorylation, which in turn activates the nuclear kinase Wee1/Myt1. Wee1/Myt1 functions to inactivate CDC25B, resulting in suppression of MPF from inducing meiotic resumption (Solc et al., 2008).

Most pathways involved in maintaining arrest contribute to the cAMP pool in the oocyte. Firstly, production of cAMP needs to occur. This is carried out by the GPR3-Gs-ADCY cascade. ADCY (adenylyl cyclase) belongs to a family of enzymes that catalyzes ATP cyclization to cAMP and is the adenylyl cyclase that is activated by the G-protein Gs. In the oocyte, the constitutively expressed G-protein coupled receptor 3 (GPR3) stimulates Gs, leading to ADCY-mediated production of cAMP that adds to the level of intraoocyte cAMP (Mehlmann, 2005). Secondly, inactivation of PDE3A is vital to maintaining cAMP levels, as PDE3A is a cAMP phosphodiesterase that dephosphorylates cAMP to AMP. Inhibition of PDE3A is mediated by cGMP, a second messenger similar to cAMP (Shuhaibar et al., 2015; Vaccari et al., 2009).

Guanylyl cyclases mediate the cyclization of GTP into cGMP. Examples are G-coupled protein type receptors such as natriuretic peptide receptor A (NPR1) and natriuretic peptide receptor B (NPR2). Of these, only NPR2 is found in follicular cells (Pan & Li, 2019). There are three known types of natriuretic peptide, named the atrial natriuretic peptide (ANP or NPPA), brain natriuretic peptide (BNP or NPPB), and natriuretic peptide type-C (CNP or NPPC). While NPPA and NPPC are both found in the follicular environment, NPPC specifically binds to NPR2

whereas the receptor for NPPA is not found. While NPPC is produced in the mural granulosa cells, its receptors are located on the cumulus (Kiyosu et al., 2012; Wigglesworth et al., 2013; Zhang et al, 2010).

NPPC stimulation of NPR2 results in cGMP production in cumulus cells which enters the oocyte through gap junctions (Richard & Baltz, 2014). Expression of the receptors is maintained through signalling by the oocyte itself, including GDF9 and BMP15. Further upstream, inosine-5'-monophosphate dehydrogenase (IMPDH) has a critical overarching role in regulating the NPPC/NPR2 pathway of mediating meiotic arrest. GTP, the substrate for cGMP cyclization by NPR2 is converted from imosine-5'-monophosphate (IMP), a process for which the IMPDH catalyzed reaction is rate-limiting (Wigglesworth et al., 2013).

Therefore, IMPDH catalyzes the provision of GTP, and activation of NPR2 cyclizes GTP to cGMP which flows into the oocytes to inhibit PDE3A, a phosphodiesterase that breaks down cAMP in the oocyte (Vaccari et al., 2009; Wigglesworth et al., 2013; M. Zhang et al., 2010). In this way, meiotic arrest is maintained. Once the oocyte is both meiotically and developmentally competent, it is able to respond to the LH surge that initiates meiotic maturation and increases both LH and FSH circulation (Eppig, 1979).

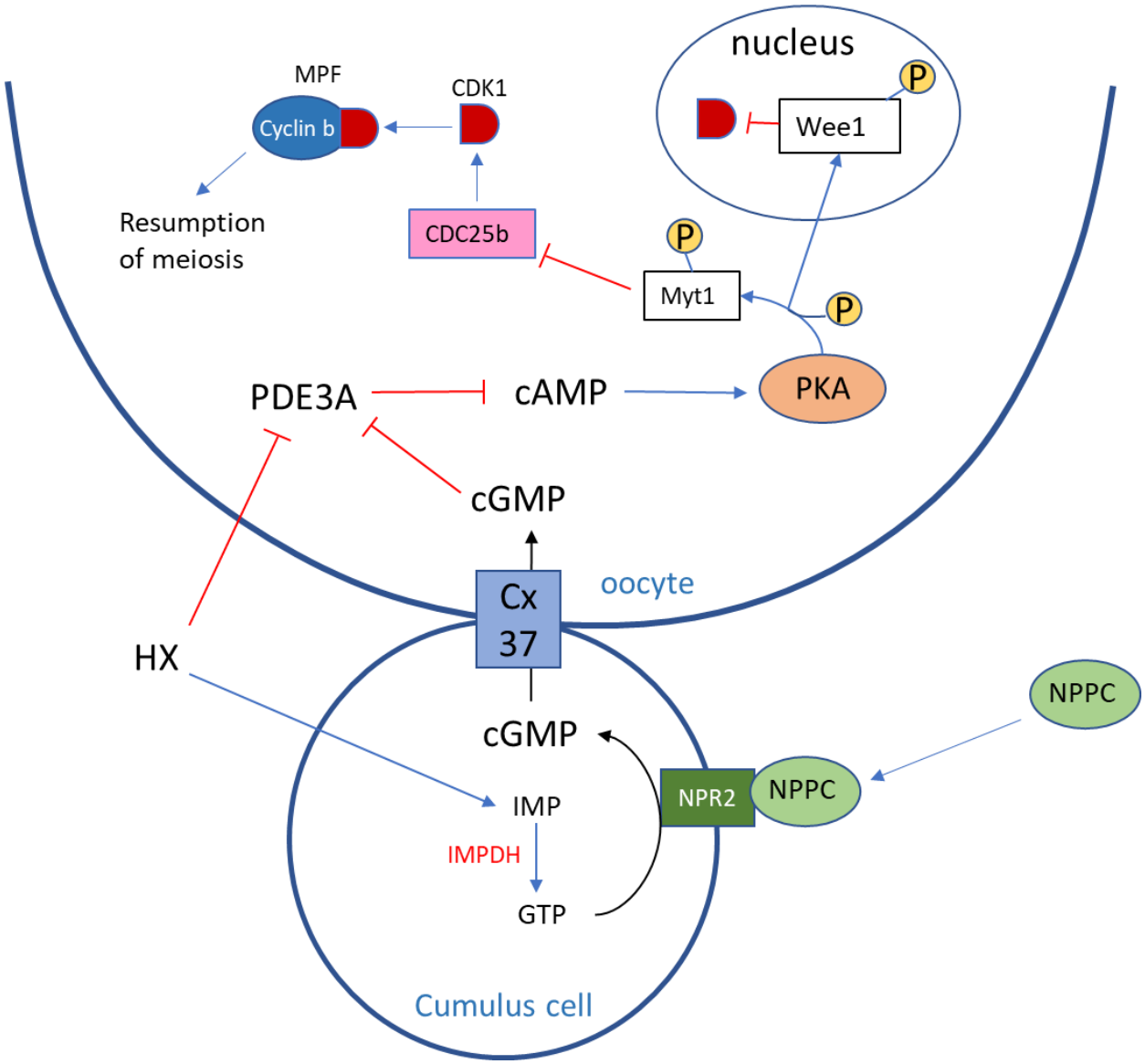

Figure 2. Meiotic arrest maintained by NPPC signalling. NPPC (light green) binds to NPR2 (dark green), which causes cyclization of GTP to cGMP. It passes through gap junctions (light blue) and enters the oocyte. Inside the oocyte, cGMP inhibits PDE3A, which when active degrades cAMP. cAMP, at high levels will activate PKA (orange). PKA phosphorylates (yellow) Myt1 in the cytoplasm and Wee1 in the nucleus. Both factors, when activated through phosphorylation, will inhibit CDK1 (red) binding to

cyclin B (dark blue). The CDK1 and cyclin B heterodimer form MPF to promote meiotic resumption.

1.1.3 LH surge, meiotic maturation, and ovulation

The preovulatory follicle induces increased synthesis of estradiol by the follicle. As estradiol accumulates, it reaches a peak level that stimulates pituitary release of LH, termed the LH surge (Micevych et al., 2003). A number of processes are triggered by the LH surge to result in meiotic resumption and meiotic maturation in preparation for ovulation and fertilization, including responses from the mural granulosa cells, the cumulus cells, as well as the oocyte and surrounding matrix. The LH receptor (LHR) is an adenylyl cyclase that increases cAMP in the follicle that can then activate protein kinase A (PKA). For much of downstream signalling, cAMP acts as the main messenger to mediate LH-induced effects (Conti et al. 2012; Park et al., 2004).

LHR activation leads to a cascade of signalling events that result in resumption of meiosis, including a decrease in cGMP levels that begins in mural granulosa cells and progresses from outward in. cGMP diffuses rapidly from oocytes and ceases to inhibit PDE3A activity, prompting PDE3A degradation of intraoocyte cAMP (Egbert et al., 2014; Vaccari et al., 2009). Simultaneously, there is decreased NPPC in the ovary accompanied by decreased NPR2 activity, leading to all around lowered cGMP in the ovary. Once cGMP levels decrease, there is also a LH-dependent closure of gap junctions (Norris et al., 2008). With lowered cGMP, a drop in intraoocyte cAMP levels is triggered, as well as the activation of PDE3A to further degrade cAMP. As a result, MPF can activate to promote meiotic maturation of the oocyte.

Meiotic resumption also relies, in part, on LH effects on epithelial growth factor (EGF) - like activation. Transient expression of amphiregulin (AREG), epiregulin (EREG), and beta-cellulin (BTC) occurs as a result of LH signalling. TACE/ADAM17, a proteolytic enzyme that cleaves EGF-like factors, plays a key role in somatic cell luteinization and ovulation. It isolates

the EGF domain from EGF-like factors to allow interaction with the EGF receptor (EGFR) (Yamashita & Shimada 2012). This activates the MAPK pathway, which plays a number of roles in meiosis, such as regulating first polar body size and inducing second meiotic arrest at metaphase II (Choi et al. 1996; Hashimoto et al. 1994).

Once meiotic maturation is initiated, meiosis resumes with the breakdown of the nuclear membrane. The visible nucleus of the immature oocyte is known as the germinal vesicle hence the process is referred to as germinal vesicle breakdown (GVBD). With the breakdown of the snuclear membrane, a spindle assembles, and the diploid DNA content condenses into chromosomes. The chromosomes then align near the oocyte periphery and divide in preparation of extruding a polar body. The polar body will contain a haploid amount of DNA, leaving a haploid fully mature oocyte to be fertilized. The chromosomes remaining in the oocyte again align with spindle and arrest in metaphase of meiosis II (Li & Albertini, 2013).

In the follicle, when meiotic resumption occurs, the mural granulosa cells respond most quickly due to its higher expression of LHR and results in secondary signals to the cumulus cells. This chain of events leads to the cumulus producing hyaluronic acid (HA). Cumulus expansion and mucification, or the deposition of a mucoelastic material in extracellular matrix (ECM) surrounding the oocyte, then occurs (Salustri et al., 1990). Several proteins, such as 1α1 and PTX-3, complex within the matrix for the formation and stabilization of the ECM which is highly important to both the ovulation process as well as fertilization success (Russell & Robker, 2007). This process requires FSH and is also regulated by the oocyte itself (Dekel & Phillips, 1979; Salustri et al., 1985).

The LH surge also induces the expression of progesterone receptors in an estradiol dependent manner though they are quickly downregulated thereafter (Couse et al., 2005).

Progesterone is a key regulator for follicular rupture, the process through which the expanded cumulus oocyte complex (COC) is released into the oviduct for fertilization (Baird et al., 2003; Loutradis et al., 1991). Cells at the follicular apex thin out, and the basement membrane is proteolytically degraded. Alongside these changes, ovarian surface epithelial cells undergo apoptosis and there is breakdown of the basal lamina.

As the follicle ruptures to release the oocyte, the oviductal ciliated infundibulum captures it through selective adhesion between its epithelium and the ECM. The oocyte is then transported along the oviduct. At the point of ovulation, the oocyte has fully matured to a second meiotic metaphase (MII) egg, having extruded a polar body and is again meiotically arrested in preparation for activation by fertilization (Combelles et al., 2002; Russell & Robker, 2007).

1.1.4 Fertilization and pre-implantation embryo development

When sperm reaches the oocyte within the oviduct, it binds to the zona pellucida (ZP), which is composed of ZP glycoproteins. In mice, these are ZP1 to ZP3 (Vazquez et al., 1989). Upon binding, a secretory vesicle referred to as the acrosome undergoes exocytosis from sperm. The acrosome contains hydrolytic and proteolytic enzymes that allow the plasma membranes to fuse. Ovastacin, a protease from the cortical granules of the oocyte, will also activate to cleave ZP2, resulting in the inability to further bind sperm thus avoiding polyspermy (Burkart et al., 2012).

Fertilization of the oocyte also releases it from the MII meiotic arrest. Half of the sister chromatids are discarded into a second polar body, and the remaining are included in the female pronucleus within the oocyte. The paternal genome is initially condensed in the male pronucleus but undergoes decondensation to eventually unify with maternal chromosomes. As the zygote

transitions from the end of meiosis to mitotic division, chromosomes reorganize within the zygote, aligning in preparation for mitotic division. While many proteins for mitosis differ from meiosis, the change is rapid. It is likely that the oocyte carries mitotic proteins into embryo development (Clift & Schuh, 2013).

As the newly formed zygote travels through the oviduct, it undergoes a series of divisions into progressively smaller cells. Initially, the zygote relies on maternal mRNA as the zygote remains still transcriptionally silent. Near the end of the 1-cell stage in mice, however, zygote genome activation begins with a minor burst of zygotic transcription. A second, more global burst follows the first division into the 2-cell stage, where more transcription of the zygote genome occurs, and maternal transcripts are degraded (Aoki et al., 1997). This same process is observed in humans at the 4- to 8-cell stages (Braude et al., 1988).

Once the embryo has divided to the 8-cell stage, a process called compaction occurs, where there is an increase of intercellular adhesion and the cells flatten and form tight junctions between each other. The compacted embryo is known as a morula. The morula continues mitotic division, and cells also begin to localize apically in the embryo. By the 32-cell stage, a fluid-filled cavity referred to as the blastocoel begins to form. Cells of the embryo begin to differentiate into two distinct cell lineages. Outside cells begin to form the trophectoderm (TE) lineage, while inner cells prepare to form the inner cell mass (ICM). With the formation of the blastocoel, the embryo is now a blastocyst and can implant into the embryo wall (Cockburn & Rossant, 2010).

1.2 Requirements of oocyte health

Culture media *in vitro* is made to imitate the *in vivo* environment. This is done through supplementation with many components that are required for healthy oocyte growth and maturation. These can include molecules such as amino acids, hormones, osmolytes and so on. When necessary nutrients are not provided, this can lead to lower egg quality and lesser blastocyst formation following fertilization.

1.2.1 *In vitro* culture of oocytes

For many couples who wish to have children, subfertility can be a stumbling block. With marriage ages and age of having a first child on the rise, fertility issues are coming to the forefront of study. In vitro fertilization has become something that can greatly improve the chances of pregnancy and has become quite widely used since its first success in 1978 (Steptoe & Edwards, 1978). However, the procedure is not without its risks, as egg retrieval for IVF requires treatment with gonadotrophins for follicular stimulation. This can result in ovarian hyperstimulation syndrome and exacerbate polycystic ovarian syndrome. In 1991, in vitro maturation (IVM) was found successful by Cha et al. (1991). With this technique, the oocytes are obtained in their immature stage and undergo the meiotic maturation process in culture and the risks above can be avoided.

Culture of oocytes through meiotic maturation requires a number of components for the energetically demanding process. IVM usually is carried out with oocytes still in COCs for optimal maturation in an *in vitro* environment. In the follicle, COCs are surrounded by follicular fluid which provides the oocyte with all the components it needs. This includes proteins, electrolytes, energy substrates, steroids and peptide hormones, growth factors, and many others

that are still under study. For the most part, commercial media are used for the purposes of IVM. These media have a focus on optimal ion concentrations and providing metabolic substrates. For example, there is usually the addition of glucose, and outcome is further improved with pyruvate inclusion as well (Downs & Hudson, 2000). Combinations of amino acids are usually a component of culture media for purposes such as being substrates for protein synthesis and to act as organic osmolytes. Macromolecules such as bovine serum albumin and fetal calf serum also serve as protein supplements that improve oocyte nuclear maturation and blastocyst formation following fertilization. Polyvinyl alcohol (PVA) is a non-biological alternative to the abovementioned macromolecules and has been shown to be an excellent replacement (Harriset et al., 2005).

Shortly following the first successful IVM procedure, Rose and Bavister (1992) tested seven different commercial media to evaluate best embryo outcomes with their use in IVM. Of the seven, it was found that SFRE 199-2 medium (SFRE) and Eagle's minimum essential medium-α (MEMα) fared the best in terms of blastocyst development, with 19% for SFRE and 18% for MEMα. Oocytes matured in those two media resulted in the highest cleavage rates to 2-cell embryos, as well as the highest development to blastocyst. However, this is a process that still requires improvement, which can only occur with better understanding of oocyte needs. Those needs are discussed in further detail in following sections.

1.2.2 Amino acids

An important part of what oocytes require consists of amino acids which serve different functions. Amino acids are in general defined as organic molecules composed of a backbone of a carboxyl end (-COOH) and an amino end (-NH2) that sandwich a carbon linked to unique

sidechains with specific characteristics that are used to categorize amino acids. The most common are those that form protein in mammalian bodies, and there are 20 of these, shown in Figure 3. Amino acids are not only the building blocks of protein, but there are also hundreds of other amino acids serving a multitude of other purposes including volume regulation, acting as signalling factors, and contributing to energy metabolites (Wagner & Musso, 1983).

One such example is glutamine, which is readily abundant in follicular fluid. This amino acid at 2mM can independently provide sufficient energy to initiate meiotic resumption in mouse oocytes and carry out GBVD, though not enough to complete meiotic maturation to the MII stage (Downs & Hudson, 2000). In combination with cysteine and proline, these three amino acids also act as precursors for glutathione (GSH) to control oxidative stress (Sutton et al., 2003).

In addition to functioning as antioxidants, some other amino acids are also required as organic osmolytes for the regulation of cell volume. A major example of this is glycine, which is shown to be highly transported in oocytes (Baltz & Zhou, 2012; Richard et al., 2017). Taurine is another organic osmolyte with various roles, including as a chelator of heavy metal ions and promoting sperm maturation (capacitation) to mediate fertilization (Hwang et al., 1998; Mrsny et al., 1979).

Importantly, amino acids also are precursors to forming DNA and RNA, specifically forming purines, pyrimidines, and thymidylates. When amino acids are added to oocyte culture media during maturation, improvements in reproductive outcome are observed. For example, embryos from those oocytes are improved in embryo development rates and result in higher cell numbers in blastocysts (Watson et al., 2000).

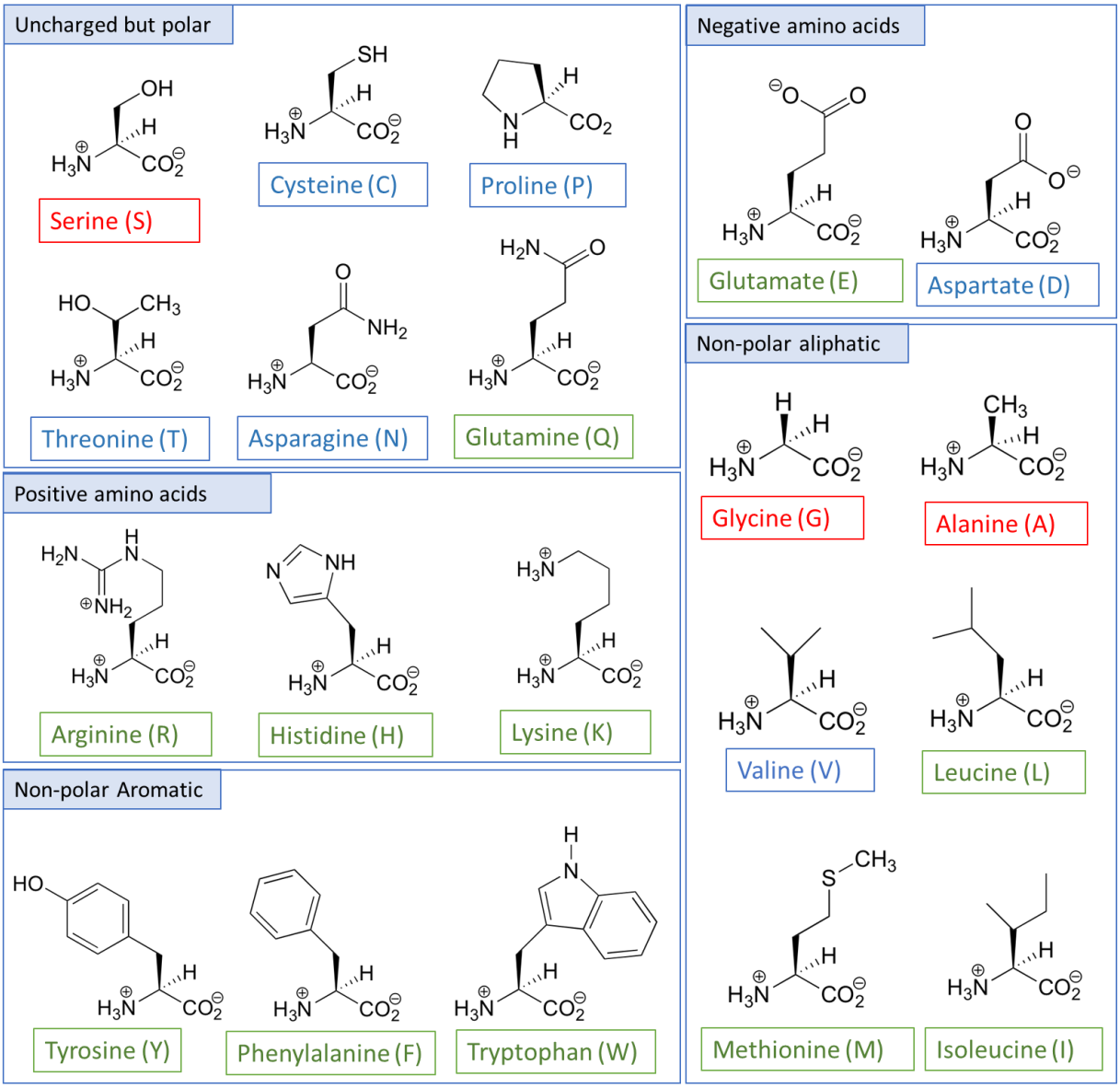

Figure 3. Protein-building amino acids. Categorized based on charge. Size is shown by colour-coding. Red = small amino acids, blue = medium-sized amino acids, green = large amino acids. Figure created using chemical structures obtained from LibreTexts Chemistry, Tim Soderberg, licensed under creative commons CC BY-NC-SA 3.0. (Soderberg, 2013).

1.2.3 Metabolism and steroidogenesis

As oocytes grow, they undergo a number of changes. Aside from increasing in size, they also proportionally increase in cytoplasmic volume and production of organelles such as mitochondria, Golgi complex, and endoplasmic reticulum (Peter & McNatty, 1980). The process of oocyte maturation requires high levels of energy; therefore, mitochondria are vital in achieving successful maturation (Tingen et al., 2009).

Mitochondria inherit their own DNA, mtDNA, and provide energy, regulate apoptosis, and mediate calcium (Ca2+) homeostasis (Van Blerkom, 2004). Oocytes primarily use oxidative phosphorylation to generate ATP through the electron transport chain. This also results in by-products such as free radicals, which in unregulated systems can compromise cell and genetic integrity. Free radicals are present in the form of reactive oxygen species (ROS) and reactive nitrogen species (RNS), both of which are managed by antioxidants such as GSH (Lu, 2013).

A major energy source used by oocytes is pyruvate, which is metabolized by the gluconeogenesis pathway, where it can be converted to 3-phosphoglycerate (3PG). Omitting pyruvate from oocyte culture media results in lowered polar body formation. Pyruvate can come from multiple sources, including from lipids, amino acids, and glucose via glycolysis (Downs & Hudson, 2000). Glucose is another required nutrient that can be metabolised, initially primarily by cumulus cells, with a preference towards the pentose-phosphate pathway (PPP) (Han et al., 2011; Xie et al., 2016). Later in development, oocytes gain the ability for some independent glucose metabolism (Brinster, 1971). The COC relies heavily on anaerobic metabolism, which results in formation of ATP for energy and also pyruvate and lactate. As a part of this process, a supply of NADPH is required, which can be renewed from NAD+ through the PPP. This process is also integral to regulating oxidative stress through the production of GSH. The PPP is also

important to oocyte maturation as a mechanism through which the ribose precursor to nucleic acid sugar backbone is formed (Dumesic et al., 2015; Songsasen, 2012).

Lipids are another group of nutrients required by oocytes. Lipids are found in oocytes in various forms, such as triglycerides, and are used as energy and co-localize with mitochondria to support oocyte processes with readily produced energy (Cetica et al., 2002). Long-chain fatty acids are another source that can be used. They are processed within the mitochondria, where through β-oxidation, the fatty acids are broken into 2-carbon acetyl-CoA groups that can be used in the citric acid cycle (Valsangkar & Downs, 2013). However, saturated fatty acids can also lead to mitochondrial dysfunction and induce endoplasmic reticulum stress. As for unsaturated fatty acids, they generally benefit embryo development, but elevated levels remain harmful to oocyte and embryo development (Dunning et al., 2014).

Lipids can also be organized into lipoproteins. Again, homeostasis is vital as too much or too little can negatively affect oocyte development. For example, while HDL is important as the primary cholesterol source in mice and is critical to fertility, an elevated level of HDL can decrease embryo quality and also result in failure to cleave in fertilized eggs (Wallace et al., 2012). In addition, saturated fats such as palmitic acid can hinder COC expansion, cause apoptosis of supporting cumulus cells, and slow meiotic progression (Leroy et al. 2005; Wu et al. 2012). This is not to say that lipoproteins do not have some very important roles. A key role for lipoproteins is steroidogenesis. This process occurs in the gonads as well as the adrenal glands and is responsible for the steroid production that is vital for oocyte maturation and fertilization. As cholesterol, they are taken up into mitochondria by the steroidogenic acute regulatory protein (StAR) where they are then converted to pregnenolone. This is a precursor for diverging conversions to form DHEA, progesterone, and other steroid hormones. In some species,

including human, the hormone estradiol triggers signalling through Ca^{2+} oscillations that mediate cytoplasmic maturation, which is a vital step in preparing an oocyte for fertilization (Tesarik & Mendoza, 1995; Zelinski-Wooten et al., 1994; Zheng et al., 2003). However, the effect of estradiol varies between species and does not always appear to be beneficial as is the case in mice (Tarumi et al., 2014). These hormones can also regulate gene expression and cell processes, such as androgen-stimulated expression of the FSH receptor gene, which is required for response to FSH, the hormone that triggers ovulation (Weil et al., 1999).

Like all the other nutrients that oocytes require, it appears that balance is key for successful preparation for ovulation and subsequent fertilization.

1.2.4 Metabolic coupling

During growth, oocytes are supported throughout by the follicle and its follicular cells. These are the granulosa cells and the cumulus, which surround the oocyte more immediately. Gap junctions are passages through which nutrients can be shared and they develop between granulosa cells and the oocyte. Communication via gap junctions begins in the primordial follicle stage, but gap junction proteins have been detected as early as in the fetal ovary and increase with oocyte growth (Mitchell & Burghardt, 1986; Pérez-Armendariz et al., 2003). Metabolic coupling refers to the improved transport of low-molecular weight molecules and nutrients into oocytes through follicular cells (Haghighat & Van Winkle, 1990). These substrates include glucose metabolites, amino acids, nucleotides, and various regulatory components such as cGMP (Sutton et al., 2003).

Granulosa cells send out filopodia referred to as transzonal cytoplasmic processes (TZPs) that penetrate the zona pellucida of the oocyte (El-Hayek, Yang, Abbassi, FitzHarris, & Clarke,

2018). At the ends of these processes sit connexin proteins that make up the gap junctions through which all these substrates can diffuse. Between oocytes and cumulus cells, the gap junctions are composed of connexin-37. Between granulosa cells, it is connexin-43 (Sutton et al., 2003).

The cumulus cells play several vital roles in providing oocytes with substrates they lack the ability to produce. For example, the majority of glucose metabolism occurs in the cumulus cells and the glycolysis products diffuse into the oocyte. A similar process occurs with cholesterol metabolism. Cumulus also enhances the transport of several amino acids into oocytes, including alanine, lysine, choline, and taurine (Haghighat & Van Winkle, 1990; Pelland et al., 2009). Research has also found that the communication is bi-directional, and that oocytes also produce signalling factors that regulate cumulus cells (Wigglesworth et al., 2013).

1.3 DNA methylation

1.3.1 Epigenetic regulation of genes

DNA can be regulated through various modifications to its structure, whether it be the histones that organize the DNA or the DNA sequence itself. Two main mechanisms of epigenetic gene regulation have been identified: chromatin remodelling and DNA methylation (Dolinoy et al., 2007).

Chromatin is the highly structured organization that DNA is wrapped into within the nucleus of the cell. Linear DNA is wrapped around octamers of core histones to form units known as nucleosomes. These then take on open or closed formations, making them euchromatin or heterochromatin respectively. Modifications can be the addition of many different groups, such as acetylation, ubiquitylation, or methylation to list a few, leading to chromatin remodelling

into either closed or open configurations, hence inhibiting any interaction with it or making the DNA available to transcription. For example, acetylation of histones most often results in relaxation of the chromatin, leading to transcription (Annunziato & Hansen, 2000; Tiedeken & Chang, 2015).

DNA methylation, which is the covalent binding of methyl groups to the DNA strands themselves, can also regulate gene expression, though the result is most often inhibited transcription. This kind of modification manifests as the addition of a methyl group to cytosine in DNA. Methylation is found almost exclusively at isolated CpG dinucleotides, which are methylated by default. However, some regions with high CG concentration, usually at 5' ends of genes co-localized with gene promoters, are not usually methylated except in the case of epigenetic regulation. These are known as CpG islands (Smallwood & Kelsey, 2012).

Methylation of these CpG islands is mediated by a group of enzymes called DNA methyltransferases (DMNTs). In humans, there have been 5 identified DNMTs to date, though two of the five share conserved sequences but do not have the ability to directly catalyse a DNMT reaction (Lyko, 2017). The ones with catalytic activity are DNMT1, DNMT3A and DNMT3B.

One of the first studied phenomena regarding epigenetics was X-chromosome inactivation, which is vital in female cells with two X chromosomes due to dose sensitivity of certain genes. In early embryogenesis, a long non-coding RNA called *Xist* binds to one X chromosome resulting in it being silenced. It was found that the *Xist* gene on the inactivated X chromosome is hypermethylated, while the active X is not methylated which is telling of DNA methylation involvement in its regulation (Brown et al., 1991; Willard & Breg 1980; Willard et al., 1993).

1.3.2 Epigenetic reprogramming

At two points in development, epigenetic marks are erased across the entire genome, followed by complete reestablishment of methylation. The first point is in the primordial germ cells during proliferation and migration. Methylation plays a major role in cell differentiation, and this erasing of methylation marks in the primordial germ cells restores them to a totipotent state (Reik & Walter, 2001). The second round of demethylation occurs following fertilization. As the embryo develops, the maternal genes passively demethylate as cells divide while paternal genes are actively demethylated (Monk et al., 1987). Unlike in the primordial germ cells, during this second global demethylation event certain gene methylation regions are untouched, known as imprinted genes (Smallwood et al., 2011). These are found at the differentially methylated regions (DMRs) and will be further discussed in the next section.

The enzymes responsible for the massive amount of methylation are DNMT3A and DNMT3B, the two *de novo* methyltransferases. DNMT3L also plays a vital role as a co-factor, despite lacking the catalytic domain. Rather, it forms a tetramer with DNMT3A. Unlike DNMT1, which carries out maintenance methylation and has a preference for hemi-methylated DNA, the DNMT3s have no such preference (Jia et al., 2007; Sharif et al., 2007). In fact, there have also been cases observed where they were capable of methylating non-CpG islands (Gowher & Jeltsch, 2001). However, in oocytes only DNMT3A and 3L appear to be active, while all three are used in the male germ cells (Smallwood & Kelsey, 2012).

Following global demethylation in the primordial germ cells, re-methylation that occurs is sex-dependent. Oocytes and sperm are methylated differently, and sperm is much more heavily methylated. In males, re-methylation begins before birth and the onset of meiosis. In female germ cells, however, the process occurs following birth, during the oocyte growth phase

(Seisenberger et al., 2012; Li et al., 2004). All the while, the oocytes are in meiotic arrest during prophase I. Areas with most methylation differences between male and female germ cells are the DMRs, and these play a vital role in fetal development (Kafri et al., 1992; Stewart et al., 2016).

The second wave of demethylation occurs once female and male germ cells have merged to create a zygote. Passive demethylation observed by the maternal genes occurs through the lack of maintenance methylation, hence the genome is less methylated with each division (Monk et al., 1987). In the paternal genes, methyl marks are actively removed by cellular machinery, the ten-eleven translocation enzymes (TETs). There are 3 TETs that demethylate the mammalian genome, and TET3 specifically is the mediator of paternal demethylation. The exception to global demethylation is the DMRs established during germ cell growth. They retain these marks, and the genes that remain methylated are known as imprinted genes (Bartolomei & Ferguson-Smith, 2011; Morgan et al., 2005).

1.3.3. Imprinted genes

Imprinted genes are still under a lot of study, but immense progress has been made in uncovering the specific roles for certain imprinted genes. These are genes that require mono-allelic expression, as in only the genes from one parent are expressed while the other is silenced by methylation-mediated imprinting. Approximately 150 imprinted genes have been found in mice, and 100 in humans (SanMiguel & Bartolomei, 2018). As a whole, it seems that maternally expressed genes and paternally expressed genes largely bias towards different aspects of fetal development. The balance between the two is what is needed for healthy embryogenesis.

Imprinted genes are highly expressed at prenatal stages and are down-regulated following birth. They have roles in a number of functions, which include brain function and prenatal

growth. The mechanism through which these genes control prenatal growth seem to function heavily through controlling placental growth. This is the medium through which nutrition is supplied to the growing fetus, and so limiting its growth indirectly limits that of the fetus as well. Many imprinted genes affect the development of the placenta, thereby restricting or promoting fetal development. Among the imprinted genes, those that are maternally expressed (or paternally imprinted) favour fetal growth restriction. Paternally expressed genes promote fetal growth instead, and it is the balance of the two seemingly conflicting functions of the parental imprinted genes that results in healthy development of the embryo (Moore & Haig, 1991).

The mechanisms of imprinting also differ between paternal and maternal chromosomes. Imprinting control regions (ICRs) are localised in intergenic regions within paternal chromosomes, and several imprinted genes can be regulated despite being at a distance from the ICR. Maternal ICRs, however, are located at the promoters of imprinted genes and therefore silence the immediate gene (Bartolomei et al., 1991; Wutz et al., 1997).

Imprinting errors can have devastating consequences including fatality, but they can also result in viable embryos with imprinting disorders. A well-studied example is the Angelman syndrome, which is identified by a particular "cheery" behaviour as well as mental disability and speech impairment. In the case of Angelman syndrome, the majority of incidences is due to chromosomal deletion rather than DNA methylation dysregulation (Horsthemke & Buiting, 2006). Others like Beckwith-Wiedemann syndrome, which manifests as pre- and postnatal overgrowth, and Silver-Russell syndrome, characterized by intrauterine and postnatal growth retardation, are primarily due to specific hypomethylation (Bartolomei & Ferguson-Smith, 2011). There have also been some reports that indicate assisted reproductive technologies such as IVF can result in higher risk for imprinting disorders (Odom & Segars, 2010).

1.4 One-carbon metabolism

One very important aspect of regulation within the body is one-carbon metabolism. One carbon groups are groups that contain a single carbon molecule, such as methyl (-CH3) and formyl (-CHO). For the context of this thesis, the primary focus will be on the methyl group. There are three components of one-carbon metabolism. The first is folate metabolism, referred to as the folate cycle. Overlapping somewhat with the folate cycle is the methionine cycle. Finally, there is the transsulfuration pathway in which homocysteine, an intermediate of the methionine cycle, undergoes transsulfuration as an alternative pathway to form cysteine (Ikeda et al., 2012).

1.4.1 Folates and the folate cycle

5-methyl tetrahydrofolate (THF) is the primary circulating form of folate in the bloodstream. Another form is folic acid, the synthetic form of folate used as a nutritional supplement to ensure sufficient folates in the diet. As shown in Figure 4, folic acid is converted to tetrahydrofolate, then into dihydrofolate in the body, which enters the folate cycle to provide methyl groups for various important processes (Kalmbach et al., 2008). Within the natural diet, it can be ingested in the form of polyglutamates, which is the reduced form of folate with a chain of glutamate residues. They can then be metabolised down to monoglutamates, which are converted to the 5-methyl THF form.

Serine passes along its methyl group to THF in a reaction catalysed by serine hydroxymethyltransferase (SHMT) with pyridoxal phosphate (PLP), or active vitamin B6, as a co-factor. This results in the simultaneous conversion of serine to glycine, and THF to 5,10-methylene THF. MTHFR then generates 5-methyl THF in a rate-limiting reaction. At this point it overlaps the methionine cycle, as homocysteine is used to convert 5-methyl THF back to THF

while the amino acid itself obtains the methyl group and turns into methionine. Meanwhile, the recycled THF can re-enter the folate cycle to shuttle more methyl groups through this pathway (Ikeda et al., 2012).

It is in the methionine cycle that the universal methyl donor, S-adenosylmethionine (SAM) is generated via methionine adenosyltransferase (MAT), converting methionine to SAM. SAM can then go on to serve many purposes, such as providing the methyl groups required for DNA methylation as well as methylation of lipids, proteins, histones and so on. Passing on its methyl group results in SAM demethylation to S-adenosylhomocysteine (SAH), which is hydrolysed to homocysteine by SAH hydrolase. SAM is also a precursor of GSH, which plays important roles in neutralizing reactive oxygen species (ROS) and reducing oxidative stress (Loenen, 2006; Lu, 2000).

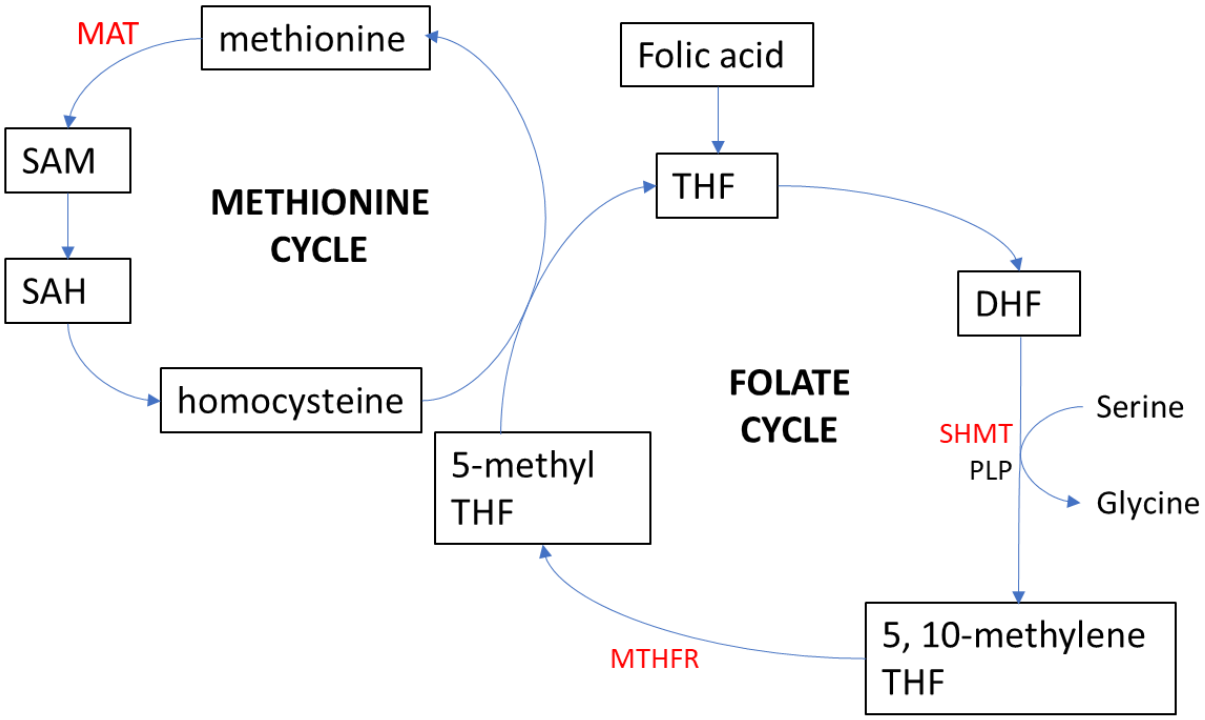

Figure 4. Diagram of the folate cycle, indicating where serine contributes its methyl group and depicting where the folate cycle overlaps the methionine cycle. SAM = S-adenosylmethionine, SAH = S-adenosyl L-homocysteine, THF = tetrahydrofolate, DHF – dihydrofolate. Direction of reactions are indicated by arrows, with key enzymes shown in red, SHMT = serine hydroxymethyltransferase, MTHFR = methylenetetrahydrofolate reductase, MAT = methionine adenosyltransferase, and PLP is a co-factor for the SHMT-mediated transfer of a one-carbon group.

1.4.2 Methyltransferases

One-carbon groups can be transferred from one component to another in the form of methyl groups by methyltransferases. They have been categorized into five classes based on structural motifs. Class I consists of all the DNA methyltransferases as well as some protein methyltransferases and is also the largest class of methyltransferases. This class also includes a wide range that can target the S-, N-, O-, C-, Se-, and As- nucleophilic cores. Class II is defined by the MetH reactivation domain, and Class III is the pre-corrin-4 methyltransferase (Schubert et al., 2003; Struck et al., 2012). The second largest class, Class IV, is composed of mostly RNA methyltransferases known as the SPOUT family, which derives its name from the founder enzymes SpoU and TrmD. Unlike Class I methyltransferases, which have highly conserved structures, this family shares a common SPOUT core but otherwise varies greatly (Krishnamohan & Jackman, 2019). The fifth and final class identified so far is class V, known as the SET-domain protein methyltransferases. As the name suggests, this is the class under which most protein methyltransferases fall (Dillon et al., 2005).

Methylation can affect properties of bioactive compounds and as such certain methyltransferases have also been the target of pharmacological study. The addition of a methyl group to a molecule can increase its lipophilicity and membrane solubility, and in the case of small molecules, can alter their conformations as well (Barreiro et al., 2011). Targets of methyltransferases include histones, nucleic acids, and small molecules. These play roles in both genetic and protein regulation but are most well-studied for their genetic activation and silencing activity (Goll & Bestor, 2005; Struck et al., 2012). Some specific methyltransferases specifically target the N-terminus of a protein and can do this multiple times to varying degrees of effects. For example, one methyl group addition can result in slightly decreased pKa due to the slight

change in polarity, but three can permanently create a positive charge and overturn N-terminal nucleophilicity (Varland et al., 2015).

The majority of methyltransferases act through SAM and rely on it for their methyl source, while SAM primarily garners methyl groups from serine (Davis et al., 2004; Schubert et al., 2003). One of the most well-studied group of methyltransferases are those that modulate DNA methylation and therefore transcription, known as DNA methyltransferases. These were discussed in section 1.3.1. Another type of methyltransferase which also regulates DNA transcription and gene activation are histone methyltransferases (HMTs). They often target the histone tails but can also be added to subunits and mediate their effect by compacting or relaxing chromatin conformation, rendering certain lengths of DNA less accessible or more accessible to transcription machinery (Tiedeken & Chang, 2015).

1.4.3 One-carbon nutrients in oocytes and preimplantation (PI) embryos

It is known that one-carbon metabolism plays vital roles in reproductive consequences. *In vitro* culture of embryos has been shown to result in imprinting loss, perhaps in part due to an imperfect balance of one-carbon nutrients. Oocytes and PI embryos alike will take up components of the one-carbon cycle. Many studies have shown that dysregulated one-carbon nutrients during oocyte growth or PI embryo development negatively affect outcome (Xu & Sinclair, 2015).

Mouse oocytes take up methionine, as do one-cell, two-cell, and morula stage embryos. A portion of this is converted to SAM. When methionine metabolism is inhibited, there is suppressed blastocyst development, indicating that this is important though not vital. Some will still grow to blastocysts despite the absence of methionine. *In vitro* embryos also experience

improved blastocyst expansion in a dose-dependent fashion with the addition of methionine to culture (Bonilla et al., 2010).

Homocysteine is another metabolite that, when dysregulated, has negative consequences on health as well as culture of oocyte and preimplantation embryo. An elevated level of homocysteine is known as hyperhomocysteinemia, where its mechanism for conversion to methionine is overwhelmed (Castro et al., 2006). In the methionine cycle, homocysteine is recycled back to methionine by methionine synthase (MTR). This reaction relies on the conversion of 5-methyl THF to THF in the folate cycle, which occurs in tandem with methionine synthesis. Among other factors, hyperhomocysteinemia can be caused by a gene variation in MTHFR, the rate-limiting enzyme that generates 5-methyl THF (Ikeda et al., 2012). With reduced MTHFR function, individuals have a higher incidence of B vitamin deficiency (Zittan et al., 2007). The condition aggravates cardiovascular risk among increasing other risk factors. Elevated homocysteine is associated with reduced recovery of oocytes for IVF, as well as the embryo quality and pregnancy outcome. With higher levels of homocysteine present in follicular fluid, ovarian follicle development appears to be limited, and lesser embryo quality has also been observed (Boxmeer et al., 2008; Ebisch et al., 2006). There is also correlation between increased homocysteine and some pathologies related to subfertility, including polycystic ovarian syndrome (PCOS) and endometriosis (Ebisch et al., 2006; Schachter et al., 2003). When homocysteine was added to embryo culture, it was found that mouse blastocyst development was suppressed, which was hypothesized to be due to oxidative stress (Menezo et al., 1989). Homocysteine auto-oxidizes, resulting in the production of ROS (Welch & Loscalzo, 1998).

As previously mentioned in section 1.4.1, folate is vital to oocyte and embryo health. In fact, taking folate supplements is conventionally recommended to pregnant women due to

evidence indicating its importance in fetal development. Folates can be transported by FOLR1, FOLR2, and reduced-folate carrier 1 (RFC1). From the 2-cell stage of pre-implantation embryo development until the blastocyst stage, folate is taken up by FOLR1. Transport was likewise observed in COCs through RFC1, though this did not appear to be for oocyte use. While cumulus cells took up folate, it did not appear to be then shuttled into the oocyte itself (Kooistra et al., 2013). Recently, Meredith et al. has shown that during murine oocyte growth, there is a brief peak of folate transport isolated to oocytes nearing but not at full size, correlating to approximately P15 during the first wave of oocyte growth and the corresponding point in oocyte growth in adult females (Meredith et al., 2016).

When folate metabolism was inhibited using the antifolate, methotrexate, in PI embryo culture, progression of development was arrested. (Kwong et al., 2010; O'Neill, 1998). It is worthy of note that with folate metabolism intact, early PI embryos cultured *in vitro* are able to support development even in the absence of folate present in the media, suggesting that folate accumulated during oocyte growth may form a sufficient pool for the early stages of embryo division (O'Neill, 1998). It was demonstrated in the same studies that the effect of methotrexate could be somewhat reversed by the addition of thymidine and hypoxanthine, which are used in DNA and RNA synthesis and are synthesized from folate, so that development to the blastocyst stage was restored. In the presence of thymidine and hypoxanthine, culturing from the 8-cell stage forward with folate metabolism inhibited by methotrexate however still resulted in the a reduced number of both inner cell mass (ICM) and trophectoderm cells in the blastocyst. This effect is exacerbated by inhibition of a parallel pathway for one-carbon generation, the betaine pathway (Zhang et al., 2015). Like the folate cycle, betaine is also a methyl donor that can contribute to the formation of SAM in the oocyte. Betaine has been found to be present in all

stages of PI embryo development, and the enzyme for transferring its methyl group into the SAM synthesis pathway, BHMT, is active in blastocysts (Lee et al., 2012). While inhibiting folate metabolism decreased the numbers of both ICM and trophectoderm cells, inhibiting BHMT only reduced ICM. Inhibiting both simultaneously had much more severe effects (Zhang et al., 2015). These could be rescued by providing downstream contributors to SAM formation such as methionine or hypoxanthine. This, in addition to decreased SAM levels upon inhibiting both pathways, indicates the importance of both folate and betaine in the regulation of one-carbon nutrients in healthy PI embryo development (Zhang et al., 2015).

Disruptions in epigenetic marks were observed as well, which can lead to a variety of lasting effects. For example, a methyl-deficient diet, defined by restriction of folate, vitamin B, and methionine, resulted in long-term health differences that may be attributed to epigenetic modification. Offspring from methyl-deficient mothers were more obese, with elevated blood pressure as well as insulin resistance (Sinclair et al., 2007). Similar results were observed in rats (Maloney et al, 2011). Methyl deficiency also negatively affected antral follicle development and oocyte maturation (Anckaert et al., 2010). In addition, some imprinted genes were observed to have reduced methylation. Other pathologies correlated with dysregulation of methylation include congenital heart disease, cognitive impairment conditions like dementia, and non-alcoholic fatty liver disease (Almeida et al., 2008; Corbin & Zeisel, 2012; Verkleij-Hagoort et al., 2006).

In humans, taking folic acid supplement resulted in elevated DNA methylation. In addition, among couples seeking IVF, those with diets rich in one-carbon metabolites such as folate and vitamin B12 from shellfish, fruit and other sources saw higher chances of pregnancy (Steegers-Theunissen et al., 2013).

During oocyte growth, there is also evidence that one-carbon metabolites are accumulated to support early PI embryo development (Kwong et al., 2010; O'Neill, 1998). This presents evidence for the importance of one-carbon nutrients in oocyte growth and embryo development.

1.5 Serine

Serine is a small, uncharged amino acid that is vitally important to the mammalian biological system. In culture, serine is considered conditionally essential as it has been shown to significantly improve cell proliferation and cell health (Eagle, 1959). It is also a precursor to many other molecules and amino acids as well as participating in metabolism and proliferation, and taking on various other important roles. This small amino acid has a one-carbon sidechain that can supply other processes with methyl groups.

1.5.1 Biological roles of serine

Serine plays a number of roles in the mammalian system, a main one being its vital part in cell proliferation. This is in part due to its function as a building block in protein synthesis and as a methyl group donor for DNA synthesis. From serine comes the synthesis of purines as well as dTMP (deoxythymidine monophosphate), which make up three of the four nucleotides that are used to build DNA (Snell et al., 1987). As DNA replication is highly active during cell proliferation, serine is essential for the process.

Not only is serine a precursor to other amino acids, it can also be incorporated into phospholipid macromolecules. These macromolecules are composed of a backbone and long chain fatty acids. The backbone for sphingolipids and sphingosine is composed of serine and

palmitoyl-CoA. Not only are these lipids important components of the cell membrane, they also contribute to apoptosis, differentiation, and also cell proliferation (de Koning et al., 2003). One such lipid is ceramide, a macromolecule that makes up a major lipid of the lipid bilayer and is synthesised from serine via sphingosine and a fatty acid. It also functions as a second messenger in regulation of apoptosis (Kolesnick, 2002).

Serine can also play a role in metabolism, specifically in gluconeogenesis, the process through which glucose can be generated to provide energy for cell function. However, its contribution is redundant and lesser than that of alanine and glutamine, which are the main contributors (Felig, 1975; Rowsell et al., 1969). There are two pathways through which serine can contribute (Figure 5); one is SPT/AGT mediated formation of hydroxypyruvate, which is then converted into pyruvate, or the direct formation of pyruvate mediated by serine dehydratase (Fell & Snell, 1988; Sallach, 1956).

Finally, it is a precursor for a number of amino acids. One example is cysteine, an amino acid required for processes such as metal ion binding and antioxidation as a component of GSH. Cysteine is generated through the trans-sulphuration pathway through the intermediate cystathionine, which is a complex of homocysteine and serine. Downstream of this, cysteine can be converted into taurine, another important amino acid that contributes to brain function as well as skeletal muscle function (de Koning et al., 2003).

Glycine can be generated from serine as well. The transfer of a methyl group from serine to THF results in glycine, and both this methyltransferase reaction as well as the generation of glycine play important roles. For example, glycine, like cysteine, is a component of GSH and is important in providing protection against ROS (Wüllner et al., 1999). It also functions as a

neurotransmitter in the central nervous system, both with inhibitory effects and as an excitatory co-agonist of the NMDA receptor (Johnson & Ascher, 1987). Yet another role for glycine is as an organic osmolyte for preimplantation embryos to regulate cell volume (Baltz & Zhou, 2012; Steeves et al., 2003).

Another notable event that spurs from the conversion of serine to glycine is the transfer of the methyl group that occurs as a result. This generates 5,10-methylenetetrahydrofolate (5,10-methylene THF), which leads into the folate cycle for one-carbon metabolism, previously discussed in section 1.4.1. The majority of methyl transfer events are from the folate cycle, where SAM is generated. Hence this serine to glycine conversion that contributes to the process makes serine the main source of carbon for methylation events (Ikeda et al., 2012).

1.5.2 Sources of serine and serine biosynthesis

Serine can be obtained one of four ways: through protein and phospholipid degradation, from dietary intake, from glycine/serine cycling, or through *de novo* synthesis. The proportions at which the different sources for serine are used vary from tissue to tissue. For example, in the fetal liver, the majority of serine is sourced from glycine conversion; however, in the kidney, most is from synthesis of the glycolytic intermediate 3-phosphoglycerate (3PG) (de Koning et al., 2003).

Mainly, for synthesis of serine, its precursors are sourced from the glycolytic or gluconeogenetic pathway, with pyruvate being the main source of 3PG (Kalhan et al., 2011). Figure 6 shows that from 3PG, dehydrogenation is carried out through phosphoglycerate dehydrogenase (PHGDH) with oxidation of NAD+ to form phosphohydroxy pyruvate. Formation of phosphoserine is then catalysed by phophoserine aminotransferase 1 (PSAT1).

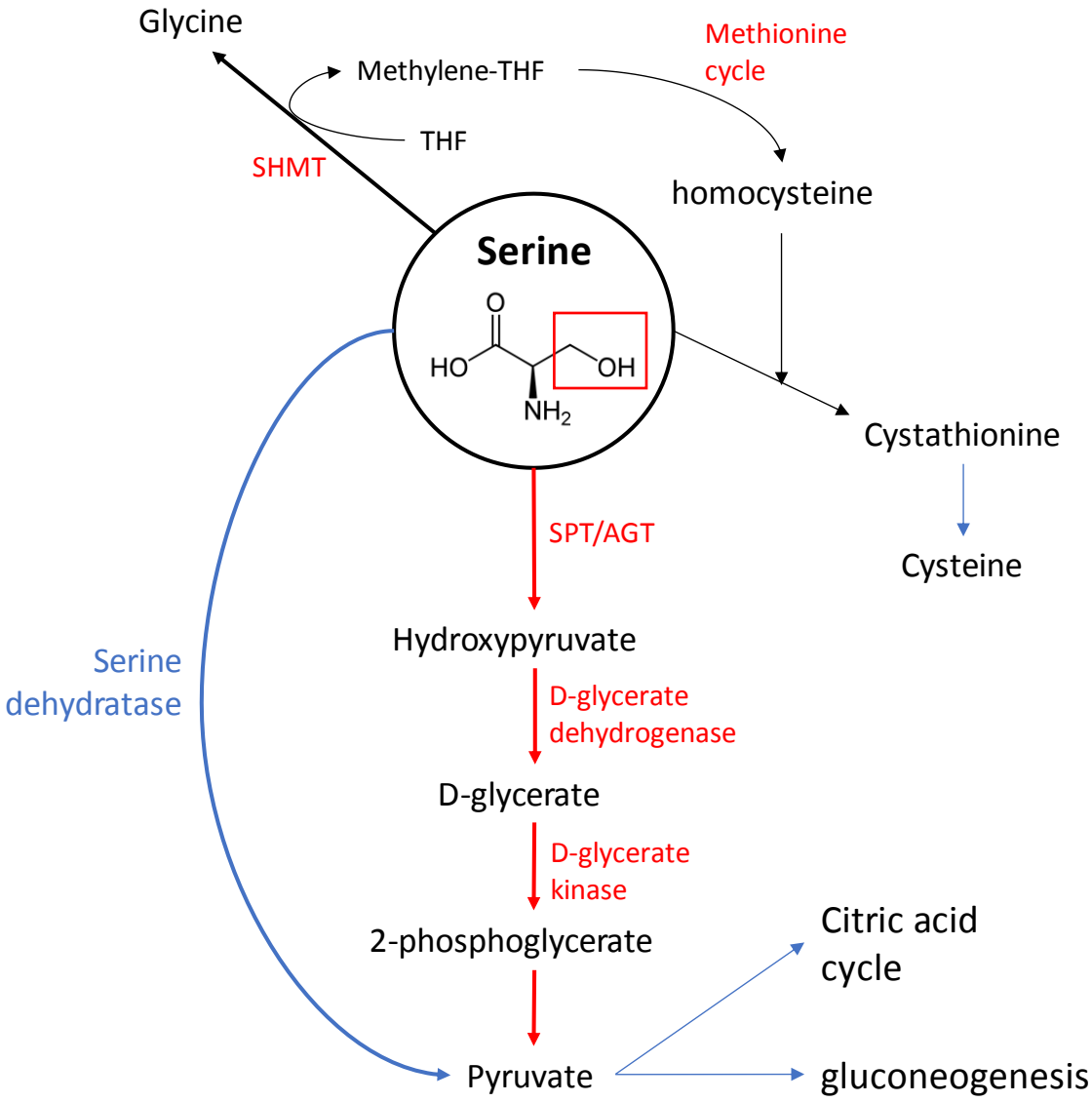

Figure 5. Metabolism of serine through the SPT/AGT (serine:pyruvate/alanine:glyoxyate aminotransferase) pathway (shown by red arrows) as well as direct conversion to pyruvate (shown by blue arrow). Serine conversion to other amino acids is also shown (black arrows). The one-carbon group of serine is marked by the red box. This is the methyl group that contributes to the methionine cycle.

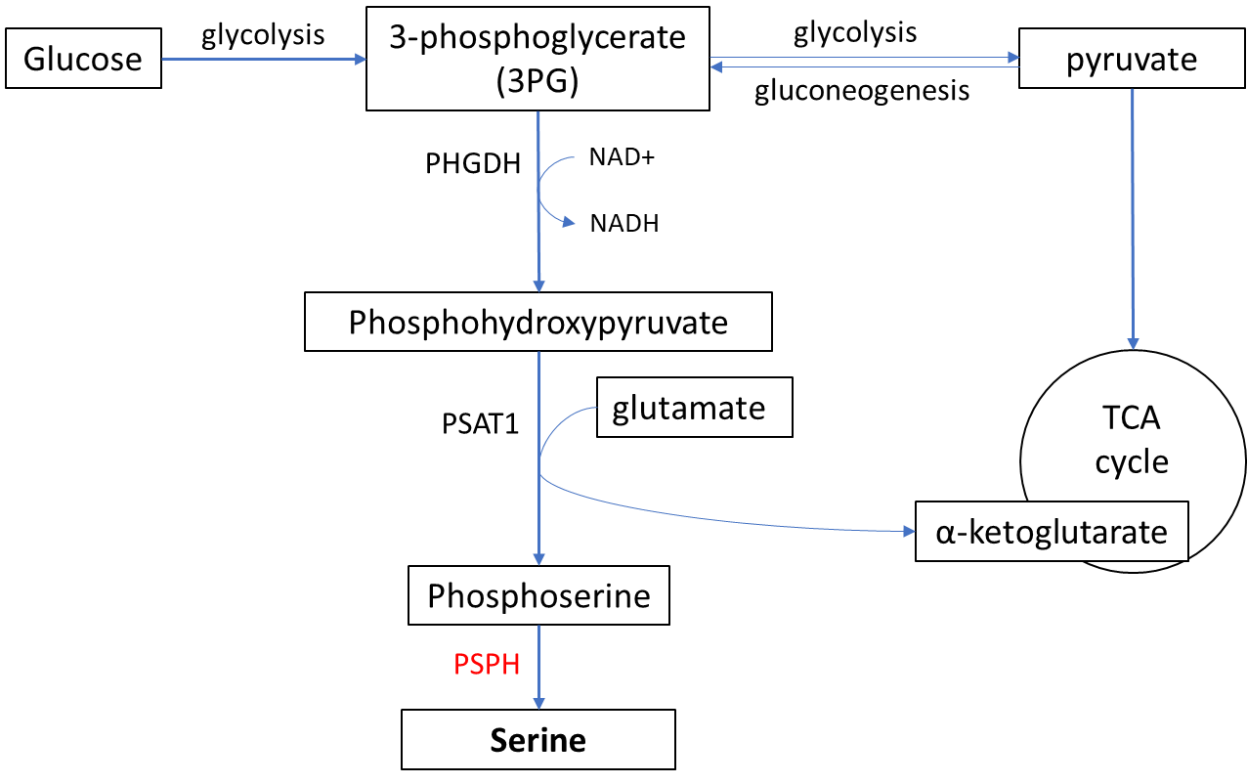

Figure 6. Biosynthesis of serine, including some sources of serine precursors. Glucose to 3PG is incomplete glycolysis, as 3PG is an intermediate product before pyruvate formation. In red is the rate-limiting enzyme. PHGDH = phosphoglycerate dehydrogenase. PSAT1 = phosphoserine aminotransferase. PSPH = phosphoserine phosphatase. 3PG for serine can be sourced from glucose via glycolysis but more frequently is obtained from pyruvate as an intermediate of gluconeogenesis.

PSAT1 during this reaction also converts L-glutamate to a-ketoglutarate, an intermediate of the citric acid cycle that can then proceed to source more pyruvate. These enzymes can be regulated by dietary changes and hormonal factors such as corticosteroids. Factors involved in metabolism such as glucagon play a regulatory role as well (Kalhan & Hanson, 2012). Phosphoserine phosphatase (PSPH) then hydrolyses phosphoserine to serine, this being the rate-limiting and irreversible final step. Being controlled primarily at the final steps, the synthesis of serine can be regulated by demand (Fell & Snell, 1988).

Synthesis of serine appears to be localized only to certain tissues, as these enzymes have highest detected activity in the kidney, testis, spleen, and brain (Snell, 1984). Other locations can also rely on cellular transport as a number of transporters are able to transport serine, which will be discussed in section 1.7.

1.6 Transport mechanisms and systems

Transport systems have previously been studied in some detail in preimplantation embryos as well as in oocytes. Understanding the mechanisms of how oocytes can obtain substrates can benefit our understanding of their regulatory processes for growth in preparation for embryo development.

1.6.1 Types of transporters

There are several types of transport, generally categorized into active or passive transport. Passive transport can be simple diffusion or facilitated, where a transporter is involved but no energy expenditure is required. Rather, the movement of substrate occurs down a concentration gradient. Active transport, on the other hand, is always carried out by a transporter through either

direct or indirect transport. Similar to facilitated transport, indirect transport relies on an electrochemical gradient. However, in this case, one substrate's movement down the gradient is coupled to the simultaneous transport of another substrate against its gradient. This can occur in the same direction (symport), or in opposite directions (antiport). Direct transport relies on energy in the form of ATP and can either couple ATP pump activity to the transport of a single substrate (uniport), or two in opposite directions (cotransport).

Transporters are estimated to make up approximately 5% of the human genome, and are located on plasma membranes, mitochondrial membranes, and vesicles. All molecules and compounds used in a biological organism require transporters, including neurotransmitters, pharmacological agents, and amino acids. Even water requires the presence of aquaporins, or water channels, to diffuse through membranes. Other transporter types consist of ion channels, ion pumps, ATP-binding cassette transporters (ABCs), coupled transporters, passive transporters, and exchangers (Hediger et al., 2013). The ABC family is powered by ATP hydrolysis and is one of the largest families of transporters that transports a broad variety of compounds. Both pumps and ABCs are ATP-dependent, thus they are also referred to as ATPases. Ion pumps transport ions across membranes and can be used to induce membrane potentials or create osmotic balance. Ion channels, on the other hand, allow for movement of ions down an established electrochemical gradient (Dunbar & Caplan, 2000).

1.6.2 Amino acid transporters

Among the different types of compounds that are transported, amino acids are of particular interest for this thesis. Traditionally, transporters are named based on their characteristics and function. An example is the naming of ASC and asc, named for their ability to transport alanine, serine, and cysteine. Furthermore, the uppercase of ASC indicates the

transporter's sodium-dependence, whereas lowercase is intended to communicate a sodium-independent mechanism. The same applies to systems $B^{0,+}$ and $b^{0,+}$, which are named partially for "blastocyst", the location where the transporter was first identified, as well as its ability to transport cationic and neutral amino acids (Van Winkle et al., 2006).

While previously these transport systems were classified based on function, newer methods of nomenclature focus more on phylogeny due to modern capabilities in gene sequencing. The solute carrier (SLC) families use this method of categorizing, by creating families of transporters that often have similar functions, but more importantly require at least 20% of the amino acid sequence to be shared among members. The SLC transporters make up nearly half of all known transporter genes in humans and are categorized into 52 families. There are further subdivisions into subfamilies, and the gene names include all this information in a common format. Each gene is headed by "SLC", followed by its family, subfamily, and finally its individual number (Hediger et al., 2013).

With more now known about the transport systems previously identified based on function, they are able to be classified based on the SLC system as well. For example, the classically named System A, which was reported as a MeAIB-sensitive transporter with variants, in fact makes up three members of the SLC38 family of transporters (Christensen, 1989; Mackenzie & Erickson, 2004). The classically named transporter systems and their corresponding SLC genes are summarized in Table 1. Four SLC families are described in more detail in a later section as candidate transporters of serine. These families are SLC1, SLC6, SLC7, and SLC38.

Table 1. Amino acid transporters (http://slc.bioparadigms.org/ and Hediger et al. (2013))

SLC genes	Protein	System	Substrates	Dependency
Slc1a1	EAAT3	X_{AG}^-	E, D	Na^+
Slc1a2	EAAT2	X_{AG}^-	E, D	Na^+
Slc1a3	EAAT1	X_{AG}^-	E, D	Na^+
Slc1a4	ASCT1	ASC	A, S, C, T	Na^+
Slc1a5	ASCT2	ASC	A, S, C, T, Q, N	Na^+
Slc1a6	EAAT4	X_{AG}^-	E, D	Na^+
Slc1a7	EAAT5	X_{AG}^-	E, D	Na^+
Slc6a6	TAUT	β	taurine	Na^+, Cl^-
Slc6a9	GLYT1	GLY	G	Na^+, Cl^-
Slc6a14	ATB0+	$B^{0,+}$	Neutral and cationic amino acids	Na^+, Cl^-
Slc6a15	B^0AT2	B^0	Large, neutral amino acids	Na^+
Slc6a18	B^0AT3	B^0	Neutral amino acids	Na^+
Slc6a19	B^0AT1	B^0	Neutral amino acids	Na^+
Slc7a5	LAT1	L	Large neutral amino acids	None
Slc7a8	LAT2	L	Small and large neutral amino acids	None
Slc7a9	b0,+AT	$b^{0,+}$	Cationic, large neutral amino acids	rBAT (*Slc3a1*)
Slc7a10	Asc-1	asc	Small neutral amino acids	4F2hc (*Slc3a2*)
Slc7a11	xCT	xc^-	Cystine, E	None
Slc7a12	Asc-2	asc	Small neutral amino acids	rBAT (*Slc3a1*) /4F2hc (*Slc3a2*)
Slc38a1	SNAT1	A	A, S, C, Q, N, H	Na^+
Slc38a2	SNAT2	A	A, S, C, Q, N, H, G, M, P	Na^+
Slc38a3	SNAT3	N	Q, H, A, N	Na^+
Slc38a4	SNAT4	A	A, S, C, N, G, T	Na^+
Slc38a5	SNAT5	N	Q, N, H, S	Na^+
Slc38a7	SNAT7	A/N	A, S, H, N, Q	Na^+

1.7 Transporters of serine

As previously described, amino acids play important roles in growth and maturation of oocytes and a number of their transporters have been characterized. For example, MII eggs express system β, L, GLY, xc^-, and $b^{0,+}$. In growing oocytes, there was activity attributed to systems $b^{0,+}$, system L, and systems asc or ASC that continued into meiotic maturation. Some activated during meiotic maturation, namely GLY and β (Pelland et al., 2009).

Transporter capacity and affinity for its substrates can be assessed by understanding the transport kinetics. The comparison to enzymatic activity has been made by many researchers in the field of amino acid transport, and the Michaelis-Menten equation used to describe enzyme catalytic activity has been used as an approximation of saturable transport kinetics as well. The equation is as follows:

$$v = \frac{V_{max} * [s]}{(K_m + [s])}$$

where v refers to the velocity of transport, V_{max} is the maximum rate reached by the transporter, and [s] is the concentration of available substrate. The K_m in this case is the Michaelis constant, which is determined by finding the substrate concentration at which the system is at half of maximal velocity. The relationship between rate of transport with increasing concentration can also provide information on whether the system is saturable, and on occasion whether multiple components may be involved (Christensen, 1989).

Noting what is currently known information regarding transporter systems recognized in oocytes and substrate profiles of a range of transporters, I have explored systems that transport serine in more detail below, as we are interested in understanding how the oocyte obtains serine due to its various potential roles in oocyte health.

1.7.1 SLC1 family: Systems X^-_{AG} and ASC

The SLC1 family is a family of high affinity glutamate transporters that consists of seven members, which have then been categorized into subgroups according to their characteristics.

Slc1a1 through *Slc1a3* and *Slc1a6* and *Slc1a7* are all categorized as system X^-_{AG} transporters, also known as excitatory amino acid transporters (EAATs). These mainly transport L-glutamate and both D- and L- aspartate (Kanai et al., 2013). However, they have not been found to be present in oocytes and they also do not transport serine, thus they are not considered for the context of this thesis (Pelland et al., 2009).

Slc1a4 and *Slc1a5* form the remainder of the SLC1 family transporters, and are known as ASC, or alanine, serine, and cysteine transporters (ASCTs). These two are neutral amino acid transporters that prefer alanine, serine, and cysteine as substrates, hence the name. While they are both sodium-dependent and potassium-insensitive antiporters sharing affinity for those same three substrates, they differ still in function as well as tissue localization.

ASCT1 (*Slc1a4)*, rather than mediating net amino acid uptake, seems to function more as a neutral amino acid exchanger (Zerangue & Kavanaugh, 1996). Aside from its three namesake substrates, it also recognizes threonine and asparagine. ASCT2 (*Slc1a5)*, on the other hand, regulates amino acid pools and has a broader range of substrates, including all those of ASCT1 and glutamine, leucine, and methionine.

ASCT2 is specifically localized, mainly in lung, skeletal muscle, large intestine, kidney, testis, adipose, and possibly oocyte; in contrast, ASCT1 is near ubiquitous in its expression (Kanai et al., 2013; Pelland et al., 2009).

1.7.2 SLC6 family: $B^{0,+}$ and B^0AT transporters

The SLC6 family is one of the largest, with upwards of 20 members that can be categorized into four subgroups and an orphan transporter. Some of these groups, including the GABA transporters, L-proline transporter, and monoamine transporters fall outside of the scope of this project. None falling within those groups transport serine. Other subgroups, namely osmolyte transporters and glycine transporters, contribute to oocyte health but also do not transport serine, therefore they will not be discussed in this section. However, the neutral and cationic amino acid transporter subgroup has several candidates to consider, as it consists of neutral amino acid transporters with serine as a substrate (Pramod et al., 2013).

B^0AT1 (*Slc6a19*) is a sodium-dependent transporter associated with Hartnup disorder. With a broad range of substrates, it prefers large aliphatic neutral amino acids such as leucine, isoleucine, valine and methionine, but also accepts serine, proline, glycine and in fact most other amino acids. This transporter has been found to be expressed mostly in kidney and intestine, and according to RNA seq analysis by Veselovska et al., it is not expressed in oocytes (Böhmer et al., 2005; Veselovska et al., 2015).

B^0AT2 (*Slc6a15*) is a transporter highly similar to B^0AT1 in both substrate affinity and mechanism. Both these transporters mediate electrogenic transport of substrate at a 1:1 stoichiometry with Na+, although the preference of B^0AT2 is for proline in addition to the large aliphatic neutral amino acids that B^0AT1 prefers, and also does not transport MeAIB. Localized to expression in brain, lung, and kidney, it also appears to have expression in pre-implantation embryos as well as oocytes (Bröer et al., 2005; Veselovska et al., 2015).

Yet another member of the B^0AT group, B^0AT3 (*Slc6a18*) differs from the previous B^0AT transporters. This transporter is a Na^+ and Cl^--dependent transporter of neutral amino acids.

Rather than the larger amino acids, it most efficiently transports alanine, glycine, serine, and cysteine. It's mainly expressed in the kidney and does not appear to be expressed in oocytes (Singer et al., 2009; Veselovska et al., 2015).

$B^{0,+}$ (*Slc6a14*) is another member of the SLC6 family and is broader in spectrum than the other transporters. It transports neutral amino acids as well as cationic amino acids such as lysine. Serine is one of its substrates, and it is both Na^+ and Cl^- dependent. Previously, it has been found to be present in mouse blastocysts, as well as in the intestine, pituitary, and lung (van Winkle 2001; Pramod et al. 2013). However, Pelland et al. has concluded the unlikelihood of $B^{0,+}$ being present in oocytes due to the lack of BCH inhibited transport, since BCH is a classical characterizing substrate for this system (Pelland et al., 2009).

1.7.3 SLC7 family: System L and y+L, system asc

The SLC7 family of transporters can be categorized into two subgroups. The first four members are cationic amino acid transporters and therefore do not recognize serine. As such they will not be discussed in this thesis. Members 5-11 are referred to as the glycoprotein-associated amino acid transporters and are the light-chains of heteromeric transporters, requiring an accessory protein to permit its function. Catalysis of transport activity is mediated by the transport system-specific light chain, whereas the shared accessory proteins are the heavy chain portion that traffics these light chains to the plasma membrane (Fotiadis et al., 2013).

LATs

The first member, LAT1 (*Slc7a5*), was identified in 1998 and transports only large neutral amino acids, thus it has no affinity for serine. LAT2 (*Slc7a8*) on the other hand transports

neutral amino acids large and small. It transports serine and functions in a sodium-independent manner. This transporter is found in many tissues, such as small intestine, kidney, brain, ovary, testis, skeletal muscle, and importantly, PI embryos from the 1-cell stage up to blastocyst as well as oocytes during both growth and meiotic maturation (Verrey et al. 2004; van Winkle 2001; Pelland et al., 2009).

y+LATs

These transporters mainly transport cationic amino acids such as lysine and large neutral amino acids, therefore they do not need to be discussed.

$b^{0,+}$

$b^{0,+}$ (*Slc7a9*) is similar in substrate profile to $B^{0,+}$ with its affinity for cationic and large neutral amino acids. It has low affinity for serine but nonetheless has sensitivity to it, but transports arginine, leucine, and cystine. It functions as a Na+-independent transporter and requires the heavy chain accessory rBAT (*Slc3a1*) (Fotiadis et al., 2013). Previously, the transporter has been found in high quantities in the blastocyst stage of mouse embryos and has been determined to likely be active in oocytes as well (Pelland et al., 2009).

asc

The asc transporters, as the name suggests, have affinity for alanine, serine, and cysteine. In fact, they specifically transport small neutral amino acids, unlike the LAT transporters previously described despite having high structural similarity to LAT2. Like the $b^{0,+}$ transporter, they function independently of Na+ and require an accessory protein, which for the asc

transporters is 4F2hc. Asc-1 (*Slc7a10*) and asc-2 (*Slc7a12)* have slightly different substrate recognition. For example, asc-2 is more stereoselective and also does not recognize the high affinity asc-1 substrate α-aminobutryic acid (Chairoungdua et al., 2001). Pelland et al. indicated that either ASC or asc was likely present in oocytes, as the two have similar transport profiles, with strong affinity for serine, alanine, and cysteine (Pelland et al., 2009). Veselovska's more recent RNA seq analysis, however, showed no asc transcripts (Veselovska et al., 2015).

1.7.4 SLC38 family: System N/A (SNATs)

This family of SLC38 encoded transporters consists of system A and N transporters in addition to some not fully characterized orphan transporters.

System A

These have a preference for small neutral amino acids, including serine, and have classically been identified by their ability to transport MeAIB. Transporters classified as System A thus far include SNATs 1 (*Slc38a1*), 2 (*Slc38a2*), and 4 (*Slc38a4*). They function in a Na+ dependent manner and are simple 1:1 stoichiometric transporters.

SNAT1 and 2 are similar in substrate affinity, with both preferring glutamine. They also transport alanine, serine, asparagine, cysteine, and histidine, though SNAT2 also has some affinity for proline. In fact, these transporters will recognize all zwitterionic aliphatic amino acids. Where SNAT1 is localized mainly to the brain, retina, placenta, and heart, SNAT2 is expressed ubiquitously. SNAT4, while still classified as system A, does not have as strong an affinity for glutamine, and also appears to transport cationic amino acids arginine and lysine

independently of Na^+. Unlike the other members of System A, SNAT4 is mostly localized to liver and has also been found in skeletal muscle of rats (Bröer, 2014).

In oocytes, no evidence of system A activity was detected nor is there evidence of this system's presence in preimplantation embryos (Pelland et al., 2009).

System N

Another group within the SLC38 family is the system N transporters, consisting of SNAT3 and SNAT5, also referred to as SN1 and SN2. When compared to system A, this system overall has a narrower profile of substrate recognition. Both transporters function through co-transport with Na^+ and also rely on proton antiport. The transporters are strongly affected by pH, and there is speculation that their roles are not limited to transport of amino acids but also contribute to regulation of pH (Bröer, 2014).

SNAT3 and SNAT5 both transport glutamine, asparagine, and histidine. Where SNAT3 only transports the above and does not recognize many of System A's substrates, serine included, SNAT5 prefers serine as a substrate in addition to the classic System N substrates. SNAT5 also transports glycine and alanine (Chaudhry et al., 1999).

SNAT3 mRNA transcripts have been found in brain, liver, kidney, and adipose, while SNAT5 has alternative splicing of mRNA into three different forms, the most prevalent of which is a 1.4kb transcript concentrated mainly in the stomach. Other forms, at 1.9kb and 2.2 kb, have been located in liver and kidney as well (Nakanishi et al., 2001).

Orphan transporters

The remainder of the SLC38 family of transporters have yet to be characterized in detail. *Slc38a6* has received little attention therefore its substrate preference is unknown, and *Slc38a8-11* have not been found to transport serine and so are irrelevant to the context of this thesis (Hägglund et al., 2015; Hellsten et al., 2017). However, *Slc38a7,* which codes for a transporter named SNAT7 in accordance with the previous members of the family, has been profiled in some detail by Hagglund et al., where its transport substrate affinity was explored. They expressed the gene in *Xenopus laevis* oocytes and tested a wide range of amino acid substrates which showed transport of glutamine that can be inhibited by serine and a number of other amino acids. From Hagglund et al.'s study, it appears that the transporter is a Na^+-dependent transporter with affinity for serine, alanine, asparagine, histidine, aspartic acid, and glutamic acid in addition to glutamine (Hägglund et al., 2011).

A later study by Verdon et al. contradicted these results, having been unable to replicate the same wide range of substrates. However, in their study SNAT7 was expressed in lysosomes rather than the plasma membrane (Verdon et al., 2017).

1.8 Summary and significance

Perturbances in the balance of one-carbon nutrients carry impact on the success and even future health of the baby in IVF. Given an association between children from IVF and imprinting disorders, it is suspected that disturbances in DNA methylation could be a cause of negative outcomes (Odom & Segars, 2010). It has been shown that establishment of a methyl pool contributed to by both betaine and folate is vitally important to embryo development (Zhang et al. 2015). But how do oocytes obtain the components to form this pool? Betaine has been shown to

be accumulated in the early pre-implantation embryo, while in oocytes it is synthesized by choline dehydrogenase (CHDH), thus providing methyl groups through the betaine/BHMT pathway (Anas et al., 2008; McClatchie et al., 2017). Early PI embryos also are able to transport folate, as are oocytes during growth (Kooistra et al., 2013; Meredith et al., 2016). Unlike betaine which is itself a methyl donor, folate needs to acquire a methyl group from serine. Therefore, knowing that oocytes transport folate, how is the upstream methyl donor serine obtained? This inspired the main question addressed in this thesis: **how are oocytes able to obtain serine to support the role of folate in establishment of a methyl pool**? This will expand the knowledge on healthy oocyte physiology in the mouse model and will ideally inform further investigation for parallel human physiology regarding one-carbon nutrients and their impact on fertility. The extent of these effects still needs to be further investigated, and knowledge stemming from this work applied to the improvement of assisted reproductive technology.

2. Objective and Specific Aims

2.1 Objective

The objective of this project was to determine how oocytes obtain serine and when during growth and development this occurs. Due to the importance of serine to one-carbon metabolism and other physiological processes in cells, this research is significant in that it furthers our knowledge of the mechanisms of healthy oocyte development.

2.2 Specific aims

Specific aim 1: To determine whether serine uptake occurs in oocytes during growth and throughout meiotic progression.

Previously, our lab had found evidence of folate transport into oocytes during growth in a unique pattern (Meredith et al., 2016). It has been hypothesized that the folate may be used for the establishment of a methyl pool that can then be used for the critical process of DNA methylation following the erasure of methyl markers in primordial germ cells. However, as the methyl donor to the folate cycle, transport of serine has yet to be studied.

Therefore, I hypothesized that serine is transported into oocytes in a pattern comparable to folate transport observed in oocytes.

Specific aim 2: To identify the mechanism through which oocytes obtain serine during growth and meiotic progression.

Serine is likely to play some vital roles in oocyte growth and capacity for fertilization, thus the mechanism through which oocytes obtain serine is important to identify. Serine can be obtained through biosynthesis or through transport. Pelland et al. had profiled transport systems

likely to be present in oocytes. Of these, some are able to transport serine, namely $b^{0,+}$, and either asc or ASC (Pelland et al., 2009). However, $b^{0,+}$ does not have strong affinity for serine.

From this information, I hypothesized that serine is actively transported into oocytes either by asc or ASC.

Specific aim 3: To determine the effects of meiotic progression and natriuretic peptide C (NPPC) on the transport of serine.

Once the mechanism of serine transport is known, its regulation then becomes important to understand. Progression of meiotic maturation is a key process that is tightly regulated through several pathways, and the NPPC/NPR2 pathway plays a vital role in this regulation. Nutrient transport in oocytes can be altered by affecting meiotic progression, thus a link between serine transport and meiotic progression may exist.

I hypothesized that the transport of serine is linked to NPPC/NPR2 signaling events associated with meiotic progression.

3. Materials and Methods

Table 2. List of Chemicals

Chemical	Source	Catalogue number
4-(2-hydroxyethyl)-1-piperazineethanesulfonic acid (HEPES)	Sigma (St. Louis, MO, USA)	H6147
[^{3}H] serine: ~1mCi/ml	Perkins-Elmer	NET248001mc
α-(methylamino) isobutyric acid (MeAIB)	Sigma (St. Louis, MO, USA)	M2383
β-mercaptoethanol	Sigma (St. Louis, MO, USA)	M-3148
Acetic acid, glacial	Fisher Scientific (Pittsburg, PA, USA)	A38-4
Agarose	Sigma (St. Louis, MO, USA)	A6877
Alanine, L-	Sigma (St. Louis, MO, USA)	A3534
Calcium chloride ($CaCl_2$)	Sigma (St. Louis, MO, USA)	C7902
Choline bicarbonate salt	Sigma (St. Louis, MO, USA)	C7519
Choline chloride	Sigma (St. Louis, MO, USA)	C7017
Cysteine hydrochloride monohydrate, L-	Sigma (St. Louis, MO, USA)	C6852
Dibutyryl cyclic AMP sodium salt (dbcAMP)	Sigma (St. Louis, MO, USA)	D0627
EDTA, disodium salt dihydrate	Sigma (St. Louis, MO, USA)	E5134
EDTA tetrasodium salt	Sigma (St. Louis, MO, USA)	E6511

Estradiol	Sigma (St. Louis, MO, USA)	E1024
Ethanol, 95%	Chaptec	
Ethidium bromide (EtBr)	Sigma (St. Louis, MO, USA)	E7637
Glucose, D-(+)	Sigma (St. Louis, MO, USA)	G6152
Glycine	Sigma (St. Louis, MO, USA)	G7403
Histidine, L-	Sigma (St. Louis, MO, USA)	H6034
Hyaluronidase, type I-S	Sigma (St. Louis, MO, USA)	H3506
K Penicillin G	Sigma (St. Louis, MO, USA)	P7794
Lactic acid, 85% w/w	Sigma (St. Louis, MO, USA)	L1250
Leucine, L-	Sigma (St. Louis, MO, USA)	L1512
Lysine monohydrochloride, L-	Sigma (St. Louis, MO, USA)	L1262
Magnesium sulfate heptahydrate ($MgSO_4$)	Sigma (St. Louis, MO, USA)	M2773
Mineral oil	Sigma (St. Louis, MO, USA)	M8410 (embryo tested) or M5904
Scintillation fluid	Scintiverse BD, Fisher Scientific (Pittsburg, PA, USA)	SX18-4
Serine, L-	Sigma (St. Louis, MO, USA)	S4311
Sodium bicarbonate ($NaHCO_3$)	Sigma (St. Louis, MO, USA)	S5761
Sodium chloride (NaCl)	Sigma (St. Louis, MO, USA)	S5886
Sodium lactate	Sigma (St. Louis, MO, USA)	L7900
Sodium pyruvate	Sigma (St. Louis, MO, USA)	P4562

Streptomycin sulfate	Sigma (St. Louis, MO, USA)	S1277
Potassium chloride (KCL)	Sigma (St. Louis, MO, USA)	P5405
Potassium phosphate monobasic powder (KH_2PO_4)	Sigma (St. Louis, MO, USA)	P5655
Polyvinyl alcohol (PVA)	Sigma (St. Louis, MO, USA)	P8136
Proline, L-	Sigma (St. Louis, MO, USA)	P5607
Pyruvic salt	Santa Cruz biotechnology	SC-296162
Tris hydroxymethyl aminomethane (Tris base)	Sigma (St. Louis, MO, USA)	252859

Table 3. Summary of Pharmaceutical Agents Used

Pharmaceutical Agent	Source	Catalogue No.
Estradiol (E2)	Sigma (St. Louis, MO, USA)	E1024
Human chorionic gonadotrophin (hCG)	Merck supplied by Intervet	Chorulon
Pregnant mare serum gonadotrophin (PMSG)	Merck supplied by Intervet or ProspecBio	Folligon or HOR-272a
Natriuretic peptide type-C (NPPC)	Sigma (St. Louis, MO, USA)	N8768

3.1 Chemicals and Solutions

L-serine (referred to simply as serine in this thesis) and other L-amino acids were obtained from sources listed in Table 2. Chemicals and compounds used for media and mineral oil all are either cell culture grade or embryo tested grade.

3.2 Animals and oocyte manipulations

3.2.1 Animals

CF1 and CD1 mice were obtained from Charles River Canada (St-Constant, QC, Canada). For experiments involving fully-grown oocytes, mice aged 5-8 weeks old were used. For growing oocytes, neonates were ordered as litters with the mother and allowed to acclimatize for minimum one week prior to use in experiments.

Animals were cared for in the University of Ottawa Animal Care and Veterinary Services facility and maintained on a 12h light-dark cycle. All adult animals had unrestricted access to Teklad Global 18% protein rodent diet 2018 (Envigo, Indianapolis, IN) and water.

Experimental mice were sacrificed by cervical dislocation.

All protocols for animal handling were approved by the University of Ottawa Animal Care Committee with the Faculty of Medicine, and all experiments comply with approved protocols.

3.2.2 Superovulation

To ensure sufficient oocytes for experimental use, adult CF1 and CD1 female mice were superovulated. Pharmaceutical agents used are listed in Table 3. Mice were injected intraperitoneally (i.p.) with 5 IU PMSG for the collection of GV oocytes 44-46h post-PMSG. To

collect MI oocytes or MII eggs, the PMSG injection was followed by injection with 5 IU hCG 47 hours following PMSG (PrespecBio, HOR-272a or Folligon, Merck supplied by Intervet) injection.

PMSG biologically imitates the effects of FSH in stimulating follicular growth, while hCG functions as LH to trigger ovulation.

3.2.3 Media

Handling and collection of oocytes was carried out in KFHM, composed of NaCl (95 mM), KCl (2.5 mM), KH_2PO_4 (0.35 mM), $MgSO_4$.7H2O (0.2 mM), Na lactate (10 mM), glucose (0.2 mM), sodium pyruvate (0.2 mM), $NaHCO_3$ (29 mM), $CaCl_2$.2H2O (1.7 mM), tetra-sodium EDTA (0.01 mM), HEPES (21mM), K penicillin G (0.16 mM), and Streptomycin SO_4 (0.03 mM) as per Lawitts and Biggers (1993). The medium was pH adjusted to 7.4 and used at an osmolarity of 240 ± 5 mM.

Oocyte culture was carried out in commercial MEMα media (Fisher Scientific, cat no. 12561-056). Otherwise, 250 mM KSOM with PVA (1mg/mL) was used, composed of the same components as listed above for KFHM but without HEPES and with 25 mM $NaHCO_3$ instead. For amino acid transport test purposes, glutamine was also excluded from KSOM media. KSOM was used at an osmolarity of 250 ± 5 mOsM.

To make modified sodium-free KSOM, all ingredients containing sodium were replaced with a sodium-free alternative. Sodium chloride was replaced with choline chloride, sodium pyruvate with potassium pyruvate, sodium lactate with 85% w/w lactic acid, and finally sodium bicarbonate was replaced with 80% choline bicarbonate. All lab-made media were filter sterilized prior to use.

3.2.4 Oocyte manipulation and culture

To collect oocytes, ovaries were excised approximately 44 hours post-PMSG injection into KFHM and minced to release COCs. COCs were then denuded by pipetting repeatedly through a narrow-bore pipette and washed through 3 drops of KFHM before proceeding with experiments.

To isolate MI oocytes, hyaluronidase enzyme was required to digest the hyaluronic acid that has begun to cause mucification of cumulus cells, rendering the COC sticky and preventing oocytes from being mechanically denuded. The enzyme was prepared at 300μg/mL in KFHM collection media. Four hours following hCG injection, the ovaries were excised and minced in hyaluronidase, which took no longer than ten minutes. MI oocytes were then collected into regular KFHM and isolated from cumulus cells by repeated pipetting. Denuded MI oocytes were then washed through 3 drops of KFHM.

MII eggs were collected 16 hours post-hCG injection. Oviducts were excised from mice and sheared with tweezers in hyaluronidase (300μg/mL in KFHM). The eggs were allowed to sit for 2-3 minutes for cumulus cells to release and were then collected and washed through 3 drops of KFHM.

Drops of culture media (50μL) were placed in 35mm culture dishes (BD falcon, VWR International (Arlington Heights, IL, USA), and mineral oil (Sigma) was used to submerge the drops. Media drops were pre-incubated at 37°C and 5% CO_2 for a minimum of 2 hours, and oocytes were washed through three drops of pre-equilibrated culture media prior to culture.

3.2.5 Maintaining meiotic arrest

To maintain meiotic arrest, dbcAMP or NPPC with estradiol (E2) was used.

300μM dbcAMP in 1mL MEMα was preincubated for at least one hour prior to use in an organ dish at 37°C and 5% CO_2. The outer ring of the organ dish was filled with MilliQ water to prevent changes in media composition due to evaporation. Denuded GV oocytes can then be transferred following collection into the prepared organ dishes.

For NPPC-mediated arrest, an organ dish with 1mL MEMα with 100nM NPPC and 100nM E2 surrounded with an outer ring of MilliQ water was incubated at 37°C with 5% CO_2 for an hour or more. Cumulus cells must be retained for NPPC and E2 to maintain meiotic arrest, therefore oocytes were collected and transferred as COCs into prepared organ dishes with NPPC.

3.3 [^{3}H] Serine transport measurements

To measure transport of serine, groups of 10-15 oocytes were washed through 3 pre-equilibrated drops of KSOM before transferring to a drop of either 1μM [^{3}H] serine in KSOM or 1μM [^{3}H] serine supplemented with 5mM non-radiolabelled (cold) serine that had been equilibrated for at least 2 hours at 37°C with 5% CO_2 before being used. Cold serine was prepared as 0.1M stocks, frozen in aliquots at -20°C. A new aliquot was used each day to make uptake drops.

KSOM drops with 1μM [^{3}H] serine yielded the total uptake, while the addition of excess unlabelled serine would isolate non-saturable transport to then be subtracted from the total to determine saturable transporter-dependent uptake. The drop containing oocytes was then incubated under the same conditions with radiolabelled serine to allow amino acid transport to occur. This process is shown in figure 7. Following the incubation period, transport was arrested by transferring the oocytes to ice-cold KFHM and washing them through six large drops of KFHM.

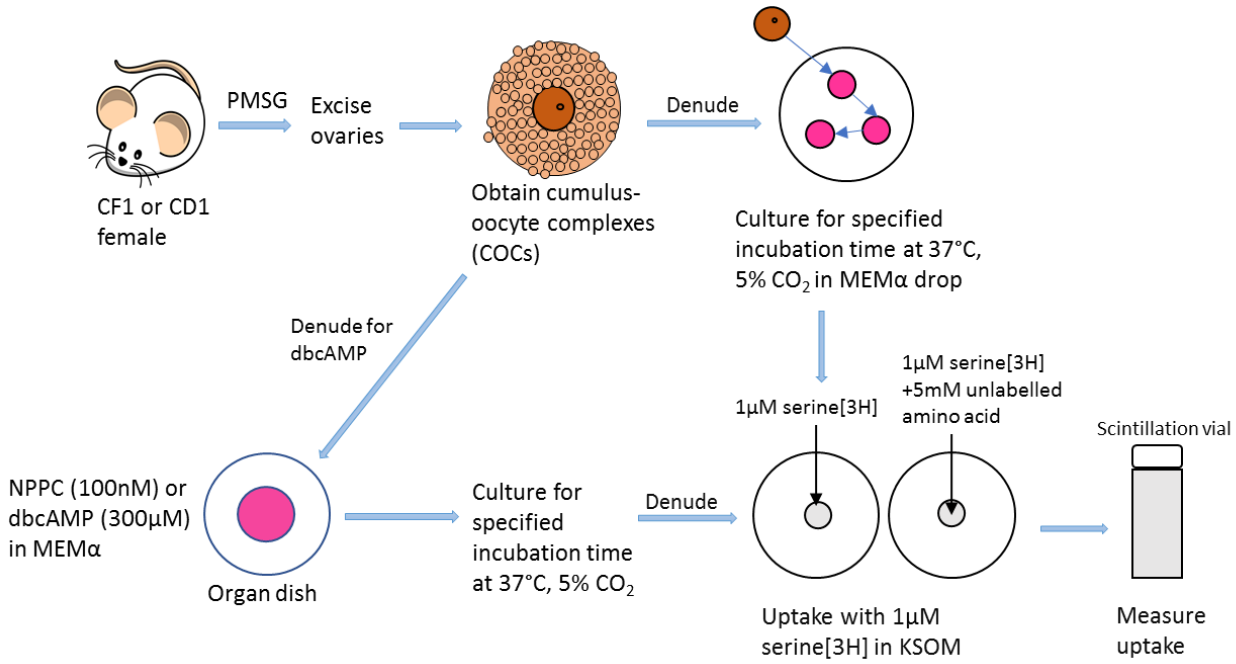

Figure 7. Workflow diagram of radiolabelled [^{3}H]serine uptake. Alterations in steps are specified for each experiment, such as age of mice used, incubation time, and length of transport time.

The oocytes were then transferred to a scintillation vial (VWR International, Arlington Heights, IL. USA, Cat no. 66022-398) and topped up with 4 mL of scintillation fluid. The activity of the samples were measured on a 2200CA TriCarb liquid scintillation counter (Packard Instrument Co., Downer's Grove, IL) in counts per minute (CPM), and each sample was counted for 5 min.

A standard curve obtained through serial dilution of [^{3}H] serine in water was used to determine molar amounts of serine per oocyte. This standard curve consisted of starting concentrations of 1:5000 and 1:7500, radiolabelled compound to water. This was prepared with 1μL of radiolabeled compound into 5 mL and 7.5mL water respectively. Two-fold dilutions were then carried out five times for each starting concentration, resulting in 12 concentrations for a standard curve. A background sample of just water was included every time as well. 5μL of each dilution and 4mL of scintillation fluid were loaded into scintillation vials and counted. These standards were prepared once a week.

3.3.1 Competition assay

Amino acids for the competition assay were prepared as 0.1M stocks and stored at -20°C for up to four weeks. Oocytes were obtained as previously described and were incubated at 37°C for 4 hours in MEMα. They were then washed through 3 drops of pre-equilibrated KSOM before being placed into an uptake drop of 1μM [^{3}H] serine for the control, or 1μM [^{3}H] serine with 5mM competitive substrate. The oocytes remained in the uptake drop for 10 or 30 minutes and were then put through the liquid scintillation counter for quantification.

Possible competitive substrates that were tested are listed in Table 4 below.

Table 4. Competitive substrates for serine transporter

Transporter system	Protein(s)	Sodium dependence	Competitor
System A	SLC38A1, SLC28A2, SLC38A4	Dependent	MeAIB
System L	SLC7A8	Independent	Leucine, alanine, cysteine
Glyt1	SLC6A9	Dependent	Glycine
$B^{0,+}$	SLC6A14	Dependent	Lysine, leucine, alanine, cysteine, histidine, glycine
$b^{0,+}$	SLC7A9/SLC3A1 heterodimer	Independent	Lysine, leucine, cysteine
ASC	SLC1A4, SLC1A5	Dependent	Leucine, alanine, cysteine
asc	SLC7A10/SLC3A2 heterodimer	Independent	Alanine, cysteine
B^0AT2	SLC6A14	Dependent	Proline, alanine, cysteine, leucine
SNAT7	SLC38A7	Dependent	Histidine, alanine, cysteine, leucine

3.3.2 Kinetics measurements

Preparation of [^{3}H] serine concentrations required evaporation and resuspension of radiolabelled serine to obtain sufficiently high concentrations. Measurements ranged from 1μM to 1000μM. Each concentration of serine was achieved using a combination of cold serine and [^{3}H] serine to be diluted in a 25μL uptake drop. Having determined sodium-dependence of the transporter, serine uptake in sodium-free media was measured to quantify activity not from the transporter of interest.

The [^{3}H] serine component was placed into a 0.6mL polypropylene microfuge tube (Fisherbrand, cat no. 05-407-24C) and allowed to evaporate at room temperature overnight. Cold serine stocks were made in either regular KSOM or sodium-free KSOM. A 1/100 dilution and a 1/1000 dilution of cold serine were made. [^{3}H] serine was then resuspended in a mixture of KSOM and cold serine in KSOM totalling 25μL by leaving the filled tubes on the bench for three hours, caps closed.

Following resuspension, the 25μL drops were plated into 35mm culture dishes and covered with mineral oil. Drops were incubated at 37°C, 5% CO_2 for a minimum of two hours before use for uptake. Counts were adjusted based on the dilution factor of serine[3H] in the total concentration of serine.

3.4 Molecular techniques

3.4.1 Polymerase chain reaction (PCR)

RNA extraction

RNA extraction was accomplished using the QIAGEN RNeasy Micro kit (Qiagen, Cat#74004). Kidney was used as the control tissue. Freshly obtained kidney (<5mg) was

homogenized in buffer RLT from the QIAGEN kit with β-mercaptoethanol (10µL for every 1 mL of buffer RLT). Groups of 60 oocytes were collected in 1.5mL Eppendorf tubes, and immediately frozen at -80°C until all biological repeats were collected. Collected oocytes were removed from the freezer and frozen-thawed 4-5 times using liquid nitrogen and a warm water bath. 20ng of carrier RNA (5µL of 4ng/µL stock) was also added to each tube of oocytes prior to extraction process. 400 µL Buffer RLT with β-mercaptoethanol was again added to each sample and vortexed thoroughly. The rest of the extraction was carried out according to the manufacturer's instructions. Oocyte RNA was double eluted by adding 22µL of RNase-free water per sample, centrifuging, and reloading the elution to centrifuge again to ensure maximal recovery of RNA.

Reverse transcription

The extracted RNA was converted to cDNA using either the RETROscript kit with random decamers (Ambion, Cat # AM1710) or the Superscript IV first strand cDNA synthesis system with random hexamers (Ambion cat# 18091050). 2µL of kidney RNA was used for each RT reaction, while the maximum of 12 or 11µL for the two kits respectively was used for oocyte RNA. All steps were carried out on ice and according to the manufacturer's instructions.

Primer design

In preparation for determining gene expression, primers were designed for a reference gene and the two genes of interest, *Slc38a7* (SNAT7) and *Slc1a5* (ASCT2). *Chdh* (CHDH) was chosen as the reference gene as it has previously been shown to be expressed in oocytes at the stage of interest. Primers for *Chdh* were 5'-CTC ATC CGG ACA TCC AGT TC-3' for forward,

and 5’-CCT CGA CAT CGG TTT CTG TT-3’ for reverse, creating a 201 bp amplicon (McClatchie et al., 2017).

The new primers were designed to span an exon-exon junction to minimize the chance of picking up genomic DNA contamination. As well, they were designed to have <60% GC content. The primer sequences for *Slc38a7* (SNAT7) were 3’-TACCTTCGGAACCTGCATCG-5’ for forward and 3’-GCTCAGGAAGCTGGCATATT-5’ for reverse that produces a 211bp amplicon. *Slc1a5* (ASCT2) primers were forward and reverse 3’-CATGGTCCAGCTTCTCTGTGA-5’ and 3’-AAGAGGTCCCGAAAGCAGTG-5’ respectively for a 401bp amplicon. These newly designed primers were estimated by the manufacturer to have melting temperatures of 61°C and 61°C for *Slc1a5* forward and reverse, and for *Slc38a7*, 57°C and 55°C. To find a common temperature to produce product, primers were tested using kidney cDNA over a temperature gradient ranging from 55°C to 62°C (Figure 19).

In order to confirm the specificity of the primers, products were sent for sequencing by the Ottawa Hospital Research Institute StemCore facilities. Sequenced products were matched using BLAST provided by the National Centre for Biotechnology Information (NCBI).

PCR

For conventional PCR, a 10mM dNTP mix was first prepared with equal parts dTTP, dCTP, dATP and dGTPs diluted 4:6 in ddH_2O. Primer stocks were prepared at 50µM in Nuclease-free water (Ambion LifeTechnologies, cat no. AM9939) and were diluted to 10µM for use in PCR. A master mix was prepared with nuclease-free water, primers, and the components of the Taq DNA recombinant kit, Taq polymerase, 10X MgCl2 buffer, and 50mM MgCl2 (Fisher, Cat # 10342053). Each reaction consisted of 13.9µL water, 2µL 10X buffer, 0.5mM

$MgCl_2$, 0.4µL dNTPs, 0.5µL forward primer, 0.5µL reverse primer, 0.2µL Taq polymerase, and 1µL cDNA. More or less cDNA was loaded as needed, maintaining the reaction volume by altering the quantity of water in the reaction. The reactions were run using a Bio-Rad T100 Thermocycler.

Gel electrophoresis

PCR products were imaged by gel electrophoresis. Gels were cast and run with the ThermoScientific Owl EasyCast B2 mini gel electrophoresis system. DNA ladders (ThermoScientific MassRuler, cat no. SM0403) were loaded on either side of samples on a 1.4% agarose gel with ethidium bromide. The Fisher Scientific FB300 power supply was used to run the gel at 105V.

3.4.2 qPCR

qPCR optimization

The range of cDNA that the qPCR instrument and PowerUp SYBR Green Master Mix (Applied Biosystems by Thermo Fisher Scientific, cat no. A25742) can tolerate was determined by testing kidney cDNA from 20ng down to less than 0.001pg. Extracted RNA concentration was determined by nanodrop, and 1:1 conversion from RNA to cDNA was assumed. Starting cDNA amounts of 20ng, 16ng, and 2ng were calculated and prepared based on nanodrop quantification. 20ng was then diluted 1/2 three times, 16ng diluted 1/2 one time, and 2ng diluted 1/2 five times and 1/10 six times to yield a total of 18 different concentrations.

Sterile PCR-grade nuclease-free water was aliquoted into 1mL Eppendorf tubes and frozen at -20°C until needed to minimize risk for contamination.

Standard curve preparation

A standard curve to be used as reference for quantification in qPCR was obtained using kidney cDNA. Four PCR reactions for each primer set was run on a 1.4% agarose gel. The bands were then cut out carefully using a razor blade and pooled in 1.5mL Eppendorf tubes. The PCR product was then extracted using the QIAGEN gel extraction kit as per the manufacturer's instructions, resulting in extracted SNAT7, ASCT2, and CHDH cDNA.

The DNA concentration of each sample was then quantified by spectrophotometry by the NanoDrop 2000 (ND-2000 ThermoFisher Scientific). The gel extraction product was serial diluted to 1pg/μL for the top concentration of the standard curve. The 1pg/μL sample was then serial diluted 1/10 six times to obtain seven concentrations for a standard curve.

Gene expression qRT-PCR

RNA was extracted from groups of 60 oocytes. 11μL of each set were reverse transcribed. A master mix consisting of water, primers, and PowerUp SYBR green master mix was loaded into the 96-well reaction plates. Each well contained 7μL water, 1μL forward primer, 1μL reverse primer, 10μL SYBR mastermix, and 1μL cDNA. Seven standard curve concentrations for each gene were loaded into a 0.1mL MicroAmp Fast 96-well reaction plate (Applied Biosystems by Life Technologies, cat no. 4346907). Prepared standard dilutions were loaded in duplicates, as were oocyte cDNA samples to be quantified. 1.5 oocyte equivalents were loaded per well, also in duplicate. The FAST system 7500 was used for qPCR quantification. The qPCR program followed the SYBR green protocol provided, followed by a melting curve program.

3.5 Statistical analysis

Data were analyzed, and statistical tests completed using GraphPad Prism 8 (GraphPad Software, La Jolla, CA). Quantitative data were presented as the mean ± standard error of the mean (SEM). Means were compared using ANOVA when more than two groups were compared using either Dunnett's post-hoc test, which compares each column with a control, or Tukey's post-hoc test, which compares all pairs of columns. When two groups were compared, Student's t-test was used.

4. Results

4.1 Serine is transported in growing oocytes and during meiotic maturation

Previous literature has suggested there is transport of folate in growing oocytes, with a large peak of transport activity occurring in oocytes from approximately postnatal day 14 (P14) mouse ovaries (Meredith et al., 2016). As such, I tested for serine transport during oocyte growth to determine whether serine was likewise transported in growing oocytes. Growing oocytes were isolated from neonatal mice aged P10 to P21 and were incubated with radiolabelled serine for transport measurements. This determined that serine transport activity began at approximately P15 and persisted into the fully-grown oocyte stage (Figure 8).

I also measured serine transport in GV oocytes, MI and MII eggs. Oocytes at each stage were isolated as previously described and immediately put into [^{3}H] serine-spiked media to measure transport. A non-specific group was included for each set as well, and it was found that GV and MI stage oocytes had detectable saturable uptake, but not MII eggs (Figure 9).

Transport during meiotic maturation was then explored in more detail through use of *in vitro* oocyte culture. For these measurements, oocytes were collected in the GV stage, then denuded and cultured in MEMα for up to 16h before measuring serine transport. As Figure 10 shows, transport increases rapidly and persists until 5h, though by 6h, the activity drops off and remains off, a result that is consistent with the previous *ex vivo* data.

However, a finding which is somewhat incongruous is the low transport observed in GV oocytes from adult females in contrast to the higher transport in fully-grown neonate GV oocytes. In growing oocytes, serine transport increases and does not appear to drop to match activity in GV oocytes from adult mice. In fact, the level observed in P21 oocytes seems to closer resemble that of MI oocytes, where there is the highest transport observed during meiotic maturation.

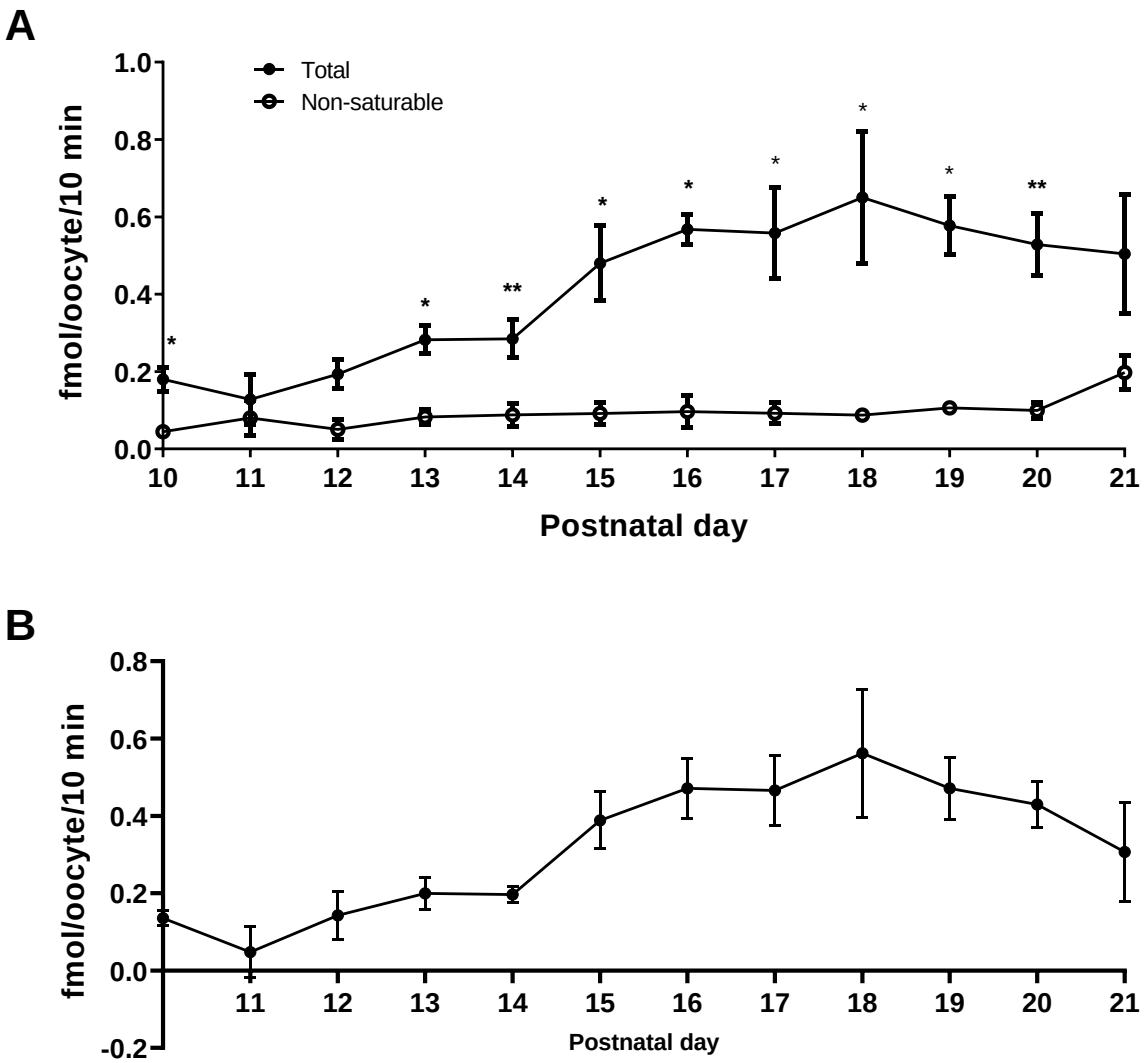

Figure 8. Serine transport measured in growing oocytes collected from mouse neonates. (n=3).

A) Measurement of serine[^{3}H] transport into oocytes, where total was measured with 1µM serine[^{3}H] added to media and non-saturable was measured with 1µM serine[^{3}H] and 5mM unlabelled serine. One-tailed paired t-test was used to assess whether saturable was significantly higher than non-saturable transport, treating each time point as a separate set of measurements. Asterisks (*) mark significance, *: $P \leq 0.05$, **: $P \leq 0.01$, ***: $P \leq 0.001$

B) This shows the saturable transport, which is calculated from subtracting the non-saturable component from total measured transport.

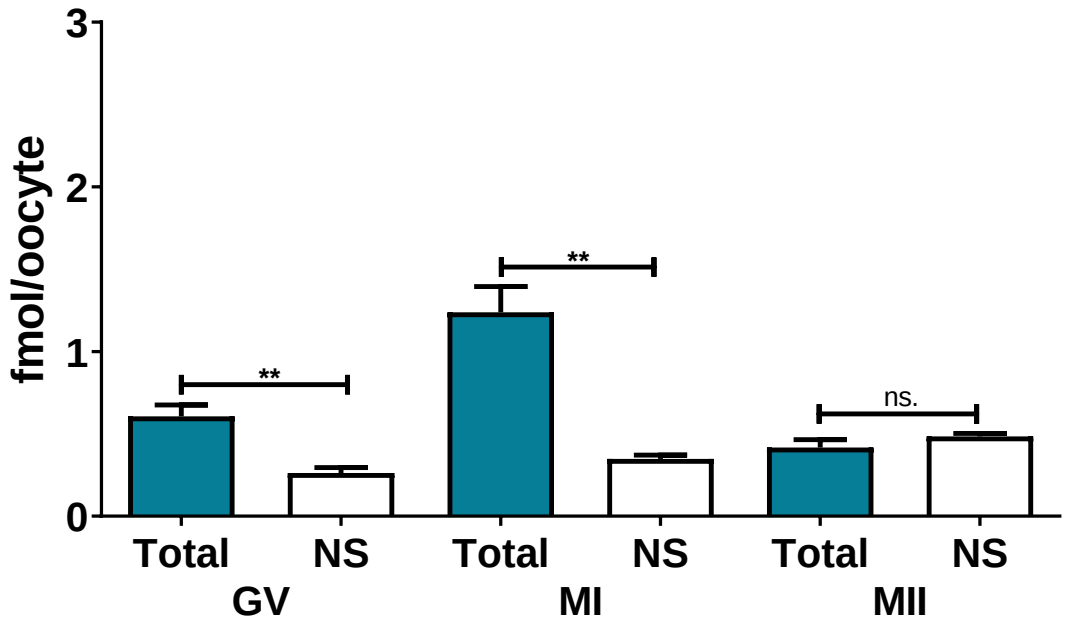

Figure 9. ***Ex vivo*** **transport measurement of serine during meiotic maturation. Oocytes were collected in GV stage, MI stage, and MII stage, then directly placed into uptake media with 1µM serine[3H] and an additional 5mM unlabelled serine for non-saturable (NS) samples (n=5). One-tailed paired t-test was used for significance calculation between total and non-saturable transport. Asterisks (**) mark significant difference, P = 0.0082 for GV, P = 0.0014 for MI. At MII, T and NS were not significant, P = 0.09.**

We considered the possibility that some activation occurred during the transition from GV to MII, and that neonatal GVs were on a higher scale of activity but could likewise be activated. In order to confirm whether this could be the case, fully grown oocytes obtained from P21 mice were cultured *in vitro* for four hours to allow maturation to MI stage oocytes in order to determine whether there would be an increase in activity corresponding to that of adult oocytes.

From this, it became clear that no significant increase in serine transport occurs. Furthermore, the level of transport activity observed in Figure 11 is comparable to that of peak activity during meiotic maturation. The lower activity observed in fresh GV oocytes where serine uptake was measured immediately may be due to physiological differences between the first wave of folliculogenesis and those from cycling adult females. It may also be due to other causes such as stress response to the mechanical denuding process, which may require a small amount of recovery time.

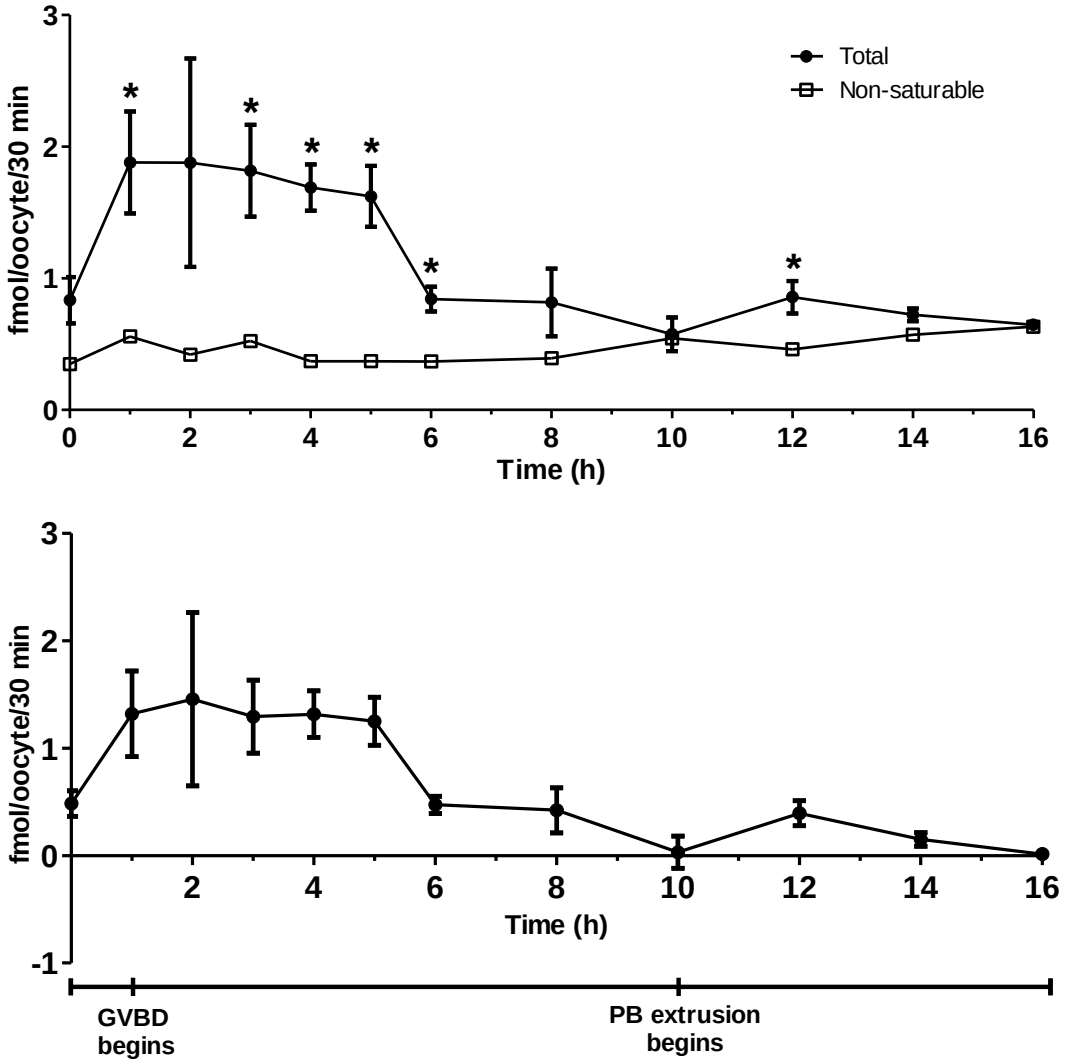

Figure 10. Time course of serine transport in oocytes during meiotic maturation. (n=3). Major morphological events are displayed in the timeline. Times are approximate and vary among mouse strains (Polanski 1997).

A) Measurement of serine[^{3}H] transport into oocytes, where total was measured with 1µM serine[^{3}H] added to media and non-saturable was measured with 1uM serine[^{3}H] and 5mM unlabelled serine. One-tailed t-test was used to assess whether saturable was significantly higher than non-saturable transport. Asterisks (*) mark significant differences between total and nonsaturable, $P < 0.05$.

B) This shows the saturable transport, which is calculated from subtracting the non-saturable component from total measured transport.

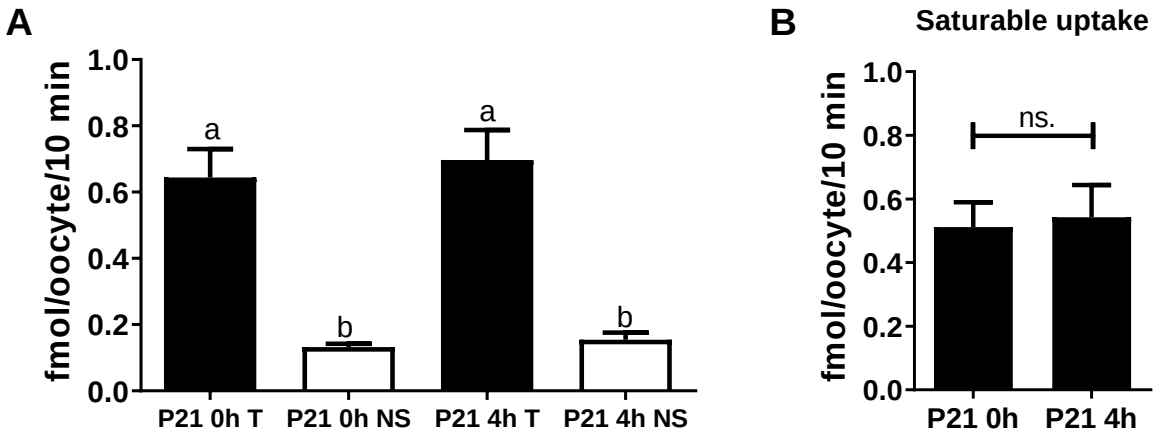

Figure 11. Measuring transport of serine in P21 GV oocytes compared to that in P21 MI oocytes. (n=3). Oocytes were obtained from P21 mouse ovaries and incubated in MEMα for 4 hours to imitate *in vitro* matured GV oocytes from adult ovaries.

A) Black bars (T) show total transport measured using 1μM serine[3H], while white bars (NS) show the non-saturable component measured with 1μM serine[3H] and 5mM unlabelled serine. Statistical significance was calculated using ANOVA with Tukey's post-hoc test, P = 0.0003. Different letters indicate groups are statistically different, where for a vs. b, $P \leq 0.01$.

B) This shows only the saturable component, calculated from the difference of T and NS. Statistical significance was determined by two-tailed t-test, P = 0.82

4.2 SNAT7 is the most likely transporter of serine in oocytes

Having confirmed the presence of active serine transport, I then aimed to identify the transporter responsible for carrying this out. A number of candidate transporters were outlined and summarized in Table 4, and their recognized substrates depicted in Figure 12. Several others were also included despite not being strong candidates, such as GLYT1, which was included in case of non-specific serine transport due to the structural similarity between serine and glycine. As well, system L, which is able to transport serine but has previously been shown to most likely not be present in oocytes during meiotic maturation, was tested. Our initial hypothesis for the most likely transporter was one of the ASC or asc transporters, and thus a first set of competition assays using asc/ASC substrates were completed in GV oocytes matured *in vitro* to MI oocytes.

As Figure 13 shows, excess serine, alanine and cysteine all inhibit the transport of [^{3}H] serine. Lysine, glycine, and MeAIB on the other hand do not, therefore they are not likely substrates of the serine transporter. From this preliminary assay, we are able to confirm that neither system L, for which MeAIB is a substrate, nor glycine transporter GLYT1 are likely to be transporting serine. Another two candidates considered, $B^{0,+}$ and $b^{0,+}$, can also be eliminated due to the transporter's insensitivity to their substrate lysine.

To further narrow down the candidates, the transporter was tested for sodium dependence using sodium-free media. As shown in Figure 14, in the absence of sodium, saturable transport of serine is eliminated. From this we inferred that our transporter of interest is sodium-dependent. This supported our ruling out of $b^{0,+}$,asc, and L, all of which are sodium independent.

Working with the hypothesis of ASC, which is sodium-dependent, being the most likely, we investigated the transporter's ability to transport leucine as a differentiating substrate between

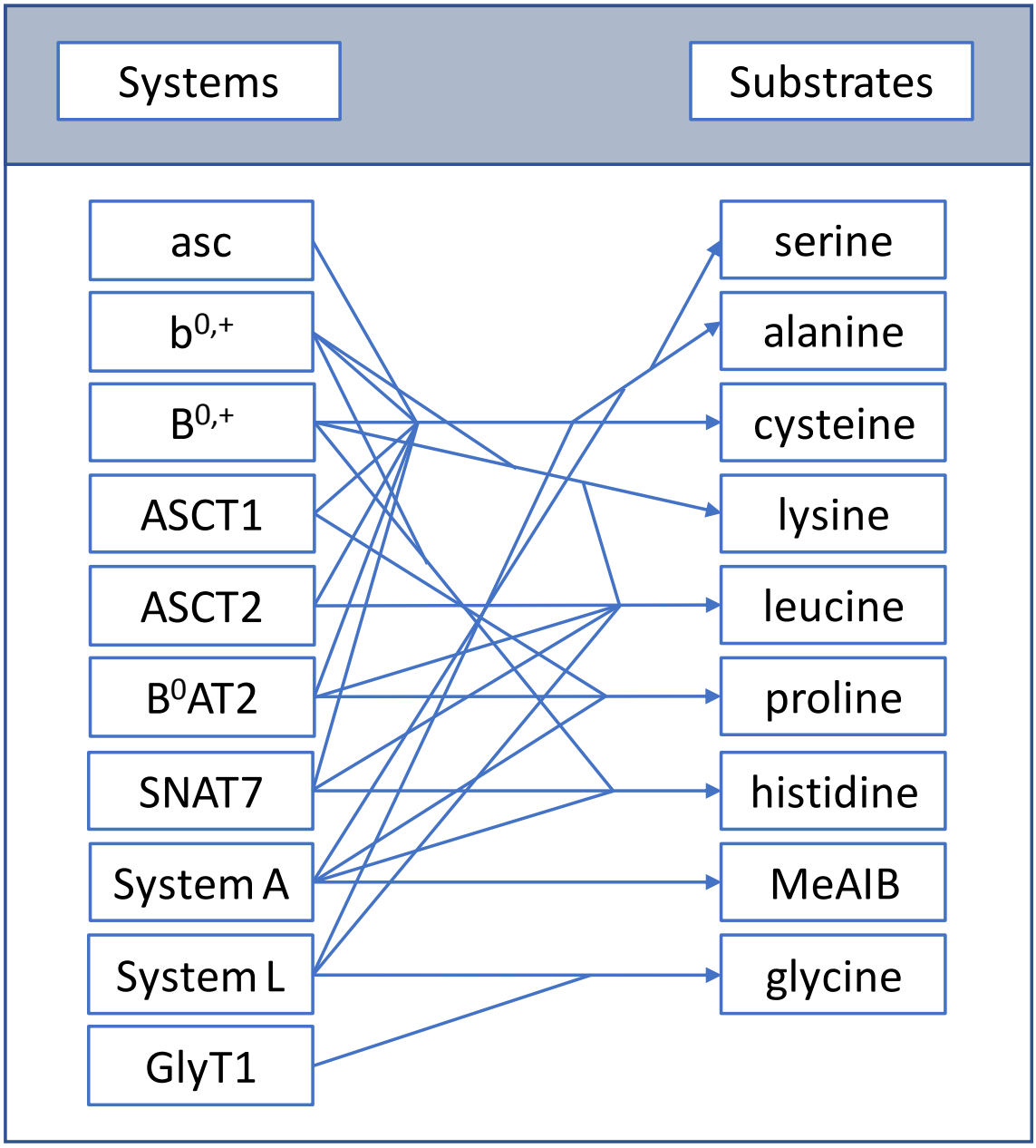

Figure 12. Schematic diagram indicating the candidate transport systems and substrates that are accepted by each transporter. Competitive substrates to narrow down candidates were established using substrate profiles shown here. Substrates recognized by the transporter are indicated with arrows.

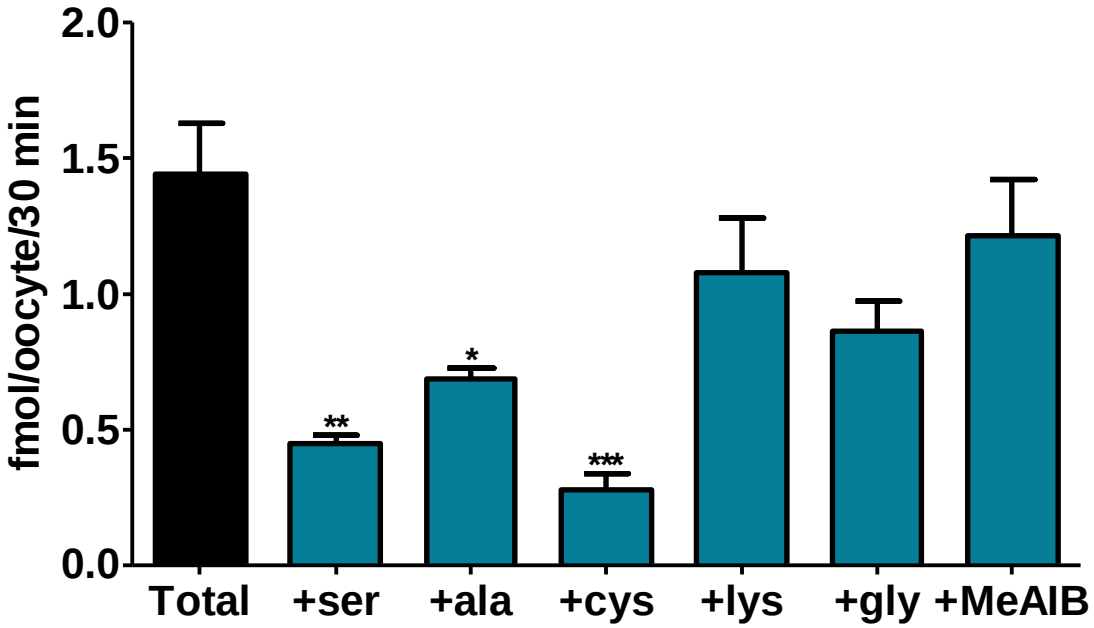

Figure 13. Competition assay to identify serine transporter in fully grown oocytes (n=5). Serine transport was measured in GV oocytes matured *in vitro* for 4 hours before transfer to uptake media. 1µM serine[3H] was used for Total, while 5mM of each competitive substrate was added to determine substrate affinity. Statistical significance obtained from ANOVA with Dunnett's post-hoc test, with 'Total' as control, $P < 0.0001$. Means compared to control, significance marked by asterisk(s), *: $P \leq 0.05$, **: $P \leq 0.01$, ***: $P \leq 0.001$

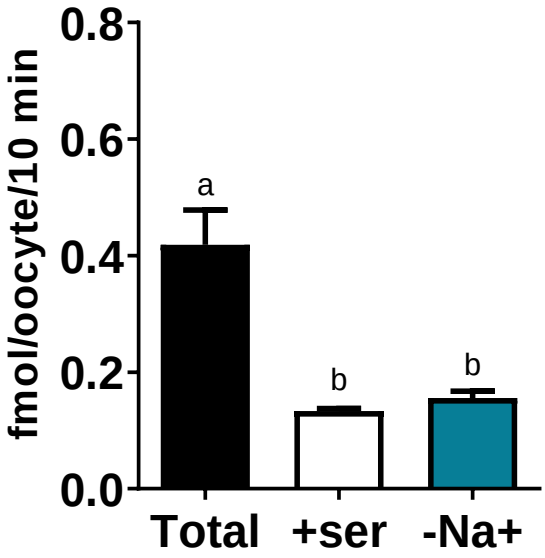

Figure 14. Determining sodium dependency of the transporter. Serine transport measurements with 1µM serine[3H] were taken in either regular KSOM or modified sodium-free KSOM, where all components with sodium were replaced with other alternatives. A "fully-inhibited" control with 5mM unlabelled serine was included. (n=5) Statistically analysed using ANOVA, Tukey's post-hoc test, P = 0.0001. Different letters indicate they are significantly different. Between a and b, P ≤ 0.001

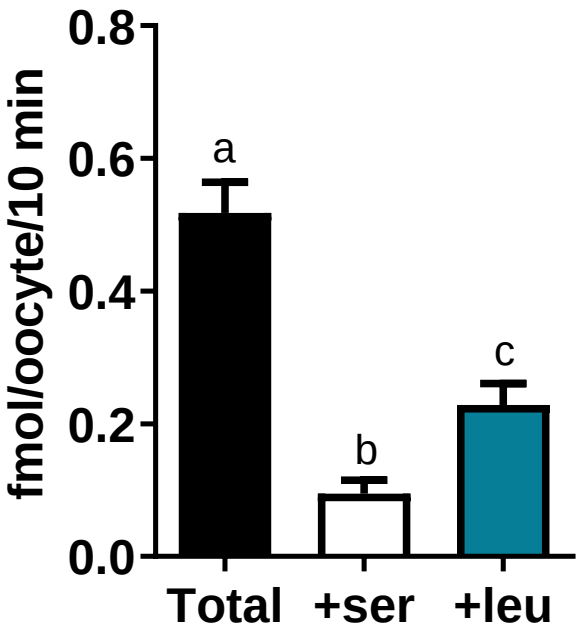

Figure 15. Determining transporter affinity for leucine. Competitive inhibition with 5mM leucine was carried out in 1µM serine[^{3}H]. (n=5) A "fully-inhibited" control with 5mM unlabelled serine was included. (n=5) Different letters indicate they are significantly different, a vs. b: $P < 0.0001$, a vs. c: $P \leq 0.001$, and b vs. c: $P \leq 0.05$. Analyzed with ANOVA, Tukey's post-hoc test $P<0.0001$.

its two isoforms. That the addition of excess leucine inhibited radiolabelled serine transport allowed us to eliminate ASCT1 as a candidate (Figure 15).

Of the transporters for which previous literature has proposed to be active in oocytes, ASCT2 is the only remaining serine transporter. However, we cannot discount other transporters less well-studied that have similar transport profiles but have not been assessed yet in oocytes. Two additional transporters that also share the transport profile outlined thus far are the B^0AT2 transporter and SNAT7.

Proline is a substrate unique to the B^0AT2 transporter among the remaining candidates, therefore it was used to test for affinity, as shown in Figure 16. The transporter was insensitive to the addition of proline. Given the established transport profile so far, SNAT7 and ASCT2 are the most likely transporters. Finally, histidine was used in a final competition assay to differentiate between SNAT7 and ASCT2. Histidine, which is a substrate for SNAT7 but not ASCT2, was able to strongly inhibit the transport of serine into the oocyte, indicating that SNAT7 is likely the transporter active during meiotic maturation in oocytes (Figure 17).

4.3 Fully grown oocytes and growing oocytes likely use the same serine transporter

In growing oocytes, a signature set of competitive substrates were used in a streamlined competitive assay to determine whether the same transporter was active during growth. This signature consists of serine, cysteine, and histidine. Using P17-19 oocytes, it was found that all three competitively inhibited serine transport (Figure 18). This indicates that the same transporter active in fully-grown oocytes is also likely active in growing oocytes.

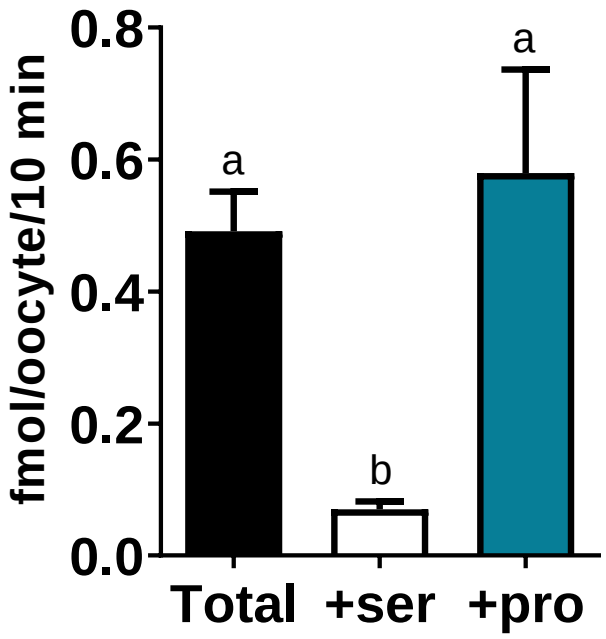

Figure 16. Determining transporter affinity for proline. Competitive inhibition with 5mM proline was carried out in 1µM serine[^{3}H] (n=5). A "fully-inhibited" control with 5mM unlabelled serine was included. Different letters indicate significance, where for a vs. b: P ≤ 0.05. Statistically analysed using ANOVA, Tukey's post-hoc test, a vs b: P < 0.0066.

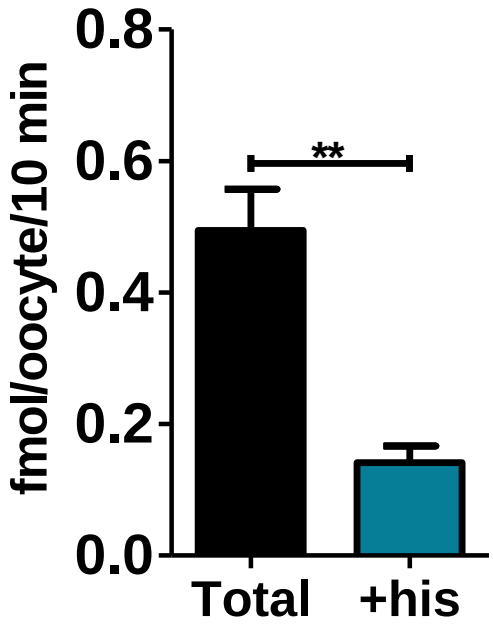

Figure 17. Competitive inhibition with histidine. (n=5) 1µM serine[3H] was used for total transport measurements, and 5mM unlabelled histidine was added to determine substrate specificity for histidine. Asterisks (**) indicate a statistical significance. Data was analysed using a one-tailed paired t-test, P=0.0021.

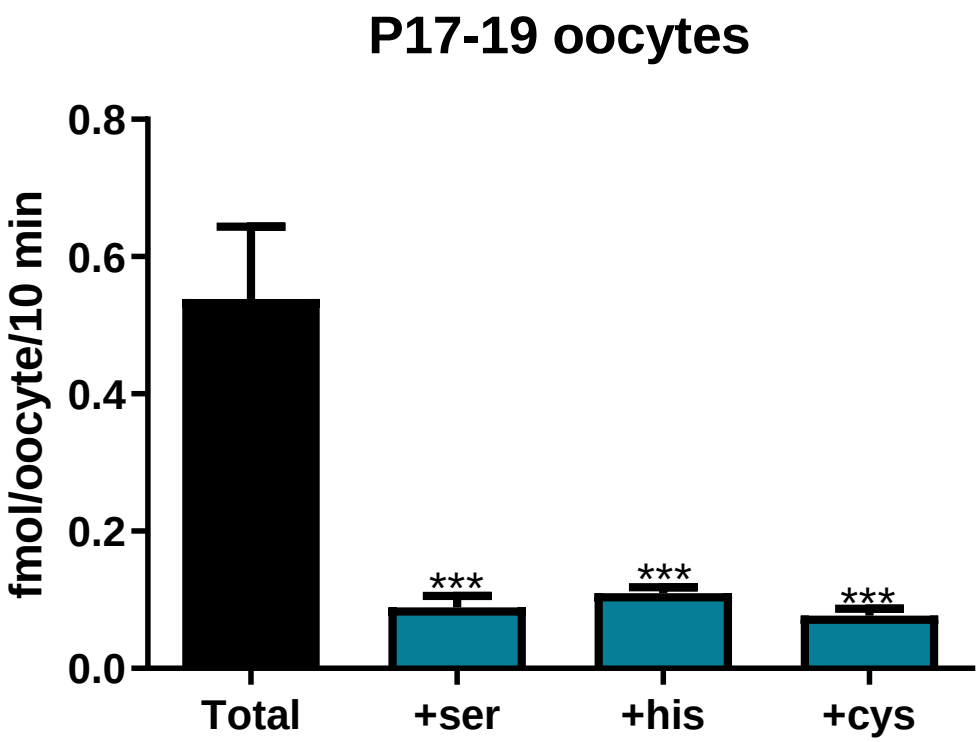

Figure 18. Competitive assay in growing oocytes collected from P17-P19 neonatal ovaries (n=5). Isolated oocytes were immediately placed into uptake media with 1µM of serine[^{3}H], and for competitive substrates, 5mM of either unlabelled serine, histidine, or cysteine. Statistically analysed using multiple comparisons one-way ANOVA, Dunnett's post-hoc test with 'Total' as control, P<0.05. Asterisks (***) indicates significance, means compared to control, P<0.0001.

4.4 *Slc38a7* (SNAT7) is expressed whereas *Slc1a5* (ASCT2) is not

Optimization of PCR and qPCR

Chdh, the control gene, which has previously been shown to be expressed in oocytes, uses a melting temperature of 60°C. The designed primers were optimized for melting temperature, and both primer sets produced bands at 60°C (Figure 19). In addition, the range of detection for the reagents and equipment is best suited for cDNA amounts ranging from 20 ng to 2E10-6 ng, as Figure 21 shows.

Expression of the genes in oocytes was first evaluated through conventional PCR. Figure 20 shows that *Slc38a7* is expressed in oocytes. However, *Slc1a5* is not, which corroborates the previous competition assay results.

In Figure 22, qPCR data quantitatively shows that while *Slc38a7* is definitively expressed, *Slc1a5* is only minimally present. During analysis of qPCR data, Ct values over that of the lowest concentration in the standard curve, corresponding to 1E-6pg was considered to indicate the gene not being present. This usually corresponded with Ct values of 31-32. The oocytes were found to have an average of approximately 1.5E-4 μg/oocyte of *Slc38a7* each. *Slc1a5* did not meet the threshold Ct value for the gene to be considered present. *Chdh*, which served as a control gene in oocytes, was present at approximately 3.5E-4μg. This, along with the results from conventional PCR, supports the hypothesis that ASCT2 is not present in oocytes whereas SNAT7 is.

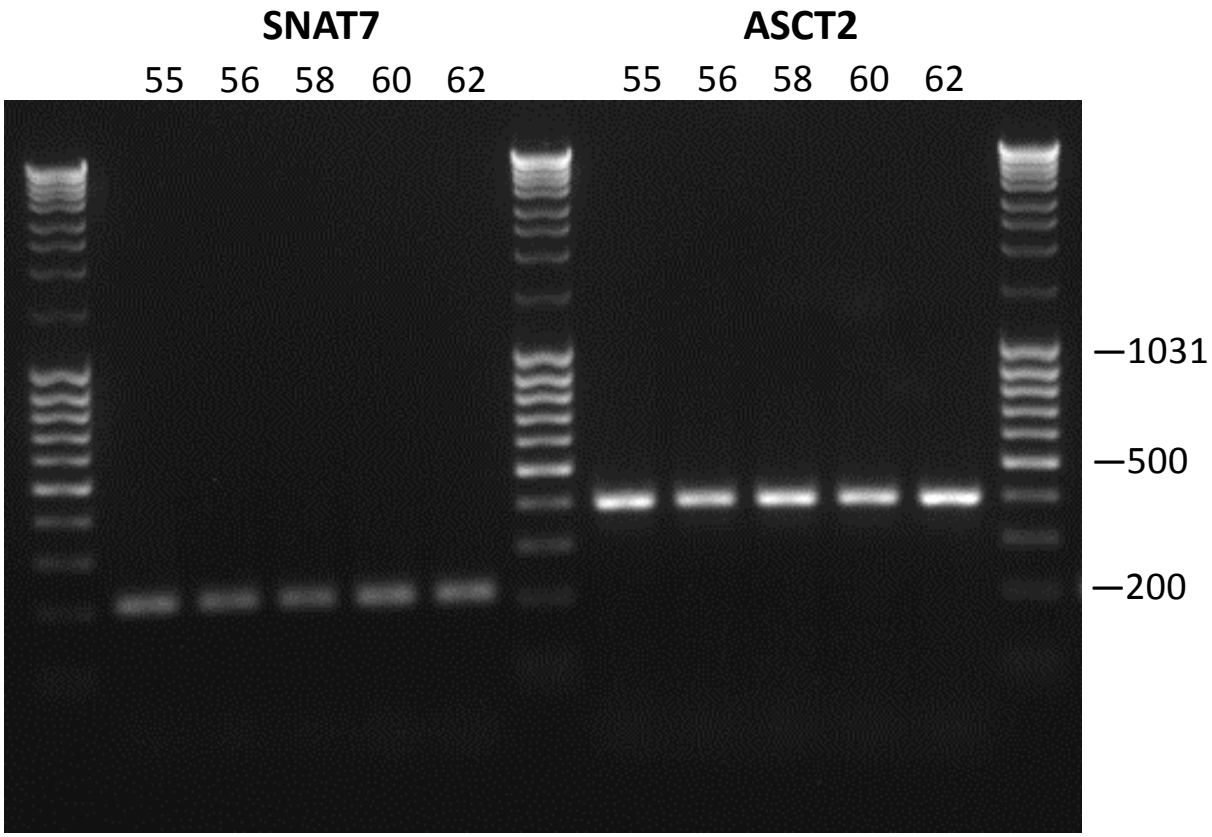

Figure 19. Temperature optimization of designed primers for *Slc1a5* and *Slc38a7* tested over a range of temperatures from 55°C-62°C using the temperature gradient function with the Bio-Rad T100 Thermocycler. Temperatures in lane labels are rounded to the nearest degree. Gel shown is 1.4% agarose with ethidium bromide. MassRuler (Thermo Fisher Scientific, cat no. SM0403) ladder was used. Gel run for 105V for 60 minutes.

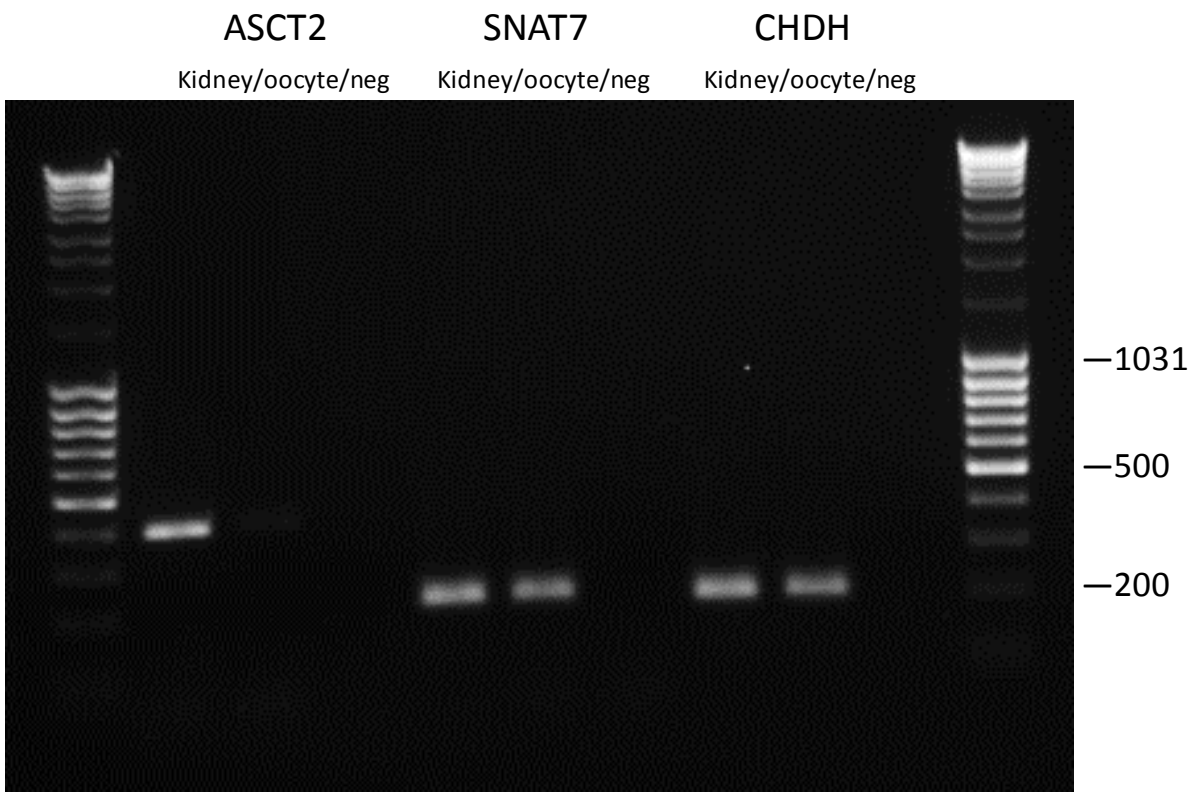

Figure 20. PCR gel showing gene expression in kidney and oocytes. *Slc1a5* (ASCT2), *Slc38a7* (SNAT7), and *chdh* (CHDH) have been run at Tm=60°C for 35 cycles. Oocyte samples contain 1.5 oocyte equivalents. A negative control with water was included for every primer set. MassRuler (Thermo Scientific) was used to estimate amplicon size. The gel was 1.4% agarose, made with ethidium bromide and was run at 105V for 60 minutes. Image acquired using UVP ChemiDoc-It TS2 imager.

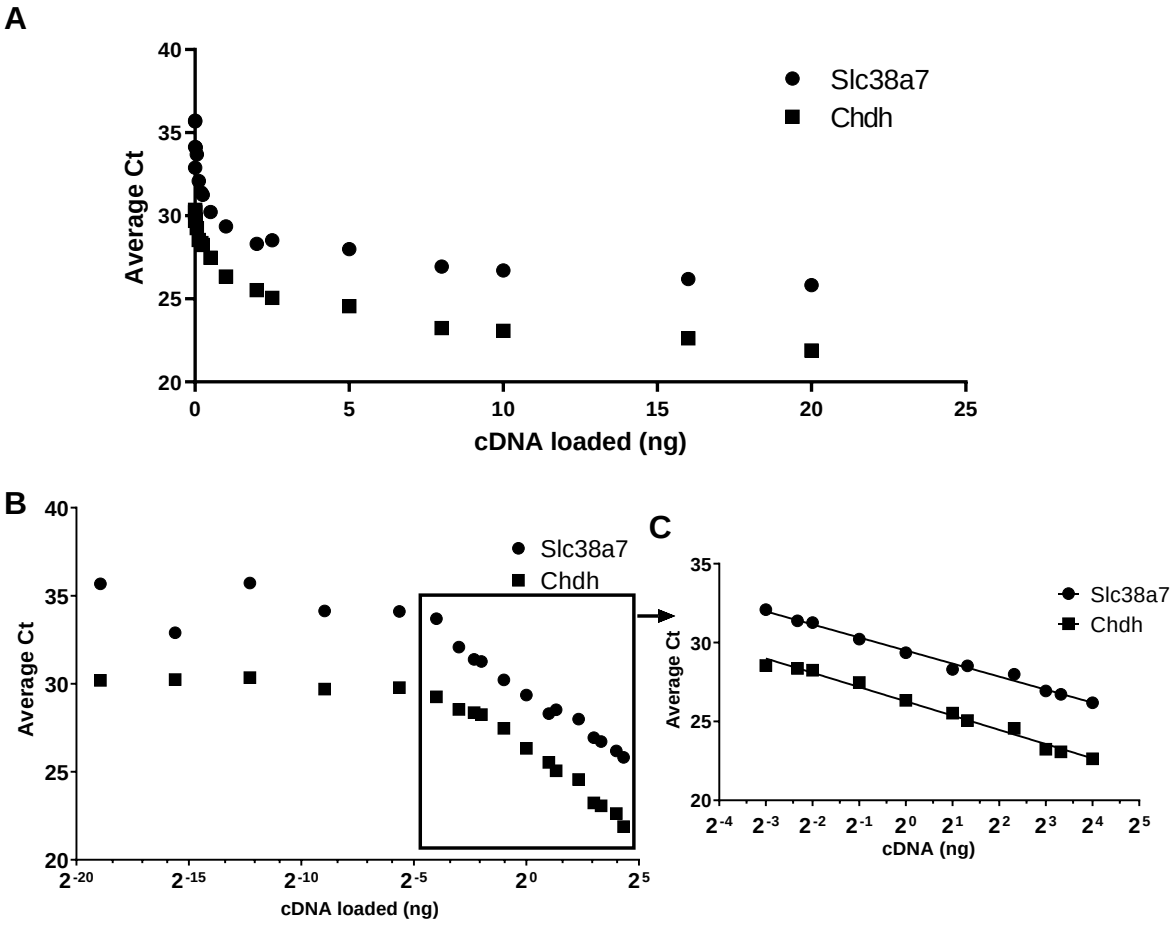

Figure 21. Calibrating the range of qPCR instrument and SYBR green reagents.

A) qPCR signal of *Slc38a7* and a reference gene, *Chdh*, shown as Ct values (cycle threshold) for kidney cDNA ranging from 20 ng to 2E10-6 ng, with level of detection threshold set at 0.24 consistently across both genes.

B) Semi-log plot with cDNA loaded graphed on a log2 scale to linearize the data. C) Plot of the most linear range, which was determined to be from 0.125 ng to 16 ng, r^2=0.99 using a semi-log fit.

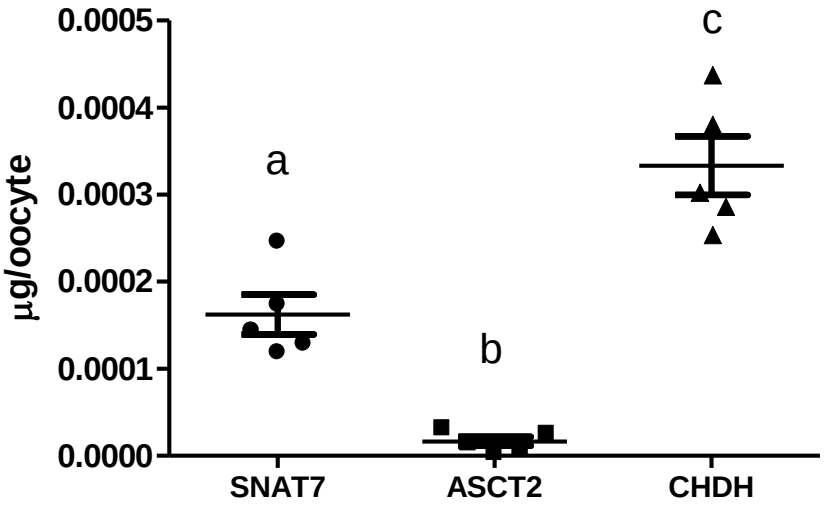

Figure 22. Gene expression of *Slc38a7* (SNAT7), *Slc1a5* (ASCT2), and *chdh* (CHDH) qPCR in GV oocytes. mRNA amount for each gene was quantified using qPCR, calculated according to a prepared standard curve ranging from 1 pg to 1E-6 pg. Different letters indicate significant difference, where for a vs. b, $P \leq 0.01$; a vs. c, $P \leq 0.01$; b vs. c, $P \leq 0.001$. Data analyzed through ANOVA, with Tukey's post-hoc test, $P<0.0001$.

4.5 Kinetics of the serine transporter in oocytes

Having established the identity of the transporter, I was also interested in characterizing it and establishing a profile for how the transporter behaves in oocytes, such as its affinity for its substrates and maximum transport rate at saturation. These properties can also be compared to other transporters in the same family to further confirm the transporter identity. To accurately determine transporter kinetics, it was first necessary to find a length of incubation time that best allows for accurate measurement of transport rate. As serine is taken into the oocyte and its intracellular concentration increases, there is also backflow of serine that exits the oocyte. Initially, the amount transported in is linear with time, but given a sufficiently long period of time for uptake it will deviate from linearity as efflux becomes significant and eventually reach a point where influx is equal to efflux and there is no longer net transport into the oocyte. To accurately evaluate rate for kinetics measurements, the length of incubation must be within the linear range of transport.

To do this, groups of 10-15 oocytes were placed in [^{3}H] serine for different lengths of time to determine at which point the transporter begins to reach steady state, or the point where influx of serine would equal efflux.

The function of transport rate (v) we approximate using the Michalis-Menten equation, which is generally defined as:

$$v = \frac{V_{max} * [s]}{K_m + [s]}$$

Where [s] is the concentration of substrate, which in the context of this project is serine. V_{max} is maximal rate that can be reached, where the transporter is saturated. K_m is the Michaelis constant that needs to be specifically determined for each transport system.

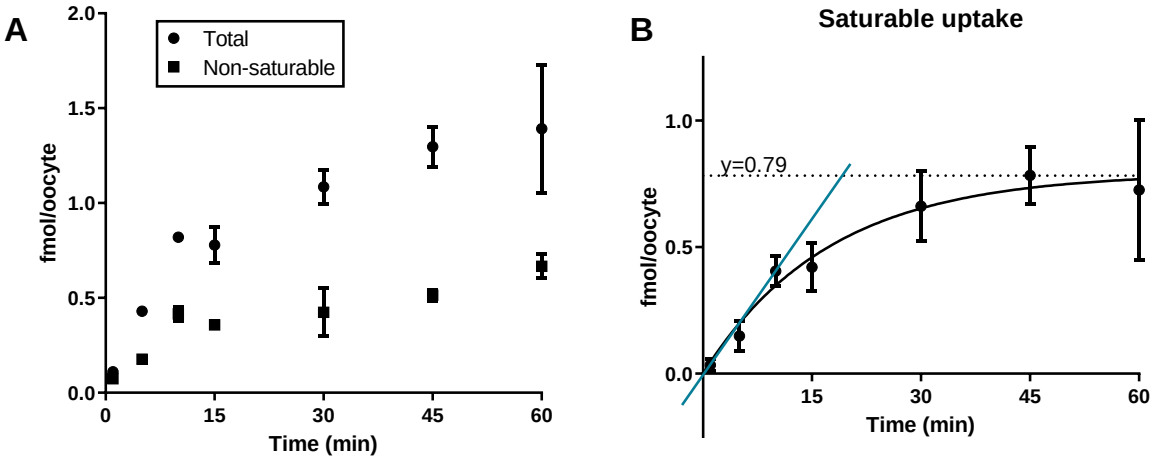

Figure 23. Optimization of the length of uptake time in oocytes with 1µM [3H] serine. 5mM unlabelled serine was included for the non-saturable component (n=3). The curve was fit according to an equation derived from the Michaelis-Menten equation. Error bars show SEM. Data were fit to a least squares one-phase association (Y=0.783*(1-exp(-0.058x)). r^2 = 0.65, plateau is estimated to be y=0.79±0.12.

We need the net rate for this derivation, which gives us

$$v = \frac{ds}{dt} = influx - efflux$$

$$\frac{ds}{dt} = \frac{V_{max} * [s]_{outside}}{K_m + [s]_{outside}} - \frac{V_{max} * [s]_{inside}}{K_m + [s]_{inside}}$$

For the purposes of this experiment, the outside [s] is approximated as a constant, with the assumption that changes due to the amount taken into the oocytes is negligible. With that same assumption, we also assume K_m >>> [s] inside the oocyte. V_{max} is also a constant, as is K_m.

Therefore:

$$A = \frac{V_{max} * [s]_{outside}}{K_m + [s]_{outside}}$$

$$B = \frac{V_{max}}{K_m}$$

Where both A and B are constants.

To determine s(t), we can now work from the simplified equation:

$$\frac{ds}{dt} = A - Bs$$

$$ds = -B(s - \frac{A}{B})dt$$

To further simplify into an easily integrated equation

$$let\ y = s - \frac{A}{B}$$

$$s = y + \frac{A}{B}$$

$$ds = dy + d\left(\frac{A}{B}\right)$$

$$ds = dy$$

Which allows us to simply again into

$$\frac{ds}{y} = -Bdt$$

$$ds = dy = (-Bdt)y$$

$$\frac{dy}{y} = -Bdt$$

And from here it can be integrated for y(t)

$$\int_{y(0)}^{y(t)} \frac{dy}{y} = \int_{0}^{t} -Bdt$$

$$ln|y|\Big|_{y(0)}^{y(t)} = -Bt$$

$$ln|y(t)| - ln|y(0)| = -Bt$$

Substituting s back in to find s(t)

$$ln\left|s(t) - \frac{A}{B}\right| - ln\left|s(0) - \frac{A}{B}\right| = -Bt$$

$$ln\left|s(t) - \frac{A}{B}\right| = ln\left|s(o) - \frac{A}{B}\right| - Bt$$

$$s(t) - \frac{A}{B} = e^{ln\left|s(0) - \frac{A}{B}\right| - Bt}$$

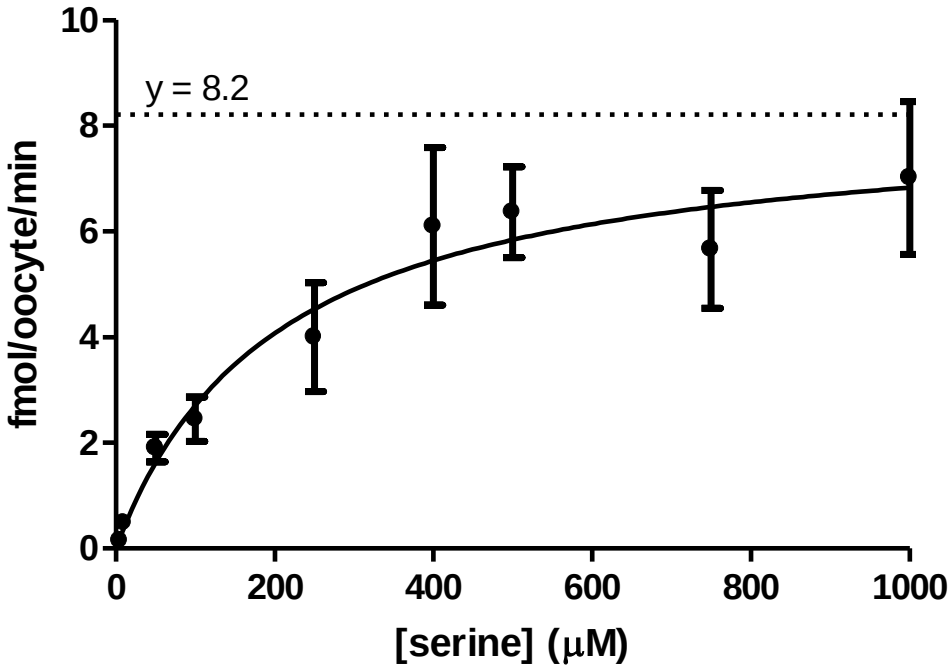

Figure 24. Transport kinetics of serine transporter in oocytes. Increasing concentrations of serine[^{3}H] used to determine changes in rate as transporter approaches saturation (n=5). Data is fit to Michaelis-Menten kinetics, V= 8.211*[S]/203+[S], r^2 = 0.63. The rate is estimated to plateau at V_{max} = 8.2±1.2 fmol/oocyte/min (indicated by the dotted line). This yields a K_m of 203 ± 96 (mean ± standard error).

Assuming s(0) = 0,

$$s(t) = -\frac{A}{B}e^{-Bt} + \frac{A}{B}$$

$$s(t) = \frac{A}{B}(1 - e^{-Bt})$$

This can be expanded according to the e^x expansion series, which is:

$$e^x = 1 + x + \left(\frac{x^2}{2}\right) + \left(\frac{x^3}{6}\right) + \left(\frac{x^4}{24}\right) \ldots$$

Substituting this into the equation for s(t), where x = -Bt,

$$s = \frac{A}{B}\left(1 - \left(1 - Bt + \left(\frac{(-Bt)^2}{2}\right) + \left(\frac{(-Bt)^3}{6}\right) + \left(\frac{(-Bt)^4}{24}\right) \ldots\right)\right)$$

$$s = \frac{A}{B}\left(Bt - \frac{B^2t^2}{2} + \frac{B^3t^3}{6} - \frac{B^4t^4}{24} \ldots\right)$$

The constant B can be determined as the inverse of time where internal concentration is 1/e of maximal concentration reached. Let this be represented by τ.

$$s = \frac{A}{B}\left(\frac{t}{\tau} - \frac{1}{2}\left(\frac{t^2}{\tau^2}\right) + \frac{1}{6}\left(\frac{t^3}{\tau^3}\right) - \frac{1}{24}\left(\frac{t^4}{\tau^4}\right) \ldots\right)$$

When $t <<< \tau$, higher order terms become negligible in comparison to the linear term t/τ. This results in a pseudolinear range that can be approximated by:

$$s(t) \approx \frac{A}{B}\left(\frac{t}{\tau}\right)$$

When the data was fit to the derived s(t) equation presented earlier, it was found to be:

$$s(t) = 0.783(1 - e^{-0.058t})$$

From this, we can determine the constant τ, knowing that B = 0.058

$$\tau = \frac{1}{B} = \frac{1}{0.058} = 17.2$$

The approximated pseudolinear range when $t <<< \tau$ yields the linear equation:

$$s(t) = 0.783\left(\frac{t}{17.2}\right)$$

This is reflected in figure 23. Transport increases linearly until steady state begins to be reached. Based on the results of this experiment, 10 minutes was used in the measurement of transport kinetics. Although it is not quite within the linear range ($t/\tau = 0.58$, $½(t/\tau)^2 = 0.12$ therefore latter terms are not negligible), it is reasonably close given the limitations of measuring sufficient radioactivity during uptake experiments.

Oocytes were then placed into increasing concentrations of [^{3}H] serine to establish the Michaelis-Menten graph from which we can identify the maximal rate of transport (V_{max}) that the transporter can achieve, as well as the concentration of substrate at ½ V_{max} (K_m). In oocytes, this transporter reaches a maximum velocity of 8.2±1.2fmol/oocyte/min, and the K_m is found at 203 ± 95.9μM. Figure 24 shows that the transporter is approaching a rate plateau and therefore is saturable.

However, there is a large margin of error. One additional concentration past 1000μM was tested, a very high concentration of 1750μM to more precisely establish the plateau. However, this revealed that a second, lower affinity transporter for serine is present at extremely high concentrations. This introduced a challenge in truly establishing the activity plateau of the transporter of interest, as concentrations this high are difficult to test and cost-prohibitive due to the large amount of [^{3}H] serine required. Furthermore, the physiological level of serine is orders of magnitude less than the concentration at which this second transporter is activated and was therefore not pursued further.

4.6 NPPC significantly increases serine transport activity *in vitro*

Meiotic maturation can sometimes affect transport of amino acids, nutrients, and small molecules in oocytes. In the follicle, NPPC maintains meiotic arrest through maintenance of elevated cAMP in the GV oocyte. Oocytes can also be kept arrested *in vitro* if cultured as COCs with NPPC. As Figure 25 shows, the presence of NPPC approximately doubles saturable transport of serine in the oocyte. However, whether this is an effect of meiotic arrest was uncertain.

4.6.1 dbcAMP does not affect serine transport activity *in vitro*

Among the effects of NPPC, its major role is in maintaining meiotic arrest albeit indirectly. Downstream of NPPC, dbcAMP, as an analogue of cAMP, can contribute to a high concentration of cAMP to maintain arrest. As such, to determine whether serine transport activity is directly affected by maintaining meiotic arrest, dbcAMP was also used to inhibit progression of meiotic maturation.

From the results shown in Figure 26, we can see that transport of serine is unchanged in the arrested group compared to the control. Based on these results, it is unlikely that the increase in serine transport observed in the NPPC-arrested group is directly due to inhibiting the progression of meiotic maturation.

4.6.2 NPPC-related transport increase is likely mediated by the SNAT7 transporter as well

Another initial hypothesis was that NPPC triggers the activation of another transporter in the oocyte. To determine whether this was the case, the signature substrate profile previously established was used. This consists of the competitive substrates serine, cysteine, and histidine.

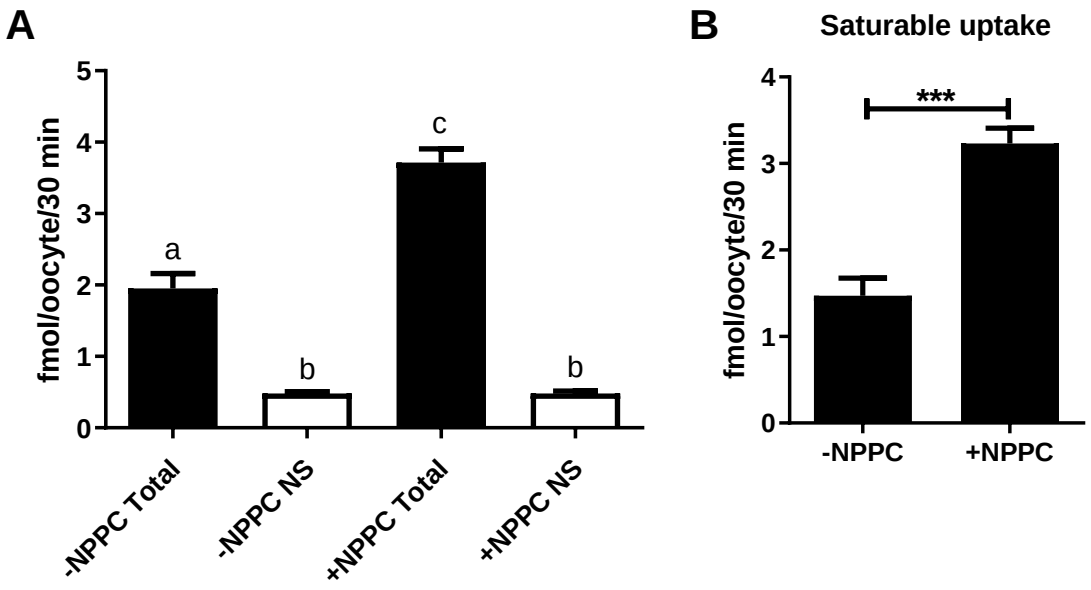

Figure 25. Transport of serine by GV oocytes in meiotic arrest mediated by NPPC (n=5).

A) Total and non-saturable (NS) serine transport measured after 4 hours of *in vitro* culture in MEMα either with or without 100nM NPPC and 100nM estradiol. 1µM serine[3H] was used for uptake measurements, and an additional 5mM unlabelled serine for NS measurements. Statistical significance calculated from one-way ANOVA, Tukey's post-hoc test $P < 0.0001$. Different letters indicate significance, for a vs. b, $P \leq 0.01$; a vs. c, $P \leq 0.01$; b vs. c, $P \leq 0.001$.

B) Saturable serine transport calculated from Total and NS measurements. Unpaired two-tailed t-test used for analysis, Asterisks (***) indicate significance, $P = 0.0002$.

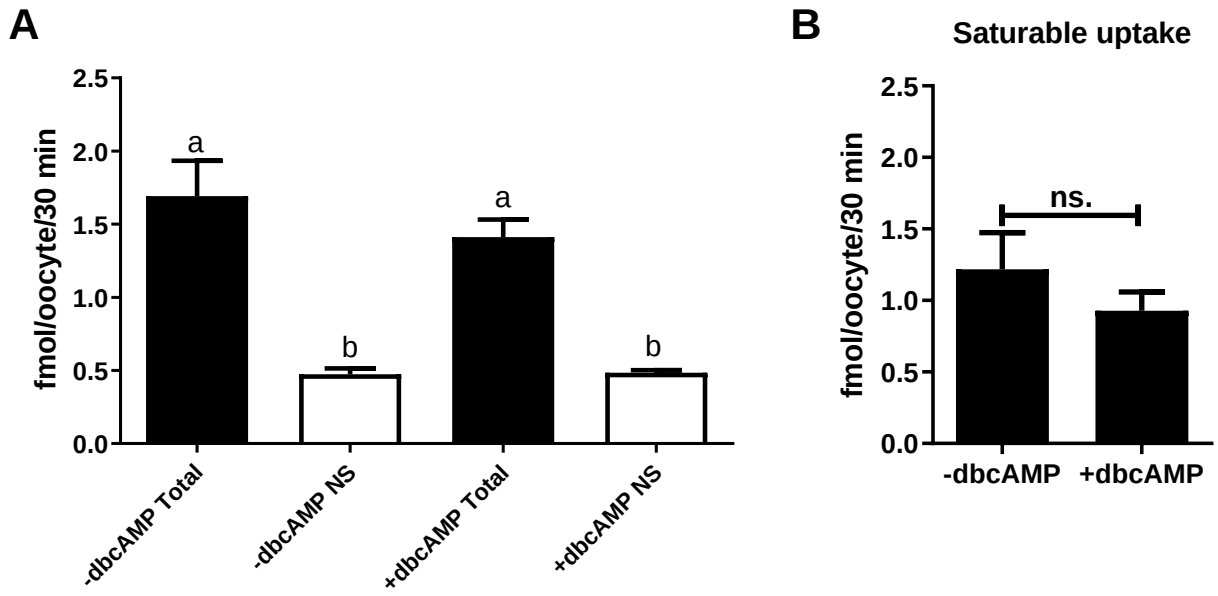

Figure 26. Transport of serine by GV oocytes in meiotic arrest mediated by dbcAMP (n=5).

A) Total and non-saturable (NS) serine transport measured after 4 hours of *in vitro* culture in MEMα either with or without 300µM dbcAMP. 1µM serine[^{3}H] was used for total uptake measurements, and an additional 5mM unlabelled serine for NS measurements. Statistical significance calculated from one-way ANOVA, Tukey's post-hoc test P=0.0028. Different letters indicate significance: a vs. b, P ≤ 0.05.

B) Saturable serine transport calculated from Total and NS measurements. Unpaired two-tailed t-test used for analysis, P = 0.34.

Results shown in Figure 27 indicate that the same transporter is likely responsible for the augmented serine transport as well. Having determined no second transporter was being activated by NPPC, we went on to pursue other possibilities.

4.6.3 High serine transport is not due to presence of cumulus

One difference that we hypothesized may account for the effect being observed with NPPC but not dbcAMP despite both maintaining meiotic arrest was the presence of cumulus cells only in culture with NPPC. We considered that perhaps the presence of cumulus cells had a priming effect on the oocytes that enhanced transporter activity. To determine whether this could be the case, oocytes were cultured with and without cumulus present, and were compared to the elevated serine transport from culture with NPPC.

Figure 28 demonstrates that the presence of cumulus cells alone during culture is not able to increase transporter activity, and that presence of NPPC is imperative to observe this effect.

4.6.4 NPPC effect initiates rapidly during MEMα culture

Thus far, transport measurements have been made following 4 hours of *in vitro* culture in NPPC. The next step was to ascertain how quickly NPPC could mediate its effect.

From the time course (Figure 29), it was found that serine transport was elevated following shorter exposure to NPPC than 4h. At 3h, transport was definitively upregulated. Intermediate timepoints appear to be ambiguously upregulated, and even at the shortest tested timepoint of 0.5h, transporter activity appears to trend higher than at 0h.

Given that NPPC is present in the follicle *in vivo*, it seemed unusual that this effect would manifest only *in vitro*. A hypothesis was that this elevated response following NPPC treatment

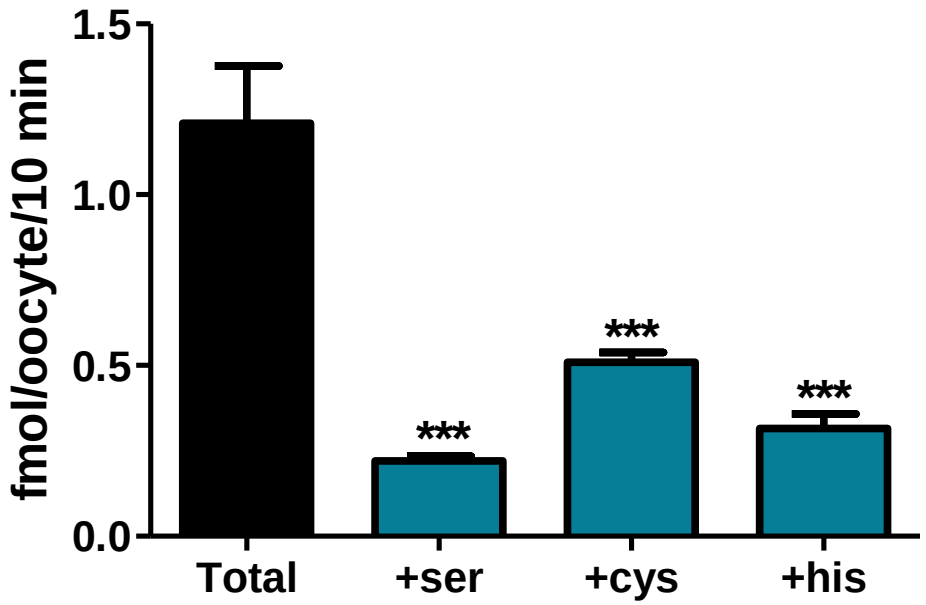

Figure 27. Competition profile for the serine transporter in oocytes cultured in NPPC (100nM) and estradiol (100nM) supplemented MEMα for 4 hours. (n=5) Total was measured with 1µM serine[^{3}H], and to determine the substrates 5mM of the competitive substrates were added. Asterisks indicate significant difference of means compared to control, P ≤ 0.001. Statistical significance calculated from ANOVA, with Dunnett's post-hoc test with 'Total' as control, P < 0.0001.

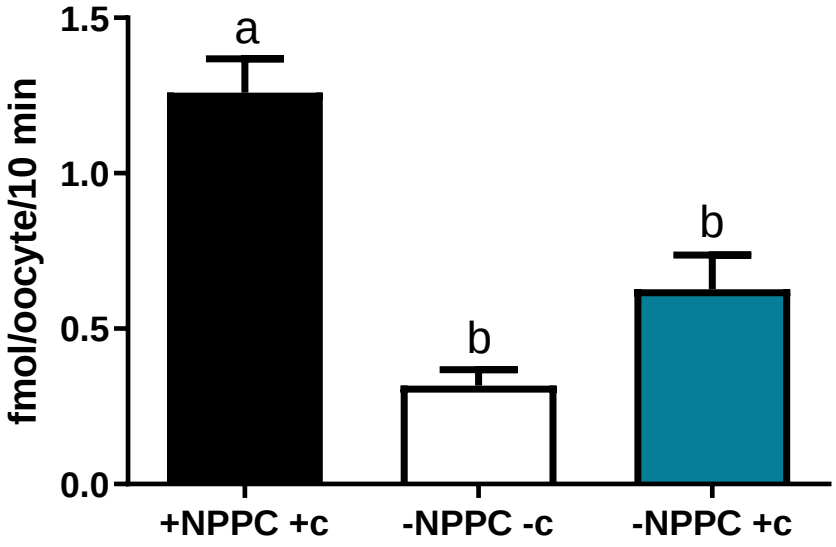

Figure 28. Identifying the role of cumulus in serine transport (n=5). A positive control of the activated transport with COCs cultured in MEMα with NPPC (100nM) and estradiol (100nM) is shown by the black bar. The negative control showing "normal" transport with denuded oocytes in MEMα with no NPPC shown by the white bar. MEMα is also used for a 4-hour culture of COCs to test the role of cumulus cells. Different letters indicate significance: a vs. b, $P \leq 0.01$. Statistical significance calculated from ANOVA, Tukey's post-hoc test, $P<0.0001$.

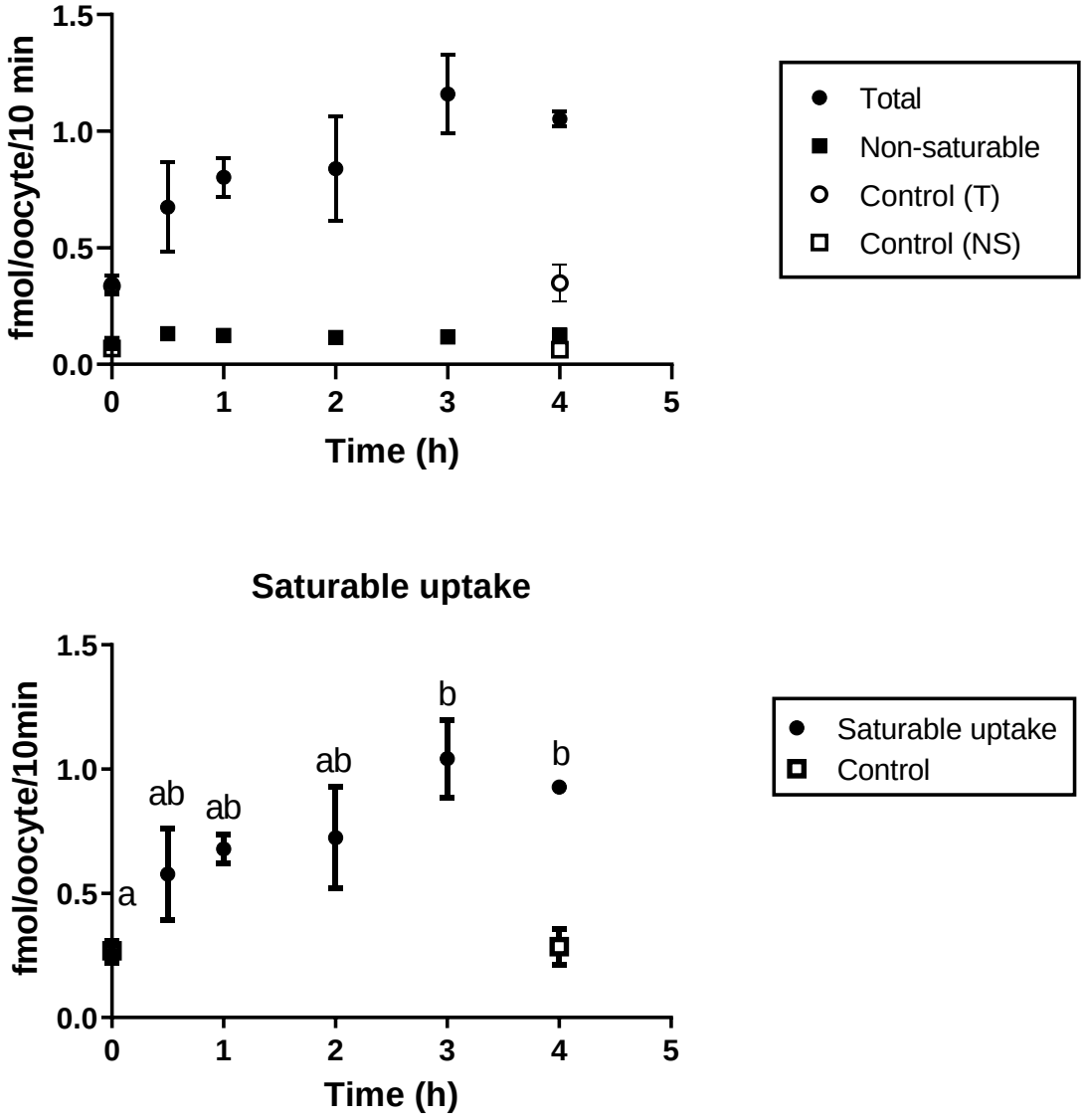

Figure 29. Time course of COC culture in NPPC (n=3).

A) Serine transport measured in oocytes cultured in MEMα with NPPC (100nM) and estradiol (100nM) as COCs for 0h to 4h. Oocytes were denuded prior to exposure to 1µM serine[^{3}H]. A non-saturable component was included for each time point with an additional 5mM unlabelled serine. Negative controls for the NPPC effect was included with total transport and non-saturable transport measured at both 0h and at 4h.

B) Saturable serine transport in NPPC, calculated from total and NS measurements, is plotted with control saturable components. Different letters indicate significance, for a vs. b, P < 0.05. Analyzed with ANOVA, Tukey's post-hoc test, P = 0.017.

was a result of NPPC absence during the collection process. Therefore, I measured serine transport in oocytes that have been treated in combinations of NPPC present in or absent from collection and culture.

Figure 30 shows that the presence of NPPC in culture media is consistently effective, whereas adding NPPC to the collection media alone does not appear to mediate the transport increase, though there is some ambiguity due to increased variance. One hypothesis we had considered was that collection in media with NPPC was sufficient to induce the increase, albeit inconsistently. To explore this possibility, serine transport was measured immediately following collection in media with or without NPPC.

To further elucidate whether the presence of NPPC during collection has any effect, serine transport in GV oocytes freshly collected in KFHM with NPPC was also measured. As shown in Figure 31, simply isolating oocytes in NPPC media is not sufficient to induce the NPPC effect. From this data, it is clear that NPPC presence during collection alone does not induce increased transport.

4.6.5 Effect of NPPC appears to be irreversible

Following this, another time course determining the persistence of this effect was completed by washing oocytes through NPPC-free media. COCs were cultured in MEMα with NPPC for three hours to ensure NPPC takes effect and were then washed three times before being transferred to MEMα without NPPC for the remaining culture time. The time course was carried out up to two hours following NPPC washout. However, even at that point it appears that the effect of increased transport is largely maintained.

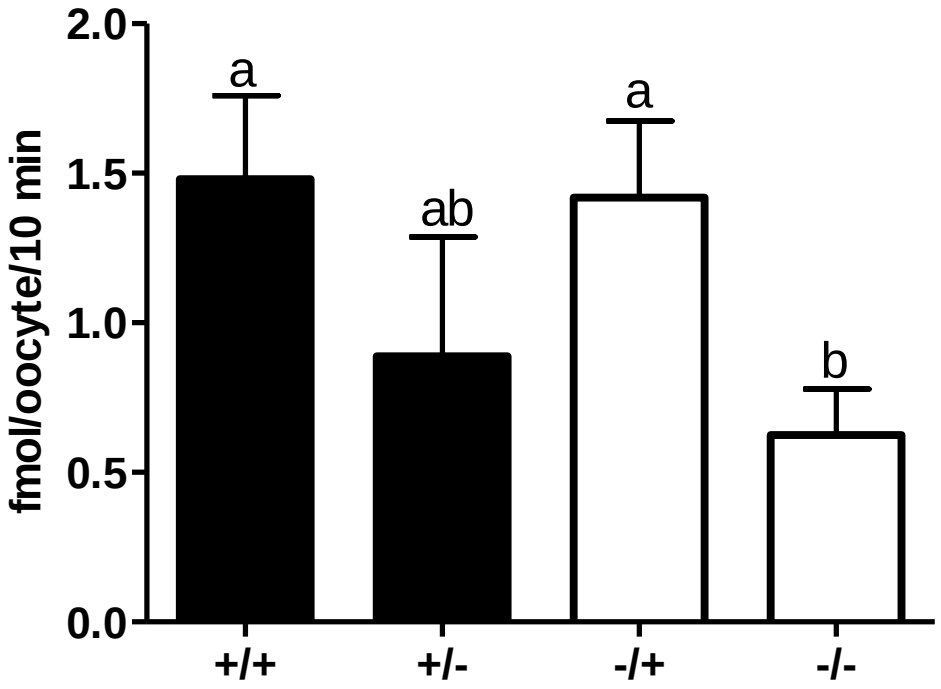

Figure 30. Effect of NPPC in collection media KFHM, culture media MEM*α*, or both. (n=5) Black bars indicate COCs collected in KFHM with NPPC (100nM) and estradiol (100nM), while white bars indicate regular KFHM for collection. COCs from both collection conditions were then cultured for 4h either with (+) or without (-) NPPC and estradiol. 1µM serine[^{3}H] was used for transport measurements. Differing letters indicate significant differences, a vs. b, P ≤ 0.05. Statistics were analyzed using ANOVA with Tukey's post-hoc test, P=0.0068.

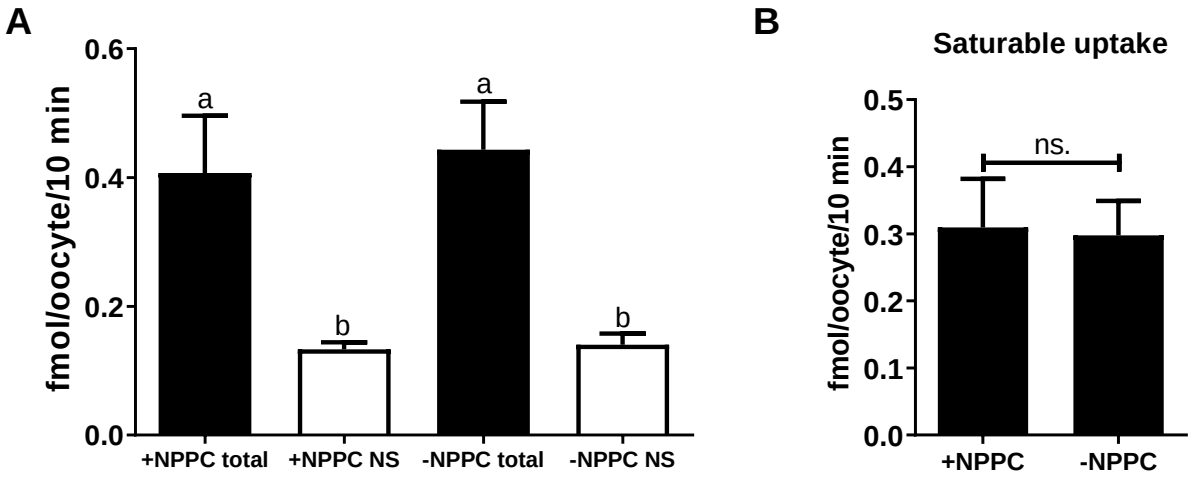

Figure 31. Effect of NPPC presence during collection.

A) Total serine transport was measured immediately following oocyte collection in KFHM either with or without NPPC present. Non-saturable (NS) was also measured for each condition with 5mM unlabelled serine in addition to the 1µM serine[^{3}H] used in total transport measurements (n=5). Statistical significance was calculated from ANOVA, Tukey's post-hoc test P=0.0016. Statistically different columns are indicated by different letters, a vs. b, P < 0.05.

B) The saturable transport component, which was calculated from the difference between total and NS measurements. Statistics analyzed by a two-tailed unpaired t-test, P=0.89.

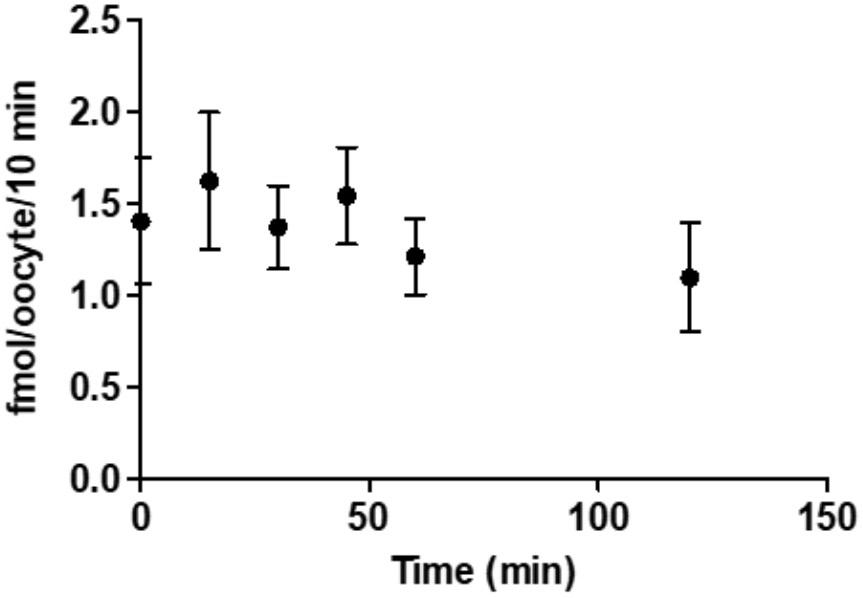

Figure 32. Duration of NPPC effect following removal from NPPC presence. Following a 4h culture in NPPC (100nM) and estradiol (100nM), oocytes were washed free of NPPC and further incubated in MEMα for increasing lengths of time ranging from 0 – 120 minutes, then measured for serine transport activity. 1μM serine[^{3}H] was used. Data analyzed using ANOVA with Tukey's post-hoc test, P = 0.24. No significant differences were found between any time points.

5. Discussion

Oocytes are benefitted by serine presence during its culture, and as the primary methyl donor to the folate cycle, serine was our target of study to better understand oocyte physiology and health. It was brought to our attention as a molecule of interest due to the observation of folate uptake in growing oocytes, and we became interested in how serine may be obtained by oocytes as well as how the process is triggered and regulated (Meredith et al., 2016). In addition to the well-documented role of serine as a methyl donor, it has been shown to be vital to other cellular processes, including many associated with metabolism and proliferation. My experiments aimed to discover the mechanisms in which serine is obtained by the oocyte as well as its regulation. Through my experiments, I have confirmed our hypothesis that serine is transported into the oocyte, and the results showed that growing oocytes and fully-grown oocytes alike take up serine. Furthermore, I have found an interesting role for NPPC in the regulation of serine transport in fully grown GV oocytes.

Serine is actively transported in oocytes

Since saturable transport was detected, we can conclude this process is likely to be facilitated transport through a transporter protein. When compared to previous work from Meredith et al. (2016) on folate transport, the starting point where serine uptake truly becomes robust corresponds to where a peak of folate transport was previously observed.

So far, we can only speculate as to what serine is used for in the oocyte, or possibly carried over to be used in the embryo. Given that both folate and serine are part of the folate cycle contributing to SAM formation, it is a strong possibility that there is a role for serine in oocytes as a methyl donor. During oocyte growth, methyl markers, including imprinted genes,

need to be established in preparation for fertilization. Accurate DNA methylation during this time, especially of imprinted genes, are important to the healthy development of the embryo (Steegers-Theunissen et al., 2013). The downstream purposes of serine transport could therefore be the creation of a methyl pool for use in DNA methylation.

Another potential role for serine is contributing to DNA synthesis (Snell et al., 1987). There is little use for that in oocytes since no DNA synthesis occurs, and even RNA synthesis stops shortly before it reaches the fully-grown oocyte stage (Schultz & Wassarman, 1977). However, it may be possible that it contributes to a pool that can be used for nucleobase synthesis once the oocyte is fertilized.

Another relevant purpose is neutralizing free radicals, as oxidative stress harms oocytes and two of the three amino acids that form GSH, cysteine and glycine, come from serine (de Koning et al., 2003). However, those components can also be independently transported into oocytes (Anas et al., 2008; Pelland et al., 2009). Furthermore, other nutrients that alleviate oxidative stress such as taurine and cystine are also transported into oocytes. The TAUT system which mediates taurine transport activates in the MI stage, as does system x_c^- mediated transport of cystine (Pelland et al., 2009). Perhaps serine is required for management of oxidative stress prior to the activation of those systems, but only future experiments where the serine transporter is inhibited, possibly by oocyte-specific gene deletion, can provide more insight as to what processes are affected by restricting serine access during oocyte growth.

Serine transport begins in growing oocytes and continue into meiotic maturation

Growing oocytes from P14 onwards transport serine steadily, as do fully grown oocytes. As discussed previously, this corresponds to a peak of folate transport that was observed at P14

by Meredith et al. (2016), which led us to explore the significance of serine as an important contributor to the folate cycle. However, unlike folate transport, which was restricted to a short period of oocyte development, serine transport follows a more gradual pattern. We observed a low baseline level of serine transport, increasing at approximately P15 to levels consistent with activity found in fully-grown oocytes. In fully-grown oocytes, serine transport turns off by approximately 6 hours into spontaneous meiotic maturation and does not return during the stages I examined.

As previously discussed, TAUT activates at the MI stage, and x_c^- activates at MII. The onset of these transporters' activation coincides approximately with the decrease of serine transport. This suggests a possible role for serine in neutralization of free radicals, which is then taken over by transporting in taurine and cystine. Another possibility is that serine, as the major methyl donor in the folate cycle, was supplying DNA methylation during oocyte growth and also provided a sufficient pool for fully remethylating the oocyte genome. Furthermore, serine transport begins shortly following the peak of folate transport, lending credence to the theory of serine's role in DNA methylation.

Serine transport in first wave GVs is not consistent with that in adult GV oocytes.

Serine transport activity increases in growing oocytes until it reaches a stable level at which the activity seems to remain relatively constant until its disappearance in fully mature eggs. The exception to this stability is serine transport measured in GV oocytes from adult mice, which demonstrated lower transport activity than fully-grown GV oocytes obtained from P21 neonatal mice. This discrepancy may in fact be a physiological difference between oocytes from the first

wave of folliculogenesis compared to ones following, or it may be an artifact of manipulation during experiments.

There are several differences between oocytes from the first wave of folliculogenesis and oocytes that follow, including their localization in the ovary and their gene expression. The first wave follicles also mature much more quickly than adult follicles (Hirshfield & DeSanti, 1995). Therefore, these two populations of fully-grown oocytes, the P21 oocytes and the superovulated oocytes of the adult mice, are not perfectly comparable. In the oocytes from adult mice, it appears that activation for serine transport occurs between the GV and MI stages to reach levels comparable to the stable level observed during oocyte growth.

Given the observed activation of serine transport in GV oocytes, it stands to consider the possibility that similar activation occurs between GV and MI stages in P21 oocytes. Experiments testing whether this was the case showed, however, that no such activation occurs in oocytes from the P21 mice. There are confirmed physiological differences between first wave oocytes and adult oocytes, thus there is a possibility that regulation of serine transport activity between the two are in fact different. Interestingly, from that experiment it became clear that both freshly obtained P21 GV oocytes and the P21 oocytes matured to MI took up serine at comparable rates to MI oocytes from adult mice.

Both groups of oocytes are nonetheless more similar than not, since oocytes matured during either process can be successfully fertilized and produce offspring, which legitimizes oocytes from neonates as a model for normal growing oocytes (Eppig et al. 2009). In addition, when the first wave follicles were traced, it was found that they contribute to dominant follicles for ovulation up to 3 months following onset of puberty (Zheng et al., 2014). By this estimation, at the time of superovulation in adult mice which are usually between 4-6 weeks old, oocytes

from first wave folliculogenesis are likely still present in the ovaries. It follows that some oocytes used in my experiments may in fact be sourced from that first wave of maturation. The fully-grown oocytes from adult mice may then be a mix of both populations. Furthermore, the comparable levels of activity between fully-grown neonatal oocytes and superovulated denuded MI oocytes suggest continuous transport activity.

Certainly, growing oocytes in later waves of folliculogenesis may simply differ in activity from the first wave, but there is also the need to consider the possibility of some non-physiological artifact. One possibility is the GV oocyte isolation process. While isolation from P21 ovaries and adult ovaries both required vigorous mincing with a razorblade, P21 oocytes would be minced until oocytes release from the COC. However, in adult ovaries, GV oocytes are collected as COCs, then denuded mechanically by pipetting the COC up and down a narrow-bore glass pipette. The denuding process is not particularly gentle and so we theorize that this mechanical stress may cause a brief and temporary drop in transporter activity that the oocyte needs to recover from. Based on the transport time course, less than an hour would be sufficient time for any such recovery.

Serine is most likely transported by SNAT7

Based on current research regarding serine transporters and their profiles of accepted substrates, we were able to eliminate many candidates. We considered that, given the presence of the GLY transporter in oocytes, the similarity in structure between glycine and serine prompted the inclusion of glycine as a competitive substrate to ensure serine transport was not due to non-specific transport by the glycine transporter. Through the unperturbed serine transport that resulted, we were able to confirm that serine was not being transported by a glycine transporter.

MeAIB also not competing for the serine transporter is corroborated by previous research showing that System A is unlikely to be present in oocytes (Pelland et al., 2009). The majority of the competitive substrates were chosen based on our initial hypothesis that either asc or ASC was the most likely candidate. This was supported by alanine transport attributed to those systems that had previously been found in oocytes in a very similar pattern to that observed for serine. Similar to serine, alanine transport was found to be low but present in GV, higher in MI, then close to absent in MII oocytes (Pelland et al., 2009).

The sodium-dependent nature of this transporter eliminated asc as well as $b^{0,+}$ and system L, but ASC seemed very likely. The transporter's strong affinity for leucine would point to ASCT2 being the main candidate rather than the other ASC isoform ASCT1, along with its affinity for alanine and insensitivity to lysine. However, contrary to previous publications suggesting the presence of either asc or ASC in oocytes based on substrate profiles, my results suggest that at the very least, ASCT2 is not expressed. Preliminary PCR testing in oocytes indicated no mRNA expression for ASCT2. This is further confirmed by deposited RNA-Seq data assessing the oocyte transcriptome (GEO GSE70116), which indicated that both isoforms of ASC were very lowly expressed. Some other transporters, however, were very highly expressed, including B^0AT2 and SNAT7 (Veselovska et al., 2015). This changed the direction of our investigation, as neither transport systems had been previously explored in oocytes or pre-implantation embryos.

B^0AT2 was eliminated as a candidate when I used its preferred substrate, proline, as a competitive substrate and found no affinity of the serine transporter for this amino acid. In addition to the previously established substrate profile, our transporter of interest was sensitive to histidine. Based on the known transport profile of SNAT7 as reported by Hägglund et al. (2011),

histidine is recognized as a substrate. Therefore, this transporter most closely fits the profile established for serine transport in the oocyte. They had attempted to measure SNAT7's transport kinetics using radiolabelled glutamine, but only extended up to 5μM at which point transport was still within the linear range. Other SNATs have large K_ms that range from around 200μM to several thousand μM (Sugawara et al., 2000; Tanaka et al., 2005). As measured in my experiments, the serine transporter in oocytes was found to have a K_m around 200μM, in contrast to the previously recorded 20μM for ASCT2 (Utsunomiya-Tate et al., 1996).

This further strengthens the possibility of the oocyte serine transporter being SNAT7. Unfortunately, considering that SNAT7 is not well studied, I cannot exclude the possibility that another transporter that has yet to be identified or characterized could be responsible instead. In addition, another group studied the substrate profile of SNAT7 in lysosomes and found it to be a much narrower range that did not include serine (Verdon et al., 2017). However, the low pH of lysosomes can affect transporter properties. For example, system ASC functioning at a low pH is so functionally different that it was once thought to be a unique transporter system known as X_A^- that transports anionic rather than neutral amino acids (Christensen, 1989). Therefore, the observed differences may be due to it being expressed in lysosomes for their study rather than the plasma membrane.

Therefore, to the best of my knowledge, this is the transporter most closely resembling what mediates serine transport in oocytes. Further experiments to confirm the transporter identity could be done with knockdown of the SNAT7 gene expression or translation in oocytes to determine its effects on serine transport. Unfortunately, no commercial antibodies were available for protein detection using Western blot, so while transcripts are present for this transporter, I am unable to say with 100% certainty that the SNAT7 protein is expressed in the oocyte. If it can be

confirmed that SNAT7 is the serine transporter in oocytes, a conditional knockdown of the gene in mouse oocytes with the Cre-LoxP system can also be explored as a potential tool to not only confirm identity of the transporter but also provide a functioning system in which effects of serine transport can be studied further.

NPPC significantly increases serine transport activity in vitro

I was next interested in the regulation of serine transport in oocytes. This exploration was prompted by the apparent activation of serine transport from the GV to MI stage, and meiotic maturation was considered a possible regulator that prompted its activity to increase. This yielded an unexpected interesting outcome: NPPC, when used to maintain meiotic arrest in the oocytes, resulted in a significantly increased transport of serine, nearly double that of what previously had been measured.

The immediate question, of course, is to determine whether this increase was directly related to keeping the oocytes in meiotic arrest. This is likely ruled out as the cause, as dbcAMP failed to induce this same increased effect. In oocytes, adding dbcAMP, a cell-permeable analogue of cAMP, can directly maintain the high level of intracellular cAMP activity required for preventing meiotic progression. NPPC, on the other hand, is released into the follicle and does not act directly on the oocyte, which could result in "off-target" effects unrelated to maintaining meiotic arrest. We also confirmed that no additional transporter other than SNAT7 was being activated by NPPC. Using a number of competitive substrates representative of SNAT7, namely serine, cysteine, and histidine, we found a similar inhibition profile to that observed without NPPC.

As cumulus cells were usually removed during oocyte culture except when arrest was maintained with NPPC, another facet we considered was whether keeping the cumulus cells during culture with NPPC could have resulted in some kind of priming effect leading to higher expression of the transporter. The results obtained were rather ambiguous. Maintaining the cumulus cells during culture without NPPC did not achieve the high level of transport observed with NPPC. However, despite it not reaching statistical significance, the cumulus cells did seem to trend higher than denuded oocytes, indicating the possibility of cumulus presence contributing in some way. Regardless, there is more to this increased activity as a result of NPPC culture that we do not understand.

Another theory was that the elevated transport was in fact representative of what is physiological *in vivo*, and removal from the *in vivo* environment led to lower transport that could be restored by adding NPPC. After running a time course, I found that thirty minutes in MEMα with NPPC and estradiol brought serine transport to a level comparable to normal MI oocytes, and with increased exposure, serine transport increased to reach maximum activation with three hours or more of NPPC exposure. Unfortunately, we cannot determine events precisely as they occur *in vivo*. However, we hypothesized that if there was a disruption when oocytes are removed from follicle, we can replicate this effect by removing oocytes from NPPC *in vitro* to produce a similar loss of activity. Instead, washing out NPPC from the oocytes had no effect on them. Once serine transport activity has been upregulated by NPPC *in vitro*, it seems that serine transport remains elevated following removal from NPPC even for up to two hours. Therefore, we concluded that the higher serine transport observed is unlikely to be a NPPC withdrawal effect.

Conversely, we explored the possibility that being without NPPC resulted in an artificial exaggerated response to NPPC when COCs are re-exposed to it following collection in the absence of NPPC. When NPPC was added to collection media, we were able to confirm that absence of NPPC during collection was not the cause of the increased serine transport. Rather, extended exposure to NPPC *in vitro* invariably resulted in increased serine transport. One point of ambiguity lies with the test group that was collected in KFHM + NPPC but was cultured in MEMα with no NPPC. There was large variation among that sample, where sometimes transport was elevated and sometimes not. This suggested either that *in vitro* exposure to NPPC for the length of time it takes to isolate COCs, usually around 10-20 minutes, could sometimes be sufficient to induce this effect, or that serine transport had been fully upregulated but decreased slowly once the COCs were no longer in NPPC. While we had found the NPPC effect to be irreversible, we tested only up until 2 hours. No timepoints were significantly different for the reversibility time course, although it appears to trend downward. As such, it is possible that by four hours, transport activity could have decreased to a level between NPPC-activated and not.

However, when we specifically tested whether isolating oocytes in the NPPC presence could in fact induce elevated transport activity, neither the group with NPPC nor without had upregulated serine transport. It seems unlikely then, that the intermediate level of upregulation observed in the previous experiment was due to full NPPC-induced activation followed by reversal during culture without NPPC. Rather, it is more likely that the brief length of NPPC exposure during oocyte isolation inconsistently induced this phenomenon due to variability in experimental handling. The length of time it takes to collect COCs can depend on the efficacy of superovulation. More effective superovulation results in more efficiency in selecting good quality COCs, whereas poor superovulation results in fewer good quality COCs. Therefore, the

latter situation would require more time isolating an adequate selection. As a result, those groups may have been exposed to NPPC longer than others.

Through my experiments, I was able to determine that meiotic progression does not affect serine transport in oocytes. Although the mechanism remains unclear, I have also shown that presence of NPPC leads to increased serine transport *in vitro.* A number of possibilities have been eliminated by the experiments done in this thesis. We determined that it is unlikely to be caused by cumulus cell priming alone. It is also not a compensatory response to the brief absence of NPPC during isolation. Unfortunately, we cannot confirm the true physiological level of serine transport activity, at least not until more is understood of NPPC and its effects on COCs and the follicular environment. While there is understanding of meiotic arrest mediated by NPPC/NPR2 and its mechanisms, it appears that all the effects of NPPC signalling pathways are not yet known.

In other cell types, NPPC/NPR2 signalling has been shown to affect gene expression (Peake et al., 2014). However, in this thesis, all NPPC tests have been done in fully-grown oocytes, which are transcriptionally silent. This likely rules out NPPC targeting of oocyte transcription to mediate increased serine transport. However, natriuretic peptides have been shown to alter protein activity as well, such as alkaline phosphatases (Hagiwara et al., 1996). Therefore, it may also increase translation or activation of the protein in a cGMP-dependent manner, or possibly influence the kinetics of the transporter.

Mural granulosa-produced NPPC is released to follicular fluid, but it is uncertain how much is present to mediate the effects of NPPC. The unanswered question remains: why does this effect occur *in vitro* when no such effect is observed from *in vivo* matured oocytes despite it being surrounded by NPPC in the follicle? Previously, a dose response experiment by Richard

and Baltz showed that 100nM - 500nM was the optimal range at which exogenous NPPC mediated meiotic arrest in COCs of the strain of mouse we use (Richard & Baltz, 2014). My experiments used the lowest dose of 100nM, but it is possible that this is not the amount present in follicular fluid and the dose differences led to altered effects.

Another difference is the use of MEMα culture media, which does not imitate follicular fluid (FF) and there are some significant differences between their composition. The majority of amino acids are present in much higher concentrations than in FF, except taurine which is not included in MEMα but is the most abundant amino acid in FF. MEMα also does not provide pyruvate but rather much higher amounts of glucose (Harris et al., 2005). Hypoxanthine is another nutrient present in follicular fluid but not in MEMα, and it not only contributes to maintaining meiotic arrest but is regulated by an enzyme that also partially regulates NPR2. Perhaps this effect is due to a combination of one of the differing components in MEMα and NPPC signalling.

Summary of thesis work and future directions

Knowing now that serine is transported into oocytes, future experiments can focus on the roles that serine plays through oocyte growth and maturation. The sodium-dependent saturable transport is not mediated by ASC, and ASC is furthermore unlikely to be present in oocytes. The evidence in this thesis show that SNAT7, instead, is not only present but may likely be the main serine transporter. However, this is something that should be confirmed in the future, possibly through use of a knockdown. In addition, the discovery of NPPC leading to dysregulation of serine transport also brings about some interesting questions regarding the regulation of serine

transport. Further research in this direction would be easier to approach with definitive knowledge of the transporter identity in the oocyte.

Another facet that has potential for exploration is the contribution of cumulus cells to the oocyte. As mentioned in the introduction, metabolic coupling is a vital process in cumulus support of oocyte growth and maturation. Amino acids are one of the substrates whose uptake by oocytes can be enhanced by the presence of follicular cells. Examples include taurine, lysine, and alanine (Pelland et al., 2009). Given that serine and alanine may share a transporter in oocytes, it is likely that serine transport would similarly be enhanced by the presence of follicular cells both in growing and GV oocytes. This is outside of the scope of this thesis, but some of my preliminary data in this direction suggests this may be the case.

Nonetheless, all these directions of research can lead to better understanding of oocyte physiology during growth and maturation, and more in-depth understanding of their regulatory pathways.

6. Conclusion

The research conducted for this thesis project shows that oocytes are able to independently transport serine during growth. Transport persists until just prior to the fully matured egg stage. Furthermore, I identified the likely mechanism of serine transport as sodium-dependent transport by the System A/N family transporter SNAT7, encoded by *Slc38a7* which is expressed in the oocyte, whereas *Slc1a5* (ASCT2) is not. Furthermore, a phenomenon affecting regulation of the transporter has been identified through NPPC presence *in vitro*. NPPC appears to irreversibly enhance SNAT7 activity.

This research answers questions regarding the accumulation of serine in oocytes that contribute to our understanding of oocyte physiology. In addition, it may provide direction for future areas of exploration to better understand the roles of serine in oocyte development. For example, researching to what extent and whether they contribute to DNA methylation during oocyte growth, or contribute to other aspects of oocyte health would be beneficial. Future directions can also include evaluation of cumulus granulosa cell contribution to serine transport. The discovery of the *in vitro* NPPC effect is also intriguing and is worth further exploration to better understand how this ligand affects COC signalling and regulation. It also exposes how much remains unknown regarding oocyte and follicular physiology and opens up future directions for study.

7. References

Almeida, O. P., McCaul, K., Hankey, G. J., Norman, P., Jamrozik, K., & Flicker, L. (2008). Homocysteine and Depression in Later Life. *Archives of General Psychiatry*, *65*(11), 1286.

Anas, M.-K. I., Lee, M. B., Zhou, C., Hammer, M.-A., Slow, S., Karmouch, J., … Baltz, J. M. (2008). SIT1 is a betaine/proline transporter that is activated in mouse eggs after fertilization and functions until the 2-cell stage. *Development*, *135*(24), 4123–4130.

Anckaert, E., Romero, S., Adriaenssens, T., & Smitz, J. (2010). Effects of Low Methyl Donor Levels in Culture Medium During Mouse Follicle Culture on Oocyte Imprinting Establishment. *Biology of Reproduction*, *83*(3), 377–386.

Annunziato, A. T., & Hansen, J. C. (2000). Role of histone acetylation in the assembly and modulation of chromatin structures. *Gene Expression*, *9*(1–2), 37–61. Retrieved from

Aoki, F., Worrad, D. M., & Schultz, R. M. (1997). Regulation of Transcriptional Activity during the First and Second Cell Cycles in the Preimplantation Mouse Embryo. *Developmental Biology*, *181*(2), 296–307.

Baird, D. T., Brown, A., Cheng, L., Critchley, H. O. D., Lin, S., Narvekar, N., & Williams, A. R. W. (2003). Mifepristone: a novel estrogen-free daily contraceptive pill. *Steroids*, *68*(10–13), 1099–1105.

Baltz, J. M., & Zhou, C. (2012). Cell volume regulation in mammalian oocytes and preimplantation embryos. *Molecular Reproduction and Development*, *79*(12), 821–831.

Barreiro, E. J., Kümmerle, A. E., & Fraga, C. A. M. (2011). The Methylation Effect in Medicinal Chemistry. *Chemical Reviews*, *111*(9), 5215–5246.

Bartolomei, M. S., & Ferguson-Smith, A. C. (2011). Mammalian genomic imprinting. *Cold Spring Harbor Perspectives in Biology*, *3*(7), 1–17.

Bartolomei, M. S., Zemel, S., & Tilghman, S. M. (1991). Parental imprinting of the mouse H19 gene. *Nature*, *351*(6322), 153–155.

Böhmer, C., Bröer, A., Munzinger, M., Kowalczuk, S., Rasko, J. E. J., Lang, F., & Bröer, S. (2005). Characterization of mouse amino acid transporter B0AT1 (slc6a19). *The Biochemical Journal*, *389*(Pt 3), 745–751.

Bonilla, L., Luchini, D., Devillard, E., & Hansen, P. J. (2010). Methionine Requirements for the Preimplantation Bovine Embryo. *Journal of Reproduction and Development*, *56*(5), 527–532.

Borum, K. (1961). Oogenesis in the mouse. A study of the meiotic prophase. *Experimental Cell Research*, *24*, 495–507.

Bowles, J., & Koopman, P. (2010). Sex determination in mammalian germ cells: extrinsic versus intrinsic factors. *Reproduction*, *139*(6), 943–958.

Boxmeer, J. C., Steegers-Theunissen, R. P. M., Lindemans, J., Wildhagen, M. F., Martini, E., Steegers, E. A. P., & Macklon, N. S. (2008). Homocysteine metabolism in the pre-ovulatory follicle during ovarian stimulation. *Human Reproduction*, *23*(11), 2570–2576.

Braude, P., Bolton, V., & Moore, S. (1988). Human gene expression first occurs between the four- and eight-cell stages of preimplantation development. *Nature*, *332*(6163), 459–461.

Brinster, R. L. (1971). Oxidation of pyruvate and glucose by oocytes of the mouse and rhesus monkey. *Journal of Reproduction and Fertility*, *24*(2), 187–191.

Bröer, A., Tietze, N., Kowalczuk, S., Chubb, S., Munzinger, M., Bak, L. K., & Bröer, S. (2005). The orphan transporter v7-3 (slc6a15) is a Na + -dependent neutral amino acid transporter (B 0 AT2). *Biochemical Journal*, *393*(1), 421–430.

Bröer, S. (2014). The SLC38 family of sodium–amino acid co-transporters. *Pflügers Archiv - European Journal of Physiology*, *466*(1), 155–172.

Brown, C. J., Ballabio, A., Rupert, J. L., Lafreniere, R. G., Grompe, M., Tonlorenzi, R., & Willard, H. F. (1991). A gene from the region of the human X inactivation centre is expressed exclusively from the inactive X chromosome. *Nature*, *349*(6304), 38–44.

Burkart, A. D., Xiong, B., Baibakov, B., Jiménez-Movilla, M., & Dean, J. (2012). Ovastacin, a cortical granule protease, cleaves ZP2 in the zona pellucida to prevent polyspermy. *The Journal of Cell Biology*, *197*(1), 37–44.

Castro, R., Rivera, I., Blom, H. J., Jakobs, C., & de Almeida, I. T. (2006). Homocysteine metabolism, hyperhomocysteinaemia and vascular disease: An overview. *Journal of Inherited Metabolic Disease*, *29*(1), 3–20.

Cetica, P., Pintos, L., Dalvit, G., & Beconi, M. (2002). Activity of key enzymes involved in glucose and triglyceride catabolism during bovine oocyte maturation in vitro. *Reproduction (Cambridge, England)*, *124*(5), 675–681.

Cha, K. Y., Koo, J. J., Ko, J. J., Choi, D. H., Han, S. Y., & Yoon, T. K. (1991). Pregnancy after in vitro fertilization of human follicular oocytes collected from nonstimulated cycles, their culture in vitro and their transfer in a donor oocyte program. *Fertility and Sterility*, *55*(1), 109–113.

Chairoungdua, A., Kanai, Y., Matsuo, H., Inatomi, J., Kim, D. K., & Endou, H. (2001). Identification and characterization of a novel member of the heterodimeric amino acid transporter family presumed to be associated with an unknown heavy chain. *The Journal of Biological Chemistry*, *276*(52), 49390–49399.

Chaudhry, F. A., Reimer, R. J., Krizaj, D., Barber, D., Storm-Mathisen, J., Copenhagen, D. R., & Edwards, R. H. (1999). Molecular Analysis of System N Suggests Novel Physiological Roles in Nitrogen Metabolism and Synaptic Transmission. *Cell*, *99*(7), 769–780.

Choi, T., Fukasawa, K., Zhou, R., Tessarollo, L., Borror, K., Resau, J., & Vande Woude, G. F. (2002). The Mos/mitogen-activated protein kinase (MAPK) pathway regulates the size and degradation of the first polar body in maturing mouse oocytes. *Proceedings of the National Academy of Sciences*, *93*(14), 7032–7035.

Christensen, H. N. (1989). Distinguishing amino acid transport systems of a given cell or tissue. *Methods in Enzymology*, *173*(1985), 576–616.

Clift, D., & Schuh, M. (2013). Restarting life: Fertilization and the transition from meiosis to mitosis. *Nature Reviews Molecular Cell Biology*, *14*(9), 549–562.

Cockburn, K., & Rossant, J. (2010). Making the blastocyst: lessons from the mouse. *The Journal of Clinical Investigation*, *120*(4), 995–1003.

Combelles, C. M. H., Cekleniak, N. A., Racowsky, C., & Albertini, D. F. (2002). Assessment of nuclear and cytoplasmic maturation in in-vitro matured human oocytes. *Human Reproduction*, *17*(4), 1006–1016.

Conti, M., Hsieh, M., Musa Zamah, A., & Oh, J. S. (2012). Novel signaling mechanisms in the

ovary during oocyte maturation and ovulation. *Molecular and Cellular Endocrinology*, *356*(1–2), 65–73.

Corbin, K. D., & Zeisel, S. H. (2012). Choline metabolism provides novel insights into nonalcoholic fatty liver disease and its progression. *Current Opinion in Gastroenterology*, *28*(2), 159–165.

Couse, J. F., Yates, M. M., Deroo, B. J., & Korach, K. S. (2005). Estrogen Receptor-β Is Critical to Granulosa Cell Differentiation and the Ovulatory Response to Gonadotropins. *Endocrinology*, *146*(8), 3247–3262.

Davis, S. R., Stacpoole, P. W., Williamson, J., Kick, L. S., Quinlivan, E. P., Coats, B. S., … Gregory, J. F. 3rd. (2004). Tracer-derived total and folate-dependent homocysteine remethylation and synthesis rates in humans indicate that serine is the main one-carbon donor. *American Journal of Physiology. Endocrinology and Metabolism*, *286*(2), E272-9.

de Koning, T. J., Snell, K., Duran, M., Berger, R., Poll-The, B.-T., & Surtees, R. (2003). L-serine in disease and development. *The Biochemical Journal*, *371*(Pt 3), 653–661.

Dekel, N., & Phillips, D. M. (1979). Maturation of the Rat Cumulus Oophorus: A Scanning Electron Microscopic Study. *Biology of Reproduction*, *21*(1), 9–18.

Dillon, S. C., Zhang, X., Trievel, R. C., & Cheng, X. (2005). The SET-domain protein superfamily: Protein lysine methyltransferases. *Genome Biology*, *6*(8), 227.

Dolinoy, D. C., Weidman, J. R., & Jirtle, R. L. (2007). Epigenetic gene regulation: Linking early developmental environment to adult disease. *Reproductive Toxicology*, *23*(3), 297–307.

Downs, S. M., Daniel, S. A. J., Bornslaeger, E. A., Hoppe, P. C., & Eppig, J. J. (1989).

Maintenance of meiotic arrest in mouse oocytes by purines: Modulation of cAMP levels and cAMP phosphodiesterase activity. *Gamete Research*, *23*(3), 323–334.

Downs, S. M., & Hudson, E. D. (2000). Energy substrates and the completion of spontaneous meiotic maturation. *Zygote*, *8*(4), 339–351.

Dumesic, D. A., Meldrum, D. R., Katz-Jaffe, M. G., Krisher, R. L., & Schoolcraft, W. B. (2015). Oocyte environment: follicular fluid and cumulus cells are critical for oocyte health. *Fertility and Sterility*, *103*, 303–316.

Dunbar, L. A., & Caplan, M. J. (2000). The cell biology of ion pumps: Sorting and regulation. *European Journal of Cell Biology*, *79*(8), 557–563.

Dunning, K. R., Russell, D. L., & Robker, R. L. (2014). Lipids and oocyte developmental competence: The role of fatty acids and β-oxidation. *Reproduction*, *148*(1), 1470–1626.

Eagle, H. (1959). Amino acid metabolism in mammalian cell cultures. *Science*, *130*(3373), 432–437.

Ebisch, I. M. W., Peters, W. H. M., Thomas, C. M. G., Wetzels, A. M. M., Peer, P. G. M., & Steegers-Theunissen, R. P. M. (2006). Homocysteine, glutathione and related thiols affect fertility parameters in the (sub)fertile couple. *Human Reproduction*, *21*(7), 1725–1733.

Egbert, J. R., Shuhaibar, L. C., Edmund, A. B., Van Helden, D. A., Robinson, J. W., Uliasz, T. F., … Jaffe, L. A. (2014). Dephosphorylation and inactivation of NPR2 guanylyl cyclase in granulosa cells contributes to the LH-induced decrease in cGMP that causes resumption of meiosis in rat oocytes. *Development*, *141*(18), 3594–3604.

El-Hayek, S., Yang, Q., Abbassi, L., FitzHarris, G., & Clarke, H. J. (2018). Mammalian Oocytes

Locally Remodel Follicular Architecture to Provide the Foundation for Germline-Soma Communication. *Current Biology : CB*, *28*(7), 1124–1131.e3.

Eppig, J. J. (1979). FSH stimulates hyaluronic acid synthesis by oocyte-cumulus cell complexes from mouse preovulatory follicles [13]. *Nature*, *281*(5731), 483–484.

Eppig, J. J., O'Brien, M. J., Wigglesworth, K., Nicholson, A., Zhang, W., & King, B. A. (2009). Effect of in vitro maturation of mouse oocytes on the health and lifespan of adult offspring. *Human Reproduction*, *24*(4), 922–928.

Felig, P. (1975). Amino Acid Metabolism in Man. *Annual Review of Biochemistry*, *44*(1), 933–955.

Fell, D. A., & Snell, K. (1988). Control analysis of mammalian serine biosynthesis. Feedback inhibition on the final step. *The Biochemical Journal*, *256*(1), 97–101.

Fortune, J. E. (2003). The early stages of follicular development: Activation of primordial follicles and growth of preantral follicles. *Animal Reproduction Science*, *78*(3–4), 135–163.

Fortune, J. E., & Eppig, J. J. (1979). Effects of gonadotropins on steroid secretion by infantile and juvenile mouse ovaries in vitro. *Endocrinology*, *105*(3), 760–768.

Fotiadis, D., Kanai, Y., & Palacín, M. (2013). The SLC3 and SLC7 families of amino acid transporters. *Molecular Aspects of Medicine*, *34*(2–3), 139–158.

Ginsburg, M., Snow, M. H., & McLaren, A. (1990). Primordial germ cells in the mouse embryo during gastrulation. *Development*, *110*(2), 521–528.

Goll, M. G., & Bestor, T. H. (2005). Eukaryotic cytosine methyltransferases. *Annual Review of Biochemistry*, *74*(1), 481–514.

Gowher, H., & Jeltsch, A. (2001). Enzymatic properties of recombinant Dnmt3a DNA methyltransferase from mouse: the enzyme modifies DNA in a non-processive manner and also methylates non-CpA sites. *Journal of Molecular Biology*, *309*(5), 1201–1208.

Hägglund, M. G. A., Hellsten, S. V, Bagchi, S., Philippot, G., Löfqvist, E., Nilsson, V. C. O., … Fredriksson, R. (2015). Transport of L-Glutamine, L-Alanine, L-Arginine and L-Histidine by the Neuron-Specific Slc38a8 (SNAT8) in CNS. *Journal of Molecular Biology*, *427*, 1495–1512.

Hägglund, M. G. A., Sreedharan, S., Nilsson, V. C. O., Shaik, J. H. A., Almkvist, I. M., Bäcklin, S., … Fredriksson, R. (2011). Identification of SLC38A7 (SNAT7) protein as a glutamine transporter expressed in neurons. *Journal of Biological Chemistry*, *286*(23), 20500–20511.

Haghighat, N., & Van Winkle, L. J. (1990). Developmental change in follicular cell- enhanced amino acid uptake into mouse oocytes that depends on intact gap junctions and transport system gly. *Journal of Experimental Zoology*, *253*(1), 71–82.

Hagiwara, H., Inoue, A., Yamaguchi, A., Yokose, S., Furuya, M., Tanaka, S., & Hirose, S. (1996). cGMP produced in response to ANP and CNP regulates proliferation and differentiation of osteoblastic cells. *American Journal of Physiology-Cell Physiology*, *270*(5), C1311–C1318.

Han, Y., Yan, J., Zhou, J., Teng, Z., Bian, F., Guo, M., … Xia, G. (2011). Acute fasting decreases the expression of GLUT1 and glucose utilisation involved in mouse oocyte maturation and cumulus cell expansion. *Reproduction, Fertility and Development*, *24*(5), 733.

Harris, S. E., Gopichandran, N., Picton, H. M., Leese, H. J., & Orsi, N. M. (2005). Nutrient

concentrations in murine follicular fluid and the female reproductive tract. *Theriogenology*, *64*(4), 992–1006.

Hashimoto, N., & Kishimoto, T. (1988). Regulation of meiotic metaphase by a cytoplasmic maturation-promoting factor during mouse oocyte maturation. *Developmental Biology*, *126*(2), 242–252.

Hashimoto, N., Watanabe, N., Furuta, Y., Tamemoto, H., Sagata, N., Yokoyama, M., … Aizawai, S. (1994). Parthenogenetic activation of oocytes in c-mos-deficient mice. *Nature*, *370*(6484), 68–71.

Hediger, M. A., Clémençon, B., Burrier, R. E., & Bruford, E. A. (2013). The ABCs of membrane transporters in health and disease (SLC series): Introduction. *Molecular Aspects of Medicine*, *34*(2–3), 95–107.

Hellsten, S. V., Eriksson, M. M., Lekholm, E., Arapi, V., Perland, E., & Fredriksson, R. (2017). The gene expression of the neuronal protein, SLC38A9, changes in mouse brain after in vivo starvation and high-fat diet. *PLOS ONE*, *12*(2), e0172917.

Hirshfield, A. N., & DeSanti, A. M. (1995). Patterns of ovarian cell proliferation in rats during the embryonic period and the first three weeks postpartum. *Biology of Reproduction*, *53*(5), 1208–1221.

Horsthemke, B., & Buiting, K. (2006). Imprinting defects on human chromosome 15. *Cytogenetic and Genome Research*, *113*(1–4), 292–299.

Hwang, D. F., Wang, L. C., & Cheng, H. M. (1998). Effect of taurine on toxicity of copper in rats. *Food and Chemical Toxicology : An International Journal Published for the British*

Industrial Biological Research Association, *36*(3), 239–244.

Ikeda, S., Koyama, H., Sugimoto, M., & Kume, S. (2012). Roles of One-carbon Metabolism in Preimplantation Period —Effects on Short-term Development and Long-term Programming—. *J. Reprod. Dev*, *58*(1), 38–43.

Jia, D., Jurkowska, R. Z., Zhang, X., Jeltsch, A., & Cheng, X. (2007). Structure of Dnmt3a bound to Dnmt3L suggests a model for de novo DNA methylation. *Nature*, *449*(7159), 248–251.

Johnson, J. W., & Ascher, P. (1987). Glycine potentiates the NMDA response in cultured mouse brain neurons. *Nature*, *325*(6104), 529–531.

Kafri, T., Ariel, M., Brandeis, M., Shemer, R., Urven, L., McCarrey, J., … Razin, A. (1992). Developmental pattern of gene-specific DNA methylation in the mouse embryo and germ line. *Genes and Development*, *6*(5), 705–714.

Kalhan, S. C., & Hanson, R. W. (2012). Resurgence of serine: An often neglected but indispensable amino acid. *Journal of Biological Chemistry*, *287*(24), 19786–19791.

Kalhan, S. C., Uppal, S. O., Moorman, J. L., Bennett, C., Gruca, L. L., Parimi, P. S., … Hanson, R. W. (2011). Metabolic and genomic response to dietary isocaloric protein restriction in the rat. *The Journal of Biological Chemistry*, *286*(7), 5266–5277.

Kalmbach, R. D., Choumenkovitch, S. F., Troen, A. M., D'Agostino, R., Jacques, P. F., & Selhub, J. (2008). Circulating folic acid in plasma: relation to folic acid fortification. *The American Journal of Clinical Nutrition*, *88*(3), 763–768.

Kanai, Y., Clémençon, B., Simonin, A., Leuenberger, M., Lochner, M., Weisstanner, M., &

Hediger, M. A. (2013). The SLC1 high-affinity glutamate and neutral amino acid transporter family. *Molecular Aspects of Medicine*, *34*, 108–120.

Kezele, P., Nilsson, E., & Skinner, M. K. (2007). Cell-cell interactions in primordial follicle assembly and development. *Frontiers in Bioscience*, *7*, d1990-1996.

Kiyosu, C., Tsuji, T., Yamada, K., Kajita, S., & Kunieda, T. (2012). NPPC/NPR2 signaling is essential for oocyte meiotic arrest and cumulus oophorus formation during follicular development in the mouse ovary. *Reproduction*, *144*(2), 187–193.

Kolesnick, R. (2002). The therapeutic potential of modulating the ceramide/sphingomyelin pathway. *The Journal of Clinical Investigation*, *110*(1), 3–8.

Kooistra, M., Trasler, J. M., & Baltz, J. M. (2013). Folate Transport in Mouse Cumulus-Oocyte Complexes and Preimplantation Embryos1. *Biology of Reproduction*, *89*(3), 1–9.

Krishnamohan, A., & Jackman, J. E. (2019). A Family Divided: Distinct Structural and Mechanistic Features of the SpoU-TrmD (SPOUT) Methyltransferase Superfamily. *Biochemistry*, *58*(5), 336–345.

Kwong, W. Y., Adamiak, S. J., Gwynn, A., Singh, R., & Sinclair, K. D. (2010). Endogenous folates and single-carbon metabolism in the ovarian follicle, oocyte and pre-implantation embryo. *Reproduction*, *139*(4), 705–715.

Lawitts, J. A., & Biggers, J. D. (1993). [9] Culture of Preimplantation Embryos. *Methods in Enzymology*, *225*(C), 153–164.

Lawson, K. A., Dunn, N. R., Roelen, B. A., Zeinstra, L. M., Davis, A. M., Wright, C. V, … Hogan, B. L. (1999). Bmp4 is required for the generation of primordial germ cells in the

mouse embryo. *Genes & Development*, *13*(4), 424–436.

Lee, M. B., Kooistra, M., Zhang, B., Slow, S., Fortier, A. L., Garrow, T. A., … Baltz, J. M. (2012). Betaine homocysteine methyltransferase is active in the mouse blastocyst and promotes inner cell mass development. *Journal of Biological Chemistry*, *287*(39), 33094–33103.

Leroy, J. L. M. R., Vanholder, T., Mateusen, B., Christophe, A., Opsomer, G., de Kruif, A., … Van Soom, A. (2005). Non-esterified fatty acids in follicular fluid of dairy cows and their effect on developmental capacity of bovine oocytes in vitro. *Reproduction*, *130*(4), 485–495.

Li, J.-Y., Lees-Murdock, D. J., Xu, G.-L., & Walsh, C. P. (2004). Timing of establishment of paternal methylation imprints in the mouse. *Genomics*, *84*(6), 952–960.

Li, R., & Albertini, D. F. (2013). The road to maturation: Somatic cell interaction and self-organization of the mammalian oocyte. *Nature Reviews Molecular Cell Biology*, *14*(3), 141–152.

Loenen, W. A. M. (2006). S-Adenosylmethionine: jack of all trades and master of everything? *Biochemical Society Transactions*, *34*(2), 330–333.

Loutradis, D., Bletsa, R., Aravantinos, L., Kallianidis, K., Michalas, S., & Psychoyos, A. (1991). Preovulatory effects of the progesterone antagonist mifepristone (RU486) in mice. *Human Reproduction (Oxford, England)*, *6*(9), 1238–1240.

Lu, S. C. (2000). S-Adenosylmethionine. *The International Journal of Biochemistry & Cell Biology*, *32*(4), 391–395.

Lu, S. C. (2013). Glutathione synthesis. *Biochimica et Biophysica Acta*, *1830*(5), 3143–3153.

Lyko, F. (2017). The DNA methyltransferase family: a versatile toolkit for epigenetic regulation. *Nature Reviews Genetics*, *19*(2), 81–92.

Mackenzie, B., & Erickson, J. D. (2004). Sodium-coupled neutral amino acid (System N/A) transporters of the SLC38 gene family. *Pflugers Archiv European Journal of Physiology*, *447*(5), 784–795.

Maloney, C. A., Hay, S. M., Young, L. E., Sinclair, K. D., & Rees, W. D. (2011). A methyl-deficient diet fed to rat dams during the peri-conception period programs glucose homeostasis in adult male but not female offspring. *The Journal of Nutrition*, *141*(1), 95–100.

McClatchie, T., Meredith, M., Ouédraogo, M. O., Slow, S., Lever, M., Mann, M. R. W., … Baltz, J. M. (2017). Betaine is accumulated via transient choline dehydrogenase activation during mouse oocyte meiotic maturation. *Journal of Biological Chemistry*, *292*(33), 13784–13794.

Mehlmann, L. M. (2005). Oocyte-specific expression of Gpr3 is required for the maintenance of meiotic arrest in mouse oocytes. *Developmental Biology*, *288*(2), 397–404.

Menezo, Y., Khatchadourian, C., Gharib, A., Hamidi, J., Greenland, T., & Sarda, N. (1989). Regulation of S-adenosyl methionine synthesis in the mouse embryo. *Life Sciences*, *44*(21), 1601–1609.

Meredith, M., Macneil, A. H., Trasler, J. M., & Baltz, J. M. (2016). Growing Mouse Oocytes Transiently Activate Folate Transport via Folate Receptors As They Approach Full Size 1. *Biology of Reproduction*, *94125*(6), 1–12.

Micevych, P., Sinchak, K., Mills, R. H., Tao, L., LaPolt, P., & Lu, J. K. H. (2003). The

Luteinizing Hormone Surge Is Preceded by an Estrogen-Induced Increase of Hypothalamic Progesterone in Ovariectomized and Adrenalectomized Rats. *Neuroendocrinology*, *78*(1), 29–35.

Mitchell, P. A., & Burghardt, R. C. (1986). The ontogeny of nexuses (gap junctions) in the ovary of the fetal mouse. *The Anatomical Record*, *214*(3), 283–288.

Monk, M., Boubelik, M., & Lehnert, S. (1987). Temporal and regional changes in DNA methylation in the embryonic, extraembryonic and germ cell lineages during mouse embryo development. *Development*, *99*, 371–382.

Monk, M., & Mclaren, A. (1981). X-chromosome activity in foetal germ cells of the mouse From the MRC Mammalian Development Unit, London. *J. Embryol. Exp. Morph*, *63*, 75–84.

Moore, R. K., Otsuka, F., & Shimasaki, S. (2003). Molecular basis of bone morphogenetic protein-15 signaling in granulosa cells. *The Journal of Biological Chemistry*, *278*(1), 304–310.

Moore, T., & Haig, D. (1991). Genomic imprinting in mammalian development: a parental tug-of-war. *Trends in Genetics*, *7*(2), 45–49.

Morgan, H. D., Santos, F., Green, K., Dean, W., & Reik, W. (2005). Epigenetic reprogramming in mammals. *Human Molecular Genetics*, *14*(1), R47-58.

Mrsny, R. J., Waxman, L., & Meizel, S. (1979). Taurine maintains and stimulates motility of hamster sperm during capacitation in vitro. *Journal of Experimental Zoology*, *210*(1), 123–128.

Nakanishi, T., Sugawara, M., Huang, W., Martindale, R. G., Leibach, F. H., Ganapathy, M. E., … Ganapathy, V. (2001). Structure, function, and tissue expression pattern of human SN2, a subtype of the amino acid transport system N. *Biochemical and Biophysical Research Communications*, *281*(5), 1343–1348.

Norris, R. P., Freudzon, M., Mehlmann, L. M., Cowan, A. E., Simon, A. M., Paul, D. L., … Jaffe, L. A. (2008). Luteinizing hormone causes MAP kinase-dependent phosphorylation and closure of connexin 43 gap junctions in mouse ovarian follicles: one of two paths to meiotic resumption. *Development (Cambridge, England)*, *135*(19), 3229–3238.

O'Neill, C. (1998). Endogenous folic acid is essential for normal development of preimplantation embryos. *Human Reproduction*, *13*(5), 1312–1316.

Odom, C. M., & Segars, J. H. (2010). Imprinting disorders and assisted reproductive technology. *Curr Opin Endocrinol Diabetes Obes.*, *17*(6), 517–522.

Ohinata, Y., Payer, B., O'Carroll, D., Ancelin, K., Ono, Y., Sano, M., … Surani, M. A. (2005). Blimp1 is a critical determinant of the germ cell lineage in mice. *Nature*, *436*(7048), 207–213.

Orisaka, M., Orisaka, S., Jiang, J.-Y., Craig, J., Wang, Y., Kotsuji, F., & Tsang, B. K. (2006). Growth Differentiation Factor 9 Is Antiapoptotic during Follicular Development from Preantral to Early Antral Stage. *Molecular Endocrinology*, *20*(10), 2456–2468.

Otsuka, F., Yao, Z., Lee, T., Yamamoto, S., Erickson, G. F., & Shimasaki, S. (2000). Bone morphogenetic protein-15. Identification of target cells and biological functions. *The Journal of Biological Chemistry*, *275*(50), 39523–39528.

Pan, B., & Li, J. (2019). The art of oocyte meiotic arrest regulation. *Reproductive Biology and Endocrinology*, *17*(1), 8.

Pangas, S. A., Choi, Y., Ballow, D. J., Zhao, Y., Westphal, H., Matzuk, M. M., & Rajkovic, A. (2006). Oogenesis requires germ cell-specific transcriptional regulators Sohlh1 and Lhx8. *Proceedings of the National Academy of Sciences*, *103*(21), 8090–8095.

Park, J. Y., Su, Y. Q., Ariga, M., Law, E., Jin, S.-L. L. C., & Conti, M. (2004). EGF-Like Growth Factors As Mediators of LH Action in the Ovulatory Follicle. *Science*, *303*(5658), 682–684.

Peake, N. J., Hobbs, A. J., Pingguan-Murphy, B., Salter, D. M., Berenbaum, F., & Chowdhury, T. T. (2014). Role of C-type natriuretic peptide signalling in maintaining cartilage and bone function. *Osteoarthritis and Cartilage*, *22*(11), 1800–1807.

Pedersen, T., & Peters, H. (1968). Proposal for a classification of oocytes and follicles in the mouse ovary. *Journal of Reproduction and Fertility*, *17*(3), 555–557.

Pelland, A. M. D., Corbett, H. E., & Baltz, J. M. (2009). Amino Acid Transport Mechanisms in Mouse Oocytes During Growth and Meiotic Maturation1. *Biology of Reproduction*, *81*(6), 1041–1054.

Pepling, M. E. (2006). From primordial germ cell to primordial follicle: Mammalian female germ cell development. *Genesis*, *44*(12), 622–632.

Pérez-Armendariz, E. M., Sáez, J. C., Bravo-Moreno, J. F., López-Olmos, V., Enders, G. C., & Villalpando, I. (2003). Connexin43 is expressed in mouse fetal ovary. *The Anatomical Record Part A: Discoveries in Molecular, Cellular, and Evolutionary Biology*, *271A*(2),

360–367.

Peter, H., & McNatty, K. P. (1980). *The Ovary*. Berkley and Los Angeles: University of California Press.

Polanski, Zbigniew. 1997. “Strain Difference in the Timing of Meiosis Resumption in Mouse Oocytes : Involvement of a Cytoplasmic f Actor (s) Acting Presumably Upstream of the Dephosphorylation of P34 Cdc2 Kinase.” *Zygote* 5 (May 2019): 105–9.

Pramod, A. B., Foster, J., Carvelli, L., & Henry, L. K. (2013). SLC6 transporters: structure, function, regulation, disease association and therapeutics. *Molecular Aspects of Medicine*, *34*(2–3), 197–219.

Rajkovic, A., Pangas, S. A., Ballow, D., Suzumori, N., & Matzuk, M. M. (2004). NOBOX Deficiency Disrupts Early Folliculogenesis and Oocyte-Specific Gene Expression. *Science*, *305*(5687), 1157–1159.

Reik, W., & Walter, J. (2001). Genomic imprinting: parental influence on the genome. *Nature Reviews Genetics*, *2*(1), 21–32.

Richard, S., & Baltz, J. M. (2014). Prophase I Arrest of Mouse Oocytes Mediated by Natriuretic Peptide Precursor C Requires GJA1 (connexin-43) and GJA4 (connexin-37) Gap Junctions in the Antral Follicle and Cumulus-Oocyte Complex1. *Biology of Reproduction*, *90(6)*(137), 1–10.

Richard, S., Tartia, A. P., Boison, D., & Baltz, J. M. (2017). Mouse Oocytes Acquire Mechanisms That Permit Independent Cell Volume Regulation at the End of Oogenesis. *Journal of Cellular Physiology*, *232*(9), 2436–2446.

Rose, T. A., & Bavister, B. D. (1992). Effect of oocyte maturation medium on in vitro development of in vitro fertilized bovine embryos. *Molecular Reproduction and Development*, *31*(1), 72–77.

Rowsell, E. V, Snell, K., Carnie, J. A., & Al-Tai, A. H. (1969). Liver-L-alanine-glyoxylate and L-serine-pyruvate aminotransferase activities: an apparent association with gluconeogenesis. *The Biochemical Journal*, *115*(5), 1071–1073.

Russell, D. L., & Robker, R. L. (2007). Molecular mechanisms of ovulation: Co-ordination through the cumulus complex. *Human Reproduction Update*, *13*(3), 289–312.

Sallach, H. J. (1956). Formation of serine from hydroxypyruvate and L-alanine*. *Journal of Biological Chemistry*, *223*, 1101–1109.

Salustri, A., Petrungaro, S., De Felici, M., Conti, M., & Siracusa, G. (1985). Effect of follicle-stimulating hormone on cyclic adenosine monophosphate level and on meiotic maturation in mouse cumulus cell-enclosed oocytes cultured in vitro. *Biology of Reproduction*, *33*(4), 797–802.

Salustri, A., Yanagishita, M., & Hascall, V. C. (1990). Mouse oocytes regulate hyaluronic acid synthesis and mucification by FSH-stimulated cumulus cells. *Developmental Biology*, *138*(1), 26–32.

Sánchez, F., & Smitz, J. (2012). Molecular control of oogenesis. *Biochimica et Biophysica Acta - Molecular Basis of Disease*, *1822*(12), 1896–1912.

SanMiguel, J. M., & Bartolomei, M. S. (2018). DNA methylation dynamics of genomic imprinting in mouse development†. *Biology of Reproduction*, *99*(1), 252–262.

Schachter, M., Raziel, A., Friedler, S., Strassburger, D., Bern, O., & Ron-El, R. (2003). Insulin resistance in patients with polcystic ovary syndrome is associated with elevated plasma homocysteine. *Human Reproduction*, *18*(4), 721–727.

Schubert, H. L., Blumenthal, R. M., & Cheng, X. (2003). Many paths to methyltransfer: a chronicle of convergence. *Trends in Biochemical Sciences*, *28*(6), 329–335.

Schultz, R. M., & Wassarman, P. M. (1977). Biochemical studies of mammalian oogenesis: protein synthesis during oocyte growth and meiotic maturation in the mouse. *J. Cell Sci.*, *24*, 167–194.

Seisenberger, S., Andrews, S., Krueger, F., Arand, J., Walter, J., Santos, F., … Reik, W. (2012). The dynamics of genome-wide DNA methylation reprogramming in mouse primordial germ cells. *Molecular Cell*, *48*(6), 849–862.

Sharif, J., Muto, M., Takebayashi, S., Suetake, I., Iwamatsu, A., Endo, T. A., … Koseki, H. (2007). The SRA protein Np95 mediates epigenetic inheritance by recruiting Dnmt1 to methylated DNA. *Nature*, *450*(7171), 908–912.

Shuhaibar, L. C., Egbert, J. R., Norris, R. P., Lampe, P. D., Nikolaev, V. O., Thunemann, M., … Jaffe, L. A. (2015). Intercellular signaling via cyclic GMP diffusion through gap junctions restarts meiosis in mouse ovarian follicles. *Proceedings of the National Academy of Sciences*, *112*(17), 5527–5532.

Sinclair, K. D., Allegrucci, C., Singh, R., Gardner, D. S., Sebastian, S., Bispham, J., … Young, L. E. (2007). DNA methylation, insulin resistance, and blood pressure in offspring determined by maternal periconceptional B vitamin and methionine status. *Proceedings of the National Academy of Sciences*, *104*(49), 19351–19356.

Singer, D., Camargo, S. M. R., Huggel, K., Romeo, E., Danilczyk, U., Kuba, K., … Verrey, F. (2009). Orphan transporter SLC6A18 is renal neutral amino acid transporter B0AT3. *The Journal of Biological Chemistry*, *284*(30), 19953–19960.

Smallwood, S. A., & Kelsey, G. (2012). De novo DNA methylation: A germ cell perspective. *Trends in Genetics*, *28*(1), 33–42.

Smallwood, S. A., Tomizawa, S.-I., Krueger, F., Ruf, N., Carli, N., Segonds-Pichon, A., … Kelsey, G. (2011). Dynamic CpG island methylation landscape in oocytes and preimplantation embryos. *Nature Genetics*, *43*(8), 811–814.

Snell, K. (1984). Enzymes of serine metabolism in normal, developing and neoplastic rat tissues. *Advances in Enzyme Regulation*, *22*, 325–400.

Snell, K., Natsumeda, Y., & Weber, G. (1987). The modulation of serine metabolism in hepatoma 3924A during different phases of cellular proliferation in culture. *The Biochemical Journal*, *245*(2), 609–612.

Soderberg, T. (2013). The 20 common amino acids - Chemistry LibreTexts. Retrieved February 25, 2019, from https://chem.libretexts.org/Bookshelves/Organic_Chemistry/Book%3A_Organic_Chemistry_with_a_Biological_Emphasis_(Soderberg)/Reference_Tables/The_20_common_amino_acids

Solc, P., Saskova, A., Baran, V., Kubelka, M., Schultz, R. M., & Motlik, J. (2008). CDC25A phosphatase controls meiosis I progression in mouse oocytes. *Developmental Biology*, *317*(1), 260.

Songsasen, N. (2012). Energy Metabolism Regulating Mammalian Oocyte Maturation. In *Meiosis - Molecular Mechanisms and Cytogenetic Diversity*.

Steegers-Theunissen, R. P. M., Twigt, J., Pestinger, V., & Sinclair, K. D. (2013). The periconceptional period, reproduction and long-term health of offspring: The importance of one-carbon metabolism. *Human Reproduction Update*, *19*(6), 640–655.

Steeves, C. L., Hammer, M.-A., Walker, G. B., Rae, D., Stewart, N. A., & Baltz, J. M. (2003). The glycine neurotransmitter transporter GLYT1 is an organic osmolyte transporter regulating cell volume in cleavage-stage embryos. *Proceedings of the National Academy of Sciences of the United States of America*, *100*(24), 13982–13987.

Steptoe, P. C., & Edwards, R. G. (1978). Birth after the reimplantation of a human embryo. *Lancet*, *2*(8085), 366.

Stewart, K. R., Veselovska, L., & Kelsey, G. (2016). Establishment and functions of DNA methylation in the germline. *Epigenomics*, *8*(10), 1399–1413.

Struck, A.-W., Thompson, M. L., Wong, L. S., & Micklefield, J. (2012). *S* -Adenosyl-Methionine-Dependent Methyltransferases: Highly Versatile Enzymes in Biocatalysis, Biosynthesis and Other Biotechnological Applications. *ChemBioChem*, *13*(18), 2642–2655.

Sugawara, M., Nakanishi, T., Fei, Y.-J., Martindale, R. G., Ganapathy, M. E., Leibach, F. H., & Ganapathy, V. (2000). Structure and function of ATA3, a new subtype of amino acid transport system A, primarily expressed in the liver and skeletal muscle. *Biochimica et Biophysica Acta (BBA) - Biomembranes*, *1509*(1–2), 7–13.

Sutton, M. L., Gilchrist, R. B., & Thompson, J. G. (2003). Effect of in-vivo and in-vitro

environments on the metabolism of the cumulus-oocyte complex and its influence on oocyte developmental capacity. *Human Reproduction Update*, *9*(1), 35–48.

Szybek, K. (1972). In-vitro maturation of oocytes from sexually immature mice. *The Journal of Endocrinology*, *54*(3), 527–528.

Tanaka, K., Yamamoto, A., & Fujita, T. (2005). Functional expression and adaptive regulation of Na+-dependent neutral amino acid transporter SNAT2/ATA2 in normal human astrocytes under amino acid starved condition. *Neuroscience Letters*, *378*(2), 70–75.

Tarumi, W., Itoh, M. T., & Suzuki, N. (2014). Effects of 5α-dihydrotestosterone and 17β-estradiol on the mouse ovarian follicle development and oocyte maturation. *PloS One*, *9*(6), e99423.

Tesarik, J., & Mendoza, C. (1995). Nongenomic effects of 17 beta-estradiol on maturing human oocytes: relationship to oocyte developmental potential. *The Journal of Clinical Endocrinology & Metabolism*, *80*(4), 1438–1443.

Tiedeken, S. D., & Chang, C. (2015). Principles of Epigenetic Treatment. In Q. Lu, C. C. Chang, & B. C. Richardson (Eds.), *Epigenetics and Dermatology* (pp. 443–465). Academic Press.

Tingen, C., Kim, A., & Woodruff, T. K. (2009). The primordial pool of follicles and nest breakdown in mammalian ovaries. *Molecular Human Reproduction*, *15*(12), 795–803.

Utsunomiya-Tate, N., Endou, H., & Kanai, Y. (1996). Cloning and functional characterization of a system ASC-like Na+-dependent neutral amino acid transporter. *The Journal of Biological Chemistry*, *271*(25), 14883–14890.

Vaccari, S., Weeks, J. L., Hsieh, M., Menniti, F. S., Conti, M., & Conti, M. (2009). Cyclic GMP

signaling is involved in the luteinizing hormone-dependent meiotic maturation of mouse oocytes. *Biology of Reproduction*, *81*(3), 595–604.

Valsangkar, D., & Downs, S. M. (2013). A requirement for fatty acid oxidation in the hormone-induced meiotic maturation of mouse oocytes. *Biology of Reproduction*, *89*(2), 43.

Van Blerkom, J. (2004). Mitochondria in human oogenesis and preimplantation embryogenesis: engines of metabolism, ionic regulation and developmental competence. *Reproduction*, *128*(3), 269–280.

Van Winkle, L. J., Tesch, J. K., Shah, A., & Campione, A. L. (2006). System B0,+ amino acid transport regulates the penetration stage of blastocyst implantation with possible long-term developmental consequences through adulthood. *Human Reproduction Update*, *12*(2), 145–157.

Varland, S., Osberg, C., & Arnesen, T. (2015). N-terminal modifications of cellular proteins: The enzymes involved, their substrate specificities and biological effects. *Proteomics*, *15*(14), 2385–2401.

Vazquez, M. H., Phillips, D. M., & Wassarman, P. M. (1989). Interaction of mouse sperm with purified sperm receptors covalently linked to silica beads. *J Cell Sci*, *92*, 713–722.

Verdon, Q., Boonen, M., Ribes, C., Jadot, M., Gasnier, B., & Sagné, C. (2017). SNAT7 is the primary lysosomal glutamine exporter required for extracellular protein-dependent growth of cancer cells. *Proceedings of the National Academy of Sciences*, *114*(18), E3602–E3611.

Verkleij-Hagoort, A., Verlinde, M., Ursem, N., Lindemans, J., Helbing, W., Ottenkamp, J., … Steegers-Theunissen, R. (2006). Maternal hyperhomocysteinaemia is a risk factor for

congenital heart disease. *BJOG: An International Journal of Obstetrics & Gynaecology*, *113*(12), 1412–1418.

Verrey, F., Closs, E. I., Wagner, C. A., Palacin, M., Endou, H., & Kanai, Y. (2004). CATs and HATs: The SLC7 family of amino acid transporters. *Pflugers Archiv European Journal of Physiology*, *447*(5), 532–542.

Veselovska, L., Smallwood, S. A., Saadeh, H., Stewart, K. R., Krueger, F., Maupetit Méhouas, S., … Kelsey, G. (2015). Deep sequencing and de novo assembly of the mouse oocyte transcriptome define the contribution of transcription to the DNA methylation landscape. *Genome Biology*, *16*(1), 209.

Vitt, U. A., Hayashi, M., Klein, C., & Hsueh, A. J. W. (2000). Growth Differentiation Factor-9 Stimulates Proliferation but Suppresses the Follicle-Stimulating Hormone-Induced Differentiation of Cultured Granulosa Cells from Small Antral and Preovulatory Rat Follicles1. *Biology of Reproduction*, *62*(2), 370–377.

Wagner, I., & Musso, H. (1983). New Naturally Occurring Amino Acids. *Angewandte Chemie International Edition in English*, *22*(11), 816–828.

Wallace, M., Cottell, E., Gibney, M. J., McAuliffe, F. M., Wingfield, M., & Brennan, L. (2012). An investigation into the relationship between the metabolic profile of follicular fluid, oocyte developmental potential, and implantation outcome. *Fertility and Sterility*, *97*(5), 1078–1084.e8.

Wassarman, P. M., Schultz, R. M., Letourneau, G. E., LaMarca, M. J., Josefowicz, W. J., & Bleil, J. D. (1979). Meiotic Maturation of Mouse Oocytes in Vitro. In C. P. Channing, J. M. Marsh, & W. A. Sadler (Eds.), *Ovarian Follicular and Corpus Luteum Function* (pp. 251–

268). Boston: Springer.

Watson, A. J., De Sousa, P., Caveney, A., Barcroft, L. C., Natale, D., Urquhart, J., & Westhusin, M. E. (2000). Impact of bovine oocyte maturation media on oocyte transcript levels, blastocyst development, cell number, and apoptosis. *Biology of Reproduction*, *62*(2), 355–364.

Weil, S., Vendola, K., Zhou, J., & Bondy, C. A. (1999). Androgen and Follicle-Stimulating Hormone Interactions in Primate Ovarian Follicle Development. *The Journal of Clinical Endocrinology & Metabolism*, *84*(8), 2951–2956.

Welch, G. N., & Loscalzo, J. (1998). Homocysteine and Atherothrombosis. *New England Journal of Medicine*, *338*(15), 1042–1050.

Wigglesworth, K., Lee, K.-B., O'Brien, M. J., Peng, J., Matzuk, M. M., & Eppig, J. J. (2013). Bidirectional communication between oocytes and ovarian follicular somatic cells is required for meiotic arrest of mammalian oocytes. *Proceedings of the National Academy of Sciences*, *110*(39), E3723-9.

Willard, H. F., & Breg, W. R. (1980). Human X chromosomes: Synchrony of DNA replication in diploid and triploid fibroblasts with multiple active or inactive X chromosomes. *Somatic Cell Genetics*, *6*(2), 187–198.

Willard, H. F., Brown, C. J., Carrel, L., Hendrich, B., & Miller, A. P. (1993). Epigenetic and chromosomal control of gene expression: molecular and genetic analysis of X chromosome inactivation. *Cold Spring Harbor Symposia on Quantitative Biology*, *58*, 315–322.

Winkle, L. J. Van. (2001). Amino Acid Transport Regulation and Early Embryo Development.

Biology of Reproduction, *64*, 1–12.

Wu, J., Nayudu, P. L., Kiesel, P. S., & Michelmann, H. W. (2000). Luteinizing Hormone Has a Stage-Limited Effect on Preantral Follicle Development In Vitro1. *Biology of Reproduction*, *63*(1), 320–327.

Wu, L.-M., Hu, M.-H., Tong, X.-H., Han, H., Shen, N., Jin, R.-T., … Liu, Y.-S. (2012). Chronic unpredictable stress decreases expression of brain-derived neurotrophic factor (BDNF) in mouse ovaries: relationship to oocytes developmental potential. *PloS One*, *7*(12), e52331.

Wüllner, U., Seyfried, J., Groscurth, P., Beinroth, S., Winter, S., Gleichmann, M., … Klockgether, T. (1999). Glutathione depletion and neuronal cell death: the role of reactive oxygen intermediates and mitochondrial function. *Brain Research*, *826*(1), 53–62.

Wutz, A., Smrzka, O. W., Schweifer, N., Schellander, K., Wagner, E. F., & Barlow, D. P. (1997). Imprinted expression of the Igf2r gene depends on an intronic CpG island. *Nature*, *389*(6652), 745–749.

Xie, H.-L., Wang, Y.-B., Jiao, G.-Z., Kong, D.-L., Li, Q., Li, H., … Tan, J.-H. (2016). Effects of glucose metabolism during in vitro maturation on cytoplasmic maturation of mouse oocytes. *Scientific Reports*, *6*, 20764.

Xu, J., & Sinclair, K. D. (2015). One-carbon metabolism and epigenetic regulation of embryo development. *Reproduction, Fertility and Development*, *27*, 667-676.

Yamashita, Y., & Shimada, M. (2012). The Release of EGF Domain from EGF-like Factors by a Specific Cleavage Enzyme Activates the EGFR-MAPK3/1 Pathway in Both Granulosa Cells and Cumulus Cells During the Ovulation Process. *Journal of Reproduction and*

Development, *58*(5), 510–514.

Zelinski-Wooten, M. B., Hess, D. L., Wolf, D. P., & Stouffer, R. L. (1994). Steroid reduction during ovarian stimulation impairs oocyte fertilization, but not folliculogenesis, in rhesus monkeys. *Fertility and Sterility*, *61*(6), 1147–1155.

Zerangue, N., & Kavanaugh, M. P. (1996). ASCT-1 is a neutral amino acid exchanger with chloride channel activity. *The Journal of Biological Chemistry*, *271*(45), 27991–27994.

Zhang, B., Denomme, M. M., White, C. R., Leung, K.-Y., Lee, M. B., Greene, N. D. E., … Both, J. M. (2015). Both the folate cycle and betaine-homocysteine methyltransferase contribute methyl groups for DNA methylation in mouse blastocysts. *The FASEB Journal • Research Communication*, *29*, 1069–1079.

Zhang, M., Su, Y.-Q., Sugiura, K., Xia, G., & Eppig, J. J. (2010). Granulosa Cell Ligand NPPC and Its Receptor NPR2 Maintain Meiotic Arrest in Mouse Oocytes. *Science*, *330*(6002), 366–369.

Zheng, P., Si, W., Bavister, B. D., Yang, J., Ding, C., & Ji, W. (2003). 17 -Estradiol and progesterone improve in-vitro cytoplasmic maturation of oocytes from unstimulated prepubertal and adult rhesus monkeys. *Human Reproduction*, *18*(10), 2137–2144.

Zheng, W., Zhang, H., & Liu, K. (2014). The two classes of primordial follicles in the mouse ovary: Their development, physiological functions and implications for future research. *Molecular Human Reproduction*, *20*(4), 286–292.

Zittan, E., Preis, M., Asmir, I., Cassel, A., Lindenfeld, N., Alroy, S., … Flugelman, M. Y. (2007). High frequency of vitamin B12 deficiency in asymptomatic individuals homozygous to

MTHFR *C677T* mutation is associated with endothelial dysfunction and homocysteinemia. *American Journal of Physiology-Heart and Circulatory Physiology*, *293*(1), H860–H865.